2020•2021
Faculteit Industriële Ingenieurswetenschappen
master in de industriële wetenschappen: chemie

Masterthesis

The impact of multiple production cycles/the introduction of recycled material on the properties of Expanded Polypropylene

PROMOTOR :
ing. Anton GINZBURG

PROMOTOR :
ing. Nancy LAEVEREN

Jules Henrotte
Scriptie ingediend tot het behalen van de graad van master in de industriële wetenschappen: chemie

▶▶ UHASSELT   KU LEUVEN

▶▶ UHASSELT   KU LEUVEN

2020•2021
Faculteit Industriële Ingenieurswetenschappen
master in de industriële wetenschappen: chemie

Masterthesis
The impact of multiple production cycles/the introduction of recycled material on the properties of Expanded Polypropylene

PROMOTOR :
ing. Anton GINZBURG

PROMOTOR :
ing. Nancy LAEVEREN

Jules Henrotte
Scriptie ingediend tot het behalen van de graad van master in de industriële wetenschappen: chemie

▶▶ UHASSELT   KU LEUVEN

Preface

The completion of this master thesis was a very challenging, yet rewarding part of my last year as a chemical engineering student. In this short section I would like to thank the people who made all of this possible. In the first place, I wish to thank my external supervisor ir. Nancy Laeveren for the guidance and constructive feedback she provided during the course of the past three months. The time she made to discuss my results as well as the overall guidance I received is very much appreciated. I feel like I have truly learned a lot over the last months working on this topic. Secondly, a token of appreciation goes out to my supervisor ir. Anton Ginzburg. He proved to be an excellent supervisor and mentor, and I have learned a lot from him on a personal and scientific level. Furthermore, I would like to thank all the lab workers and colleagues for maintaining a very positive atmosphere to work in and being open for questions at any point in time. Finally, my thanks go out to all my friends and family who have supported me during these months and the years before that. I want to thank my fellow students, my friends from Tongeren and Diepenbeek, and of course my parents. They have provided me with everything I needed and showed me a never-ending support. Thank you.

Table Of Contents

List of Tables

List of Figures

Nomenclature

Term	Definition
Complex Shear modulus (G*)	This value describes the entire viscoelastic behaviour of a sample and is calculated by oscillatory tests. It is the combination of the elastic G' or storage and viscous or loss G" shear modulus: $G^* = \sqrt{G'^2 + G''^2}$
Crystallisation	By cooling a polymer from the melt, certain polymers can arrange themselves into regular crystalline structures, so called lamellae. Polymers are usually semi-crystalline as they differ in MW. Furthermore, the crystallinity is influenced by the tacticity of the polymer.
Dynamic Viscosity (η)	Also known as the shear viscosity, is calculated by reformulating Newton's law: $\tau = \dot{\gamma} \cdot \eta$
Extensional Viscosity (η_e)	Also known as the elongational viscosity, when a rheometer applies an oscillating extensional stress to the system, one is able to calculate this type of viscosity using the following formula: : $\eta_e = \frac{\sigma_e}{\dot{\epsilon}}$
Relaxation time (τ)	When a deformation is applied to a material, part of the energy is dissipated leading to a lowering or relaxation of the stress in time. The time it takes for the stress to flatten out is called the relaxation time.
Sharkskin	Sharkskin refers to the phenomenon of a loss of surface gloss of an extrudate, also sometimes termed surface mattness.
Shear modulus (G)	Is calculated by dividing the shear stress by the shear strain: $G = \frac{\tau}{\gamma}$
Strain Hardening	During a strain deformation, a large scale orientation of chain molecules can strengthen a material. The molecules tend to orient themselves in the direction of the load, and in doing so increasing the strength an stiffness of the material in that direction. This parameter is not influenced by the crystallinity, but by the entanglement density of the amorphous phase.
Ultimate Tensile Strength (TS)	It is the maximum stress a material can withstand, while being stretched, before breaking. Furthermore, it can be seen as the highest point in the stress-strain curve. In case of compression, it is called the compressive strength.
Yielding point	At the yielding point, polymers experience a strong irreversible plastic deformation. This deformation is usually followed by necking or strain hardening.
Young's modulus (E)	Tensile property of polymers. It is, following Hooke's law, the slope of the stress-strain curve or the ratio between the increase in stress and strain. It is a measure for the stiffness of a material.

Zero Shear Viscosity (η_0)	Is the viscosity measured when the angular frequency (ω) is zero and the complex viscosity function is reaching a constant plateau value. It is an important value with it being proportional to the molecular weight (MW) of the polymer and can be calculated using creep, oscillatory and rotational tests. It displays the viscosity of a material at rest.

Abstract

The chemical company Kaneka Belgium N.V. provides polypropylene-based foam particles, used to produce moulded parts which are applied in different sectors. Today, the company's customers are striving for sustainability following the European guidelines for 2030, which directly involve recycling of end products. In this context, it is compulsory for KB to start re-introducing a fraction of reprocessed material into their process. In order to do so, it is necessary to assess its effect on the properties and deterioration of the end product. First, this work focusses on the impact of going through multiple extrusion cycles on virgin material. In addition, the influence of adding stabilizers to the recipe at different reprocessing steps to prevent further deterioration is evaluated. Thirdly, the impact of implementing a fraction of external recycled particles into the recipe is elaborated. Different characterization techniques were performed: rheology, DSC and mechanical techniques. Generally, it can be concluded that the reprocessed samples remain stable with favourable properties, in contrast to the recycled samples who do not guarantee this stability. The rheological results demonstrated a decrease in viscosity, caused by β-chain scission. Adding the recycling stabilizer minimized this decrease. Secondly, the DSC curves indicated a small rise in crystallinity. Finally, the mechanical tests indicated a decrease in tensile strength, compression strength and elongation at break for both the recycled and reprocessed blends.

Abstract in Dutch

Het chemisch bedrijf Kaneka Belgium N.V. produceert op polypropyleen gebaseerde schuimdeeltjes, dewelke hun toepassingen vinden in verschillende sectoren. Vandaag de dag streven hun klanten naar duurzaamheid gezien het produceren van duurzamere producten en het recycleren van eindproducten deel uit maakt van de richtlijnen opgesteld door de Europese Commissie voor 2030. In deze context is het noodzakelijk voor KB ook zelf een fractie aan herwerkt of gerecycleerd materiaal te verwerken in hun proces om zo de globale hoeveelheid aan afval te beperken. Gezien dit materiaal reeds door het productieproces is gegaan, hetgeen globaal voor een degradatie van het materiaal zorgt, is het noodzakelijk het effect van het invoegen van beide soorten materiaal bij standaard materiaal na te gaan op vlak van eigenschappen van het eindproduct. Deze thesis focust eerst op de impact van het doorlopen van meerdere extrusiecycli op het standaard materiaal. Vervolgens wordt de invloed van de toevoeging van stabilisatoren in het recept nagegaan op vlak van degradatie. Ten derde wordt de impact van het toevoegen van een extern gerecycleerde fractie aan schuimpartikels uitgewerkt. Verschillende karakterisatietechnieken werden gehanteerd: reologie, DSC en mechanische technieken. Algemeen kon er geconcludeerd worden dat het herwerkte materiaal stabiel bleef. Dit gold niet voor de gerecycleerde recepten, dewelke een duidelijkere daling in eigenschappen zagen. De resultaten verkregen uit de reologische tests toonden aan dat de viscositeit daalde t.g.v. het β-chain scission mechanisme. Het toevoegen van de, speciaal voor de gerecycleerde recepten ontworpen, stabilisator minimaliseerde deze daling in viscositeit. Verder toonden de DSC curves een lichte toename in kristalliniteit na 5 extrusiecycli. Ten slotte toonden de mechanische testen een afname in treksterkte, compressiesterkte en uitrekking tot breuk voor zowel de recepten met gerecycleerd als het herwerkte materiaal.

Chapter 1

Introduction

1.1   Context

The master's internship took place in Oevel at the chemical company Kaneka Belgium NV (KB). The company operates in a business-to-business context, providing the intermediate products for manufacturing a wide variety of final products such as chemicals, functional plastics and applications in building and construction. This master's thesis was executed at the Eperan-PP section of KB, which produces expanded polypropylene foam particles (EPP), also called "beads". These beads are the base component for other companies to manufacture moulded end-products. Several applications of the beads are shown in figure 1, adapted from [1]. This wide range of possible applications is due to the fact that many grades of Eperan-PP are produced. They differ in bead-size, the amount of stabilizer added or the added pigment.

Figure 1: EPP-applications

The different production steps starting from the raw polymer material to producing an EPP-moulded end-product are depicted in figure 2.
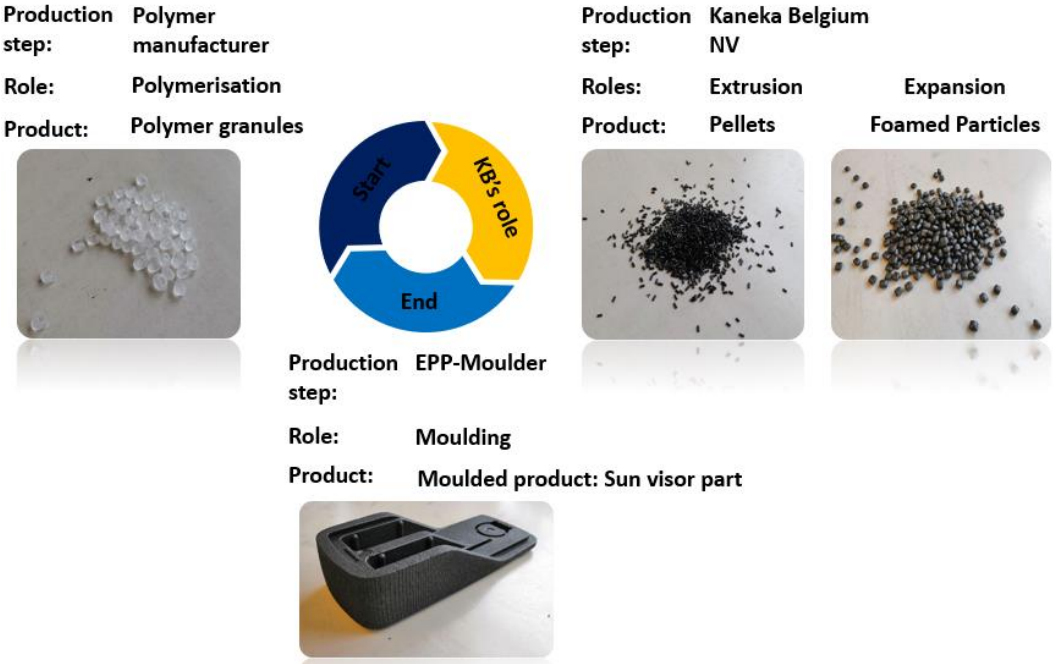
Figure 2: Production process of an EPP moulded product

Kaneka's contribution lies in the extrusion and expansion of the received polymer (being PP) granulate into foamed particles. The extrusion process provides pellets, starting from the bought PP-granulate in combination with other additives. Extrusion is a shaping process in which heated material is pushed through a die.

Afterwards, the expansion takes place under high temperature and pressure using CO_2 as a foaming agent. In doing so, the volume of the pellets is increased with preservation of their mass, thus lowering the density of the product massively. Next to developing new types of foamed particles, recycling old EPP-products into virgin material is also a relevant and important topic nowadays as currently only a small percentage of produced EPP-material is recycled.

Since both the customers and the company itself are increasingly striving for a more sustainable process and a lower residual waste content, their aim for the future is to produce beads from a combination of virgin and recycled EPP, while maintaining proper material characteristics. This thesis is sustainability driven and focusses on the effect of the introduction of recycled-EPP into virgin material and the effect of going through different production cycles on the material properties. The recycled material currently originates from two sources. On one hand, it can originate from internally re-worked off-spec EPP material. On the other hand, externally collected end-of-life moulded parts can also serve as a base for recycling. Collecting, shredding and remelting old EPP products into EPP granulate gives a base component to form new EPP materials. Since 2021, KB has been participating in a project which focusses on creating a circular economy in collaboration with several other companies. The aim of this project is to reintroduce end-of-life EPP back into the manufacturing chain and form a closed loop. This circular economy project is depicted in figure 3.
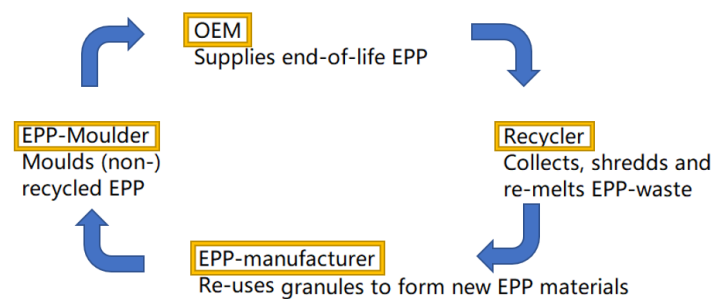
Figure 3: Circular economy implemented on EPP

1.2   Problem Definition/Research Question

The entire recycling project has only recently been launched and is therefore still in its early stages. A demand for the introduction of a recycled fraction of product into the production line came partly from the customer, who is obliged to reduce its waste material by the European Parliament. The EU commissioned an action plan for creating a circular economy wherein plastic waste is the key priority. Furthermore, the goal is to work towards using only recyclable plastic packaging by 2030. This objective lays the foundation to a new plastics economy, relating the design and production of plastics and plastic products directly to the reuse, repair and recycling of the produced plastics. In doing so, they strive for creating and developing more sustainable materials [2].

Thus, reusing waste materials or closing the product life cycle is one of the main objectives of KB for the future. Currently, the introduction of a higher percentage of recycled fraction in the

16

production line, i.e. a weight percentage (wt%) higher than 10%, has not yet been applied, nor have possible side effects on the production line been explored. This lack of knowledge raises questions whether the material undergoes a significant level of degradation going through multiple production cycles. In addition, the introduction of a higher percentage of recycled fraction may have an incidental impact on this degradation of the material.

First of all, what is the effect of going through several production cycles on the end-products? As the extrusion step is the most aggressive step in this process (due to exposure to temperature, oxygen and shear), this question could be simplified to: "What is the effect of multiple extrusion cycles on the pellets?". During the formation of the pellets of different EPP grades, stabilizers are added, among other raw materials, in order to limit the degradation of the material. Thus, does the presence or absence of these stabilizers in the recipe have a significant effect on the flow behaviour and degradation of the pellets after extrusion? Furthermore, the impact of adding a higher fraction or percentage of recycled material to virgin material is still unknown. Does adding 25 wt% of recycled material to the standard recipe have a large impact on the flow and degradation properties of the formed product? Will the properties of the combined materials remain within the company's quality standards or will additional stabilizer need to be introduced here? Does using a specially designed recycling stabilizer give better end properties?

1.3   Research Objectives

The focus of the project lies on the development of the dominant foamed particle grades with regard to sales volume, i.e. VB20-VB24. VB20 is a material-ID and stands for Very small Black particles, which are expanded 20 times in comparison to the size of the original pellets. Every produced grade gets its own specific ID. The goal is to characterize these grades in terms of flow behaviour and degradation after several extrusion cycles and verify the influence of adding recycled material and/or stabilizers to their recipe.

The first objective of this thesis is to visualize the flow behaviour (i.e. the MFI or melt flow index) of the mini-pellets produced by the extruder in function of the number of extrusion cycles. A clear comparison is needed between the varying properties of the non-stabilized product and the stabilized product in order to show the influence of the stabilizer on the process behaviour. Once this comparison has been made, a full characterisation of the most advantageous pellets is desired in order to determine their different physical properties and compare them with the virgin product. Furthermore, the physical properties of the beads are required to compare these to the ones of the expanded virgin material. This comparison will indicate to which extend the material has degraded and after which extrusion cycle it is still reusable.

The second objective is to introduce a fraction of 25% recycled material into newly produced stabilized and non-stabilized pellets and identify again the degradation and flow properties of this combined material in function of the number of extrusion cycles. Next, the properties of this material need to be compared to those of virgin material in order to conclude whether the 25% recycled material is sufficiently stable and provides the desired properties for the end-product useful for the customers to implement in their moulding processes.

A third and final objective is to check the effect of the addition of a newly designed recycling stabilizer or to enlarge the amount of the already added stabilizer to the recycling recipe in order to obtain more stable pellets with more favourable properties. The desired parameters from this type of test are the same as those for the previously mentioned purposes.

Chapter 2

Literature Survey

The goal of this thesis was an in-depth study of the influence of implementing recycled EPP material into the recipe, in combination with the effect of going through multiple extrusion cycles on the final product's mechanical properties. These properties will give a quantification of ongoing degradation of the material. On top of that, a new kind of recycling stabilizer was tested to see its impact on the end product. In order to understand the influence of each of the recipe components and each process step on the mechanical properties of the final product and the possible occurring degradation, a preliminary study is needed. Possible improvements and working points are also explored. Section 2.1 starts with an elaboration of what is needed to form the EPP foamed particles and a further analysis of their expansion necessities and possibilities. Next, section 2.2 discusses the possible degradation mechanisms occurring during the extrusion. As the extrusion and pelletizing step is the more degrading step, an in dept analysis of this degradation is needed to fully understand its influence on end-properties. Section 2.3 addresses the current knowledge of reprocessing (expanded) polypropylene, which in its turn gives an indication of the info which is still lacking in literature. Degradation, crystallization and processibility in PP blends are furtherly discussed to give an insight of what is to be expected during the experimental work. Finally, section 2.4 provides a short overview of the most useful stabilizers counteracting degradation during extrusion. The different types, specific mechanisms and inclusion methods are mentioned, as well as how a loss of stabilizers might occur.

2.1 Basic concepts of Expanded Polypropylene

Currently, these foamed particles are widely investigated commercial products having numerous desirable and beneficial properties such as: a good chemical-resistance, outstanding mechanical properties, low electrical conductivity, low cost and a unique porous honeycomb structure. PP-foams have a wide range of industrial applications in the fields of packaging, aerospace, automobiles, acoustic absorbent, dielectric materials, energy storage materials, thermal insulators, as well as tissue engineering [3]. As the gross part of the produced particles by KB will be destined for use in the automotive sector, the mechanical properties like compression strength, tensile strength and elongation are the main focus points and should be preserved. Furthermore, processing of the produced particles should also be convenient and stable.

The introduction tipped that the produced products are not simply resulting from only one component, but that a mixture of components is used which changes dependent on what the customer desires from the produced polymer's properties. KB produces expanded polypropylene (EPP), which differs from normal polypropylene in terms of manufacturing, properties and applications. The following paragraphs will elaborate on the basic concepts of foaming and other needs to produce expanded PP particles. Given that every processing step and recipe ingredient contributes to the final mechanical properties, all are elaborated.

2.1.1 Expansion necessities and possibilities

Expanded polypropylene foam particles (beads) are made using a multi-step process by which the base polypropylene is expanded into beads following a foaming process. The starting component is propylene. This polymer is polymerised and granulated into a polypropylene resin which can be bought as a raw material. The resulting PP-granules are, depending on the end-product, mixed with other ingredients (section 3.1). Next, all ingredients are added into

the extruder (figure 20), which melts the polymers, mixes the different components and produces strands of material. These are then cut into smaller pellets of a certain size, which are in their turn the base component for the expansion. The size of the pellets is correlated to the desired particle size and properties. In order to make the pellets expandable, a couple of factors are necessary:

- correct temperature and pressure;
- foaming agent;
- dispersant.

Moreover, different foaming techniques are available creating foams useful in multiple applications. Furthermore, the exact texture of the by KB produced particle foam is strongly bound to the formed foam cells. As a result, cell size and density are key parameters in creating a stabile foam and are further elaborated in the following paragraphs.

2.1.1.1 Foaming techniques

An expansion of PP-pellets can be carried out using multiple mechanisms and foaming techniques. Depending on the desired final products, sheet and particle foams are the more conventional types of manufactured foams both having different properties and drawbacks [4]. The first type of foam is mostly used as a packaging and insulation material and is not manufactured by KB. The reason being it not providing the desired impact strength, toughness, and thermal stability needed for the customer's applications. Thus, only the particle foaming technique is elaborated.
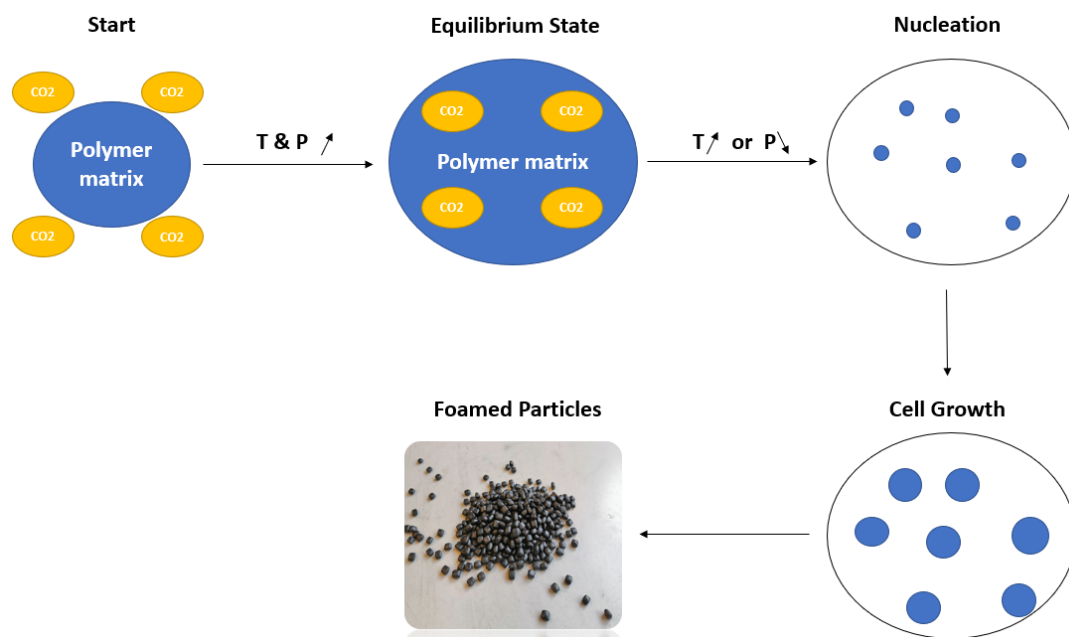
Figure 4: Cellular foaming mechanism of PP

The foaming process is a four-step process, of which a schematic overview is given by figure 4 [5]. An example of an experimental set-up is given in section 3.3 followed by the process conditions. First, a gas is dissolved in the pellets forming a polymer/gas solution. During this process step, the temperature and pressure rise, which consequently causes the solubility of the gas in the polymer matrix to increase. A so called "plasticization" takes place, which corresponds to an increase of the segmental mobility of the polymer chains which in its turn decreases the glass transition temperature (T_g) and makes the mixture more processable. The T_g is an important polymer characteristic, it is the temperature below which the physical

20

properties of the polymer change similarly to those of a glassy or crystalline state and the mobility is restricted. Above this temperature, the polymer chains are able to move more freely, increasing their flexibility and resulting in a more rubbery behaviour. With PP being a semi-crystalline polymer, the gas molecules are able to penetrate through the free volumes of the amorphous regions as these are not as structured and dense. This penetration enlarges the amount of free volumes and in doing so expanding the polypropylene. Current foam manufacturers use CO_2 as a foaming gas, although hydrocarbons like butane are also possible. Both dis-and advantages are later discussed in 2.1.1.3. The dissolution of gas takes place until an equilibrium is reached. Secondly, the nucleation takes place. This step is started following a thermodynamic instability. Both a temperature increase and a pressure decrease can be used as an initiation of nucleation or cell growth. The cells grow by a combination of heat and mass transfer. In the final step, the cell growth is stopped by a natural (or imposed) ending of the driving force, resulting in the formation of a cellular foam [5].

2.1.1.2 Important foaming properties: Cell size, melt strength and crystallization

During the foaming mechanism of PP, an in-depth understanding of the crystallization behaviour is necessary for a controllable foamability of the polymer. After melting the EPP, it stays in its molten state until the crystallization temperature is reached by cooling. Once this temperature is reached, the foamed particles start solidifying. Hereby, the outer shell of the particles solidifies first. Too low temperatures make the semicrystalline polymer chains freeze quickly, hereby increasing the viscosity and inhibiting the growth of the foam cells. If on the other hand the temperature stays to high, a low viscosity is observed and the solidification process is extended resulting in a possible collapse of the foam. Too high temperatures also cause the solubility of the CO_2 to decrease. Therefore, the correct temperature processing window is narrow and should be respected [6], [7].

Secondly, the elongational properties of the formed melt should endure the cell growth and a rupture of the cells should be avoided at all cost, which indicates the necessity of a high melt strength. The correct foam morphology consists of: a low average cell size, a narrow cell size distribution and a low density in order to have a favourable melt strength. Standard linear PP is known to possess a low melt strength and a low expansion ratio. However, the addition of some form of cross-linkage (via a copolymer) could enhance this property. Furthermore, the addition of a LCB (long chain branch) causes the elongational properties of PP to increase even more by means of the strain hardening principle, which is further discussed in sections 2.1.2.3 and 2.2.1.3 [6].

2.1.1.3 Impregnation of a polymer matrix

Impregnation is a process of infusing solute molecules, already dissolved in a solvent (for example CO_2), into a polymer matrix using high temperature and pressure. By infusing the matrix with other components, its physical and visual properties get modified by physically or chemically binding the solute impregnates to the matrix or by absorption to the surface. The impregnates can range from functional dyes, flame retardants and antioxidants to even fragrances and insecticides dependant on the end-product's applications. These impregnates modify the polymer by: changing its colour, preventing degradation of the material and thus preventing the mechanical properties to change by giving it antioxidant properties, inserting insecticides using pyrethrins [8], [9]. Lately, polypropylene was impregnated with thymol using CO_2 as a working fluid to generate an antimicrobial activity in the material [10].

The impregnation itself is fulfilled by bringing CO_2 to its supercritical state ($ScCO_2$) at which both its pressure and temperature rise above the critical values (which lie at 72.9 atm and 31°C). The super critical pressure causes an increase in density and diffusivity. However, the

supercritical temperature causes the density to drop but increases the solubility of the solvent. A more in-depth review of this supercritical state is given by [11]. Attaining the supercritical state gives the CO_2 solvent-like properties and the possibility to act as a "carrier" in which dyes, additives, medical compounds and other substances useful for the end-product can be dissolved. At this stage, the enhanced CO_2 is infused into the polypropylene bringing the other substances into the PP. During this infusion, the small CO_2-molecules penetrate the free volume of the amorphous regions of the polymer matrix and swell the material creating even more free volumes. It should be clear that this penetration step is the exact same as step one of the foaming process, and both can be combined into one process. Again, the plasticization takes place, increasing of the segmental mobility of the polymer chains giving the dissolved solutes the possibility to penetrate and diffuse into the swollen polymer matrix. Finally, a depressurization takes place and the CO_2-molecules are removed from the matrix leaving the impregnates trapped in the polymer matrix. It should be clear that the different impregnation steps going from penetration to depressurization are similar to the foaming process itself, resulting in the possibility of combining both processes into one. The impregnation mechanism of a tubular polymer fibre is depicted in Figure 6 [12].
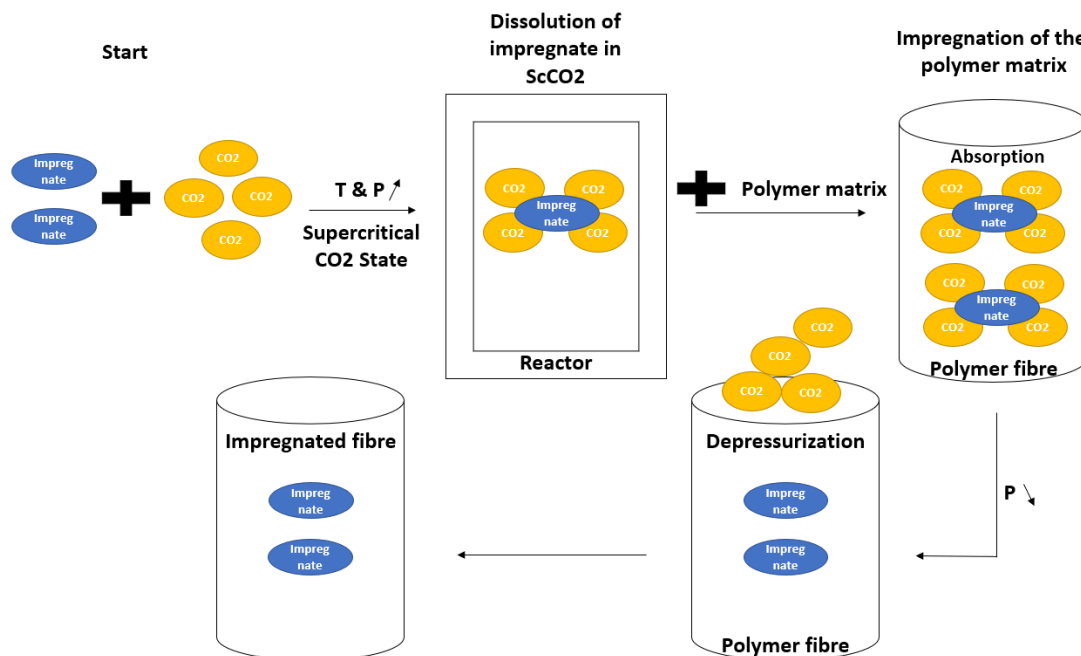
Figure 5: Schematic overview of the impregnation mechanism using ScCO2

2.1.1.4 CO_2

The use of CO_2 has a couple of advantages over the more conventional hydrocarbons useful for the foaming process. CO_2 offers: a low toxicity, low cost, non-flammability, environmental sustainability and chemically inert conditions. In addition, more than 90% of the introduced amount can be recovered, which reduces the total production cost and is favourable in terms of waste reduction. Moreover, other organic solvents have higher critical values and viscosity and a lower diffusivity in comparison to CO_2, making the dissolution of CO_2 molecules into the polymer matrix more efficient in the latter. In terms of solubility of the desired impregnates in CO_2, its solvent character is comparable to that of a hydrocarbon solvent like n-hexane. Nonpolar molecules like dyes will disperse easily and have a high solubility, polar compounds on the other hand are poorly soluble [12], [13].

2.1.1.5 Foaming or blowing agent

Naturally, a foaming agent is needed to realize the actual expansion of polyolefins. In section 2.1.1.1, a gas (CO_2) was used to simplify the process, but in general there is a wide range of foaming agents available on the market. These range from chemical non soluble foaming agents such as azodicarbonamide, to volatile physical foaming agents such as CO_2-and N_2-gas. The foam application defines the used type of foaming agent. If high production rates of foamed particles and low foam densities are desired, the volatile foaming agents yield a lower processing cost following the use of a continuous extrusion process (see section 3.2). Densities of 50-200 kg/m^3 are reached, which is way below the range of the chemical blowing agents giving a range of 400-700 kg/m^3 and lower production rates [14].

In conclusion, CO_2 plays a dual role being the plasticizing agent at the preliminary stage of the process, and a foaming agent during the main stage of the expansion. Before the foam-inducing pressure drops, the raw material is plasticized by means of exposure to the initial pressures of carbon dioxide. This exposure provides a total and homogeneous plasticization of the polymer matrix. As a result, the gas is a determining factor of the cellular structure, expansion ratio, and crystallization parameters of the resultant foams [4].

2.1.1.6 Dispersion agent

Lastly, the formed beads can agglomerate as a result of the Van Der Waals attractions between the polymer chains being larger than the electrostatic repulsion between those chains. To counter this agglomeration, a dispersant or dispersion agent is added. Dispersants lead to a certain form of steric hinderance and electrostatic stabilization, preventing agglomeration. In polymer processing, the sterically hindered dispersion agents are favoured. All dispersants consist of an anchor and buffer or head and tail to couple and prevent coupling to the particles.

Generally, steric dispersants rely on two main aspects to ensure proper functionality. First, their head should guarantee a strong anchoring to the particles. Secondly, the tail should be long enough to prevent the particles from agglomerating following the van der Waals interactions. Moreover, the tail should have a certain solubility in the surrounding polymer matrix as it acts like a molecular spring. If these dispersants were not added, the agglomerated foamed particles could give problems during the following processing steps, i.e. the moulding process. In addition, these larger agglomerates would reduce impact resistance as they concentrate stresses and act as flaws. Subsequently, the cracking of moulded products appears near these agglomerates of smaller particles after impact. A more in-depth overview of dispersants and their mechanism is given by [15].

An example of dispersants used during polypropylene processing are organosilanes. Both functionalized and unfunctionalized organosilanes cannot react with polypropylene because of its inertia, thus resulting in only dispersion taking place by means of the long hydrocarbon chain. Following the mentioned reasoning for steric stabilization, an alkyl dispersant tail suffices for polypropylene as it is compatible with the polymer. A schematic representation of the dispersant and its protective mechanism is given in figure 6.
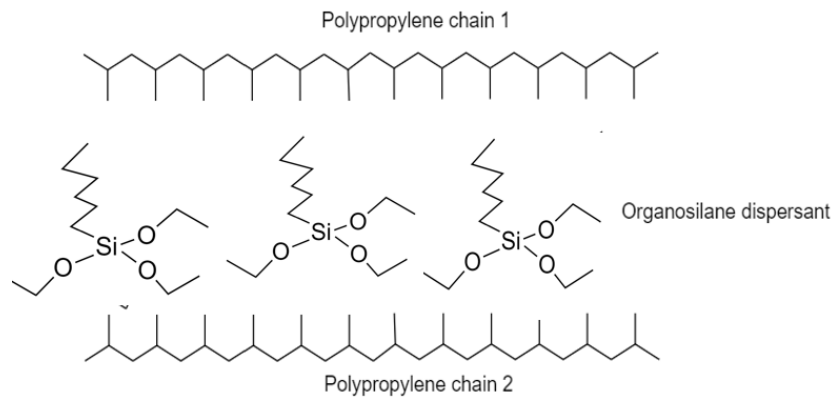
Figure 6: Functioning of Organosilane as a steric dispersants

2.1.1.7 Uncertainties

The past decades brought many research efforts focussing on the effect of plasticization on foaming polymer parts. In particular, its influence on the mechanical characteristics of synthesized or modified materials. However, besides empirical data related to foamed polymer behaviour, the formation process is still far from being fully understood as the occurring physical processes are complex and the transition between different steps of the expansion process are still hard to examine. For example the transition of cell birth or nucleation into cell growth in the plasticized polymer is a complex process, still providing many uncertainties [5], [3].

2.1.2   (dis)Advantages & Possibilities

A first difficulty of the particle foaming technique lies in the nature of the base components of foaming itself. PP is a semi-crystalline polymer, resulting in a higher difficulty in controlling the cellular structure of the formed foam. This higher level of difficulty is due to the fact that the gases used for expansion do not dissolve in the crystalline regions, creating a non-uniform foam. Furthermore, cell nucleation will also happen in an inhomogeneous way because of the heterogeneity of PP. Secondly, pure polypropylene cells usually exhibit a poor melt strength. A low melt strength results in weaker cell walls, which in their turn result in a possible rupture of the cells during the foaming process [5]. To improve these properties, efforts were made to optimize the foaming process enhancing the EPP's properties and improving the cellular structure. Like mentioned is the implementation of CO_2 or other hydro carbons beneficial for the polymer's properties following the plasticizing effect. Moreover, adding other components to the pellets could give new possibilities for the future. Two examples of improvements are the addition of peroxides and fluoro-elastomers. Furthermore, the addition of a LCB can improve the melt strength massively.

2.1.2.1 Addition of Peroxides

A possible opportunity or consideration to make in the future is to add a percentage of peroxide, which could influence the mechanical and morphological properties of the produced materials. Results described in [16] indicate that adding an amount of peroxide to the polymer mixture (here being a mixture of PP/EPDM) could induce crosslinking, which results in a higher density of the end-product and a higher melt strength. This higher network density results in fewer solvent molecules being able to get in between the macromolecules to drive them apart. Apart from this higher cross-linkage is an increase in peroxide concentration also

resulting in an increased tensile strength and elongation. However, if the peroxide concentration surpasses a certain percentage, a continuous decrease in both properties is found, which could be attributed to the fact that a higher availability of free radicals also results in a higher degradation of the PP (see section 2.2.2). An in-depth review of the influence of peroxides on propylene degradation can be found in [17]. Moreover, the decrease can also be explained by an inextensibility of highly cross-linked rubbery particles and a deterioration of the interface interactions between the these rubber particles and the polymer matrix. Lastly, the viscosity decreased with increasing peroxide percentage. This phenomenon could be explained by the absence of coagents in the used matrix, which provide ionic as well as covalent crosslinks. Without these coagents, the degradation of the molecular chains increases with increasing peroxide content leading to lower viscosities [16]. The question still remains whether this small percentage of peroxides will have the same crosslinking effect on a pure PP blend as a deterioration of the PP material is more likely. In [18], there is stated that low-temperature decomposing peroxides and dialkyl peroxides result in a free-end long-chain branching of the PP. This branching provided an improved strain hardening as seen by the elongational viscosity, which is further discussed in section 2.2.1.3. Furthermore, this PP-branching is more efficiently done using electron beam irradiation resulting in the addition of an LCB [19].

2.1.2.2 Addition of Fluoro-Elastomers

Besides adding peroxides to the mixture, the addition of a fluoro-elastomer (FMK) could also be beneficial as it enhances the diffusion of CO_2 into the polymer matrix. Moreover, adding FMK could result in a smaller cell size, higher density and a more uniform cell size distribution leading to an improved tensile and compression strength and a favourable expansion ratio. Finally, FMK possesses a great chemical and weather resistance, has flame retardant properties and has a high melting point, all features favourable in the end product [20].

2.1.2.3 Long chain branching of the base polymer

Finally, the addition of long chain branches (LCB) to the starting PP-base polymer in the recipe has a major influence on the foamability of polypropylene. Like previously discussed is standard PP a convenient base component for foaming providing favourable mechanical and chemical properties. However, the low melt strength and fast crystallization provide difficulties in terms of the cellular foam morphology and foam properties. The addition of a LCB introduces the strain hardening effect into the recipe resulting in a higher melt strength and difference in crystallization speed due to a decrease in cell rupture and a change in relaxation mechanism. A more detailed examination of long chain branching the PP and its influence on foaming properties is given in section 2.2.1.3.

2.2 Polymer Degradation During Extrusion

In general, reprocessing (non)-recycled polypropylene is inevitably accompanied with degradation, crystallization and processability problems. Degradation results in a decrease in tensile and impact strength, while crystallization on the other hand increases the Youngs modulus. In addition, reprocessing results in a decrease in viscosity of the PP-mixture which changes its processability in comparison to virgin material. Therefore, it is of scientific and technological importance for the recycling and reprocessing of PP-waste to form a good understanding of the degradation, crystallization, and processability of the material.

During the first part of the process, extrusion and pelletizing are the main contributors in the degradation of the used polymers. The main degrading processes are the thermal and mechanical mechanisms both being examples of chemical ageing of polymers. These

phenomena are elaborated, focussing on the influence of degradation on the polymer during its production and lifespan. Furthermore, only structural changes at macromolecular scale can induce dramatic consequences on the mechanical properties. As maintaining stable and beneficial mechanical properties is the company's main goal in terms of having full control over their process, this study only covers those chemical ageing processes. The most common influencing factors are the process temperature, the oxidation time or the amount of dissolved oxygen in the molten polymer matrix and the amount of shear put upon the polymer. Favourable extrusion parameter settings result in more beneficial end-properties, for example the mechanical strength and optical properties, as well as a better further processability. Moreover, degraded polymers could even cause stoppages in the extruder [21]. Many quantitative methods have been developed to determine the amount of degradation in polymers after extrusion.

2.2.1 Parameters Influenced by Degradation

A quantification of the amount of polymer degradation can be done by doing an examination of the polymer's most profound parameters over time being: the tensile strength, elongation, viscosity, compression strength and density. All these properties are related to the molecular structure of the polymer. In short, having a great knowledge of this structure unveils its properties. Three common polyolefin characterization techniques are used to define this microstructure: the molecular weight (distribution), the chemical composition distribution and the long chain branch distribution.

2.2.1.1 Molecular weight & Molecular weight distribution (MWD)

The molecular weight of a polymer or macromolecule resembles to the sum of the atomic weights of all present molecules in the molecule, which is in its turn the relative mass of an atom of the elements present in the molecule. Hence, it is expressed in g/mol. Moreover, the parameter is mostly used to determine the composition of the elements in the molecule and represents the length of the molecular chain for polymers, which can be automatically coupled to the degradation (see section 2.2.2.1). In our case, this degradation of the polymer will be directly linked to a change in mechanical properties of the produced foamed particles, which should be minimized to form a stable foamed product. Therefore, it is important to characterize and track this parameter.

The MWD on the other hand is a representation of the distribution in molecular weight of polymers present in the polymer matrix itself. Like all three polyolefin characterization methods, this model is based on the equation of the general distribution for the microstructure of polyolefins. This general distribution of the chains is a function of the length of the chains, the comonomer fraction and the amount of long chain branches (LCB) per chain. The exact equation and its derivatives is given by [22]. Stating that linear chains are used and integrating the general equation over all monomer compositions finally gives an equation corresponding to the MWD, the so called Flory's distribution. Dependent on the used catalyst can the MWD curve also be formed out of a combination of Flory's distributions. A conventional measurement for the MWD is using gel permeation chromatography (GPC see section 2.2.3), which expresses the value in a log scale.

The polymer matrix is often a mixture of several polymers with different molecular weights. In addition, the same type of polymer could differ in molecular weight. The importance of the MWD lies in the processability of a polymer. The wider the MWD, the easier the processing. A more narrow MWD results in a better performance of the polymer in terms of properties, but makes processing harder [23]. Figure 7 gives an example of a MWD curve constructed with GPC. In terms of the desired product, a constant MWD for the PP is desired giving both great

26

mechanical properties and making processing relatively easy. A shift to lower values would result in great processability, but a reduction in properties of the PP and should be avoided.
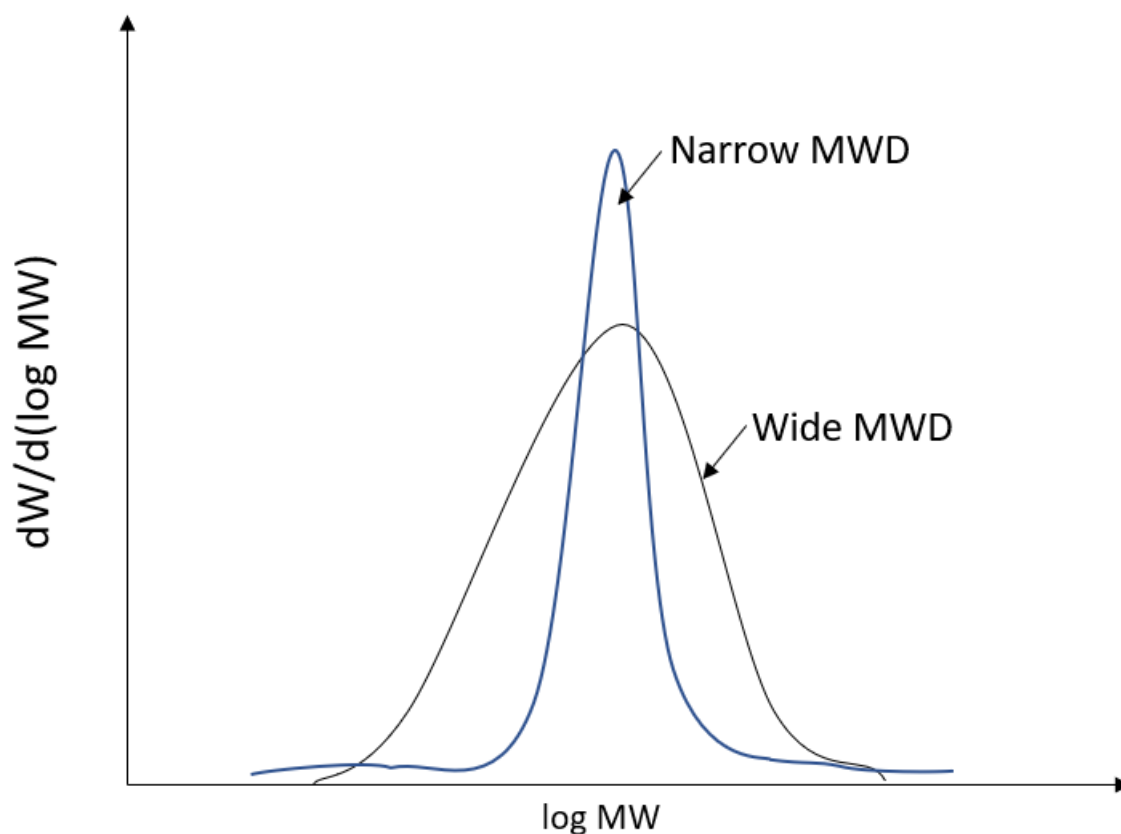
Figure 7: MWD curve of two different samples

2.2.1.2 Chemical Composition Distribution (CCD)

The CCD represents the distribution of chemistry across the chains and its calculation is again based on the equation of the general distribution for the microstructure of polyolefins. A derivation of this equation is done, resulting in the Stockmayer's distribution equation given by [22]. Based on this equation, the CCD curves for polyolefins can be constructed following different instrumental methods. Given the CCD curve, a sequence distribution of the copolymers is received looking at the width of the peaks. A random or alternating configuration of the copolymers resembles to more narrow peaks, more broad peaks on the other hand resemble to a more blocky sequence distribution. This is because the long blocks of the same comonomer increase the intermolecular heterogeneity. In contrast, longer chains and a higher MW result in more narrow and higher peaks, while shorter chains result in a broader CCD. Following this reasoning, the CCD could give an indication of a decrease in chain length as well as a change in chemical structure of the samples during the experimental work. Figure 8 depicts the essence of olefin copolymer microstructure by comparing the CCD curves of two different samples. In this curve, the β stands or the blockiness and an increase in τ results in a decrease in chain length. Similar to the curves constructed for the MWD, a weighted superposition of all curves is to be taken if multiple-site catalysts like the heterogenous Ziegler-Natta catalysts are used.
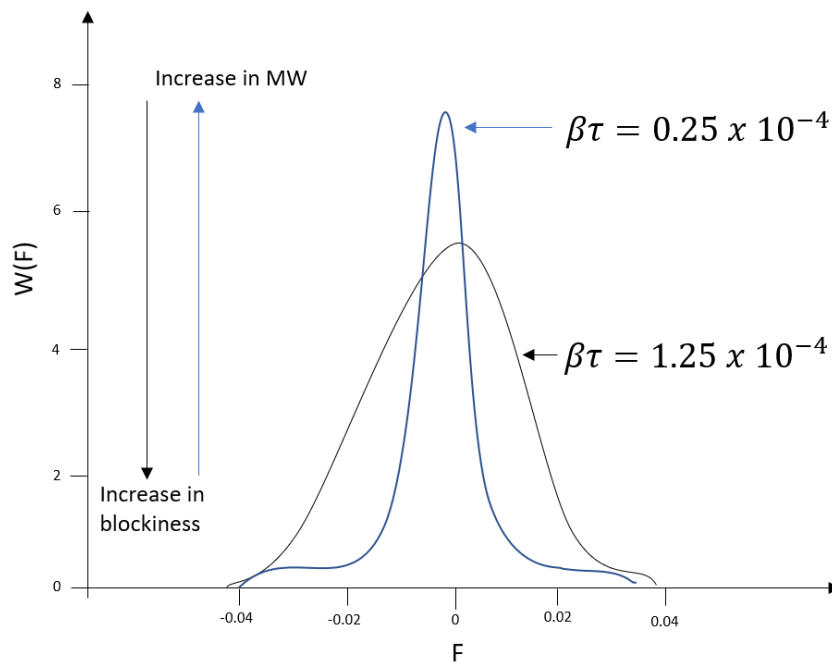
Figure 8: CCD curves of two samples based on the of Stockmayer's distribution equation

In general, a higher percentage of copolymer results in a higher amount of branching and a decrease in crystallinity due to an increase in distance between the chains. A more in-depth analysis as well as the constructed equations backing the generated curves are given by [22]. Moreover, this article gives a wide variety of examples, equations and plots to elaborate more in the CCD topic.

If this reasoning is applied to a PP-based copolymer, which often uses C2C3 as a copolymer in industrial applications, a higher amount of PE comonomer would result in a reduction of the crystallinity and therefore causes both the crystallization and the dissolution temperatures to be lower than the one in a PP homopolymer [24]. However, if on the other hand a PP homopolymer has to be characterized, one should discuss the tacticity, stereo sequence distribution and amorphous fraction. It is known that the stereochemistry or tacticity of the polypropylene backbone is directly related to the crystallinity, which influences in its turn other mechanical properties. Isotactic PP possesses a higher degree of crystallinity than atactic or syndiotactic PP. Furthermore, the distribution in stereo sequence has to be discussed as well. Most commercially produced PP grades are highly isotactic, however they can be manipulated by adding more atactic chains to the blend resulting in a decreased crystallinity. The stereochemistry is mainly influenced by the ligand of the used catalyst for polymerization and the growing polymer. The most recent stereochemistry trends and catalyst developments are depicted in [25].

The CCD will not be discussed any further during this thesis due to the given polymer recipe being confidential and not having the equipment available for these measurements.

2.2.1.3 Long chain branching

Like mentioned in section 2.1.2.3, the addition of LCBs to the recipe is a major influencing parameter during the foaming of PP. A LCB changes the chemical structure of the PP matrix, thereby changing the important foaming properties, respectively the elongational properties of the melt during expansion and crystallization properties, for the better. This change is by means of the strain hardening effect.

The strain hardening effect is increases the strength and stiffness of the material in the orientation of its deformation. As a result, it is seen in the viscosity curve means of a rise in elongational viscosity and zero shear viscosity. A difference in relaxation mechanism of the branched molecule results in a slower relaxation of the melt, thus resulting in a slower relaxation process [26]. Like described by [27], a higher amount of entanglement of the PP hinders the main chain's lateral motion causing it to relax by sliding along its own contour following a snake-like movement, the so called reptation mechanism. The PP chains are confined to a tube-like region by their entanglements, enlarging the relaxation time in comparison to the non-entangled state [28], [29]. A schematic representation of this tube-like behaviour of standard entangled PP is given by figure 9.
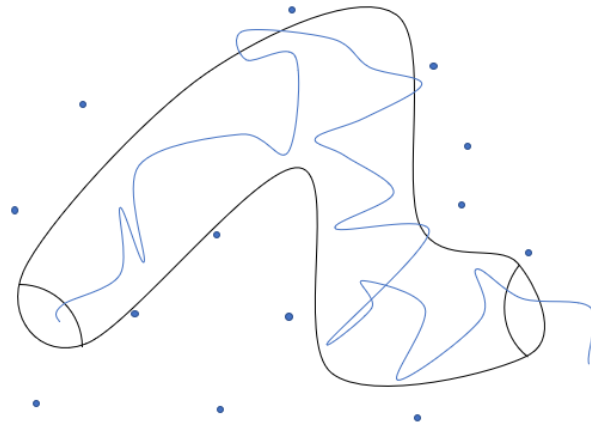
Figure 9: PP chain is constraint in a tube-like manner in a melt by other chains (small circles)

However, the addition of a LCB hinders this reptation and a retraction of the long chain branch is first needed before the reptation can take place. A reconfiguration of this dangling arm occurs many times before the relaxation of the deeper segments can take place, as seen in figure 10. The mechanisms of reptation, retraction and the overall constrained relaxation are greatly visualized by [27], [29] and [30]. Now, by restricting the movements of the chains, the deformations by means of elongational stress are restricted, hereby enlarging the total elongation before breaking and increasing its ability to "stretch" [31]. Furthermore, instead of a brittle breakage, the material becomes more ductile.
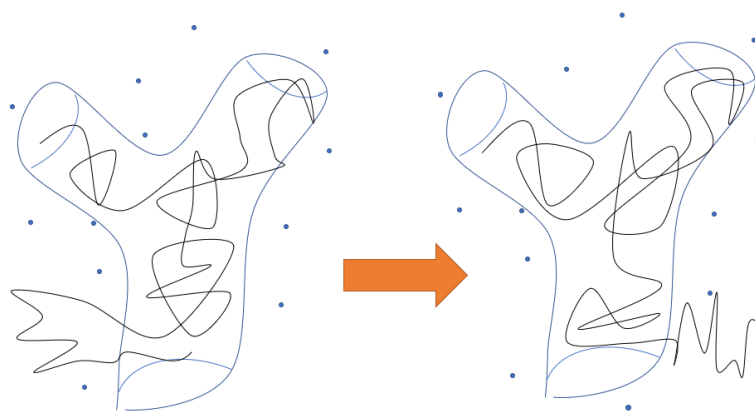
Figure 10: Schematic of the arm retraction mechanism of a LCB

In doing so, the LCBs protect the cell walls from rupture during the bubble growth of the foamed particles as this is an extensional process. Moreover, the strain hardening improves the dispersion between the cells and widens the processing window, as demonstrated by [32].

Figure 11 compares the rise in elongational viscosity of linear PP to that of a long chain branched PP at different extensional rates ($\dot{\varepsilon}$). Although different PP grades with different zero elongational viscosities are used, a rise in elongational viscosity is clearly visible in the curve of the branched PP. A more in-depth analysis of the used model (being the 'pom-pom'-model) and the corresponding equations is given by [33].
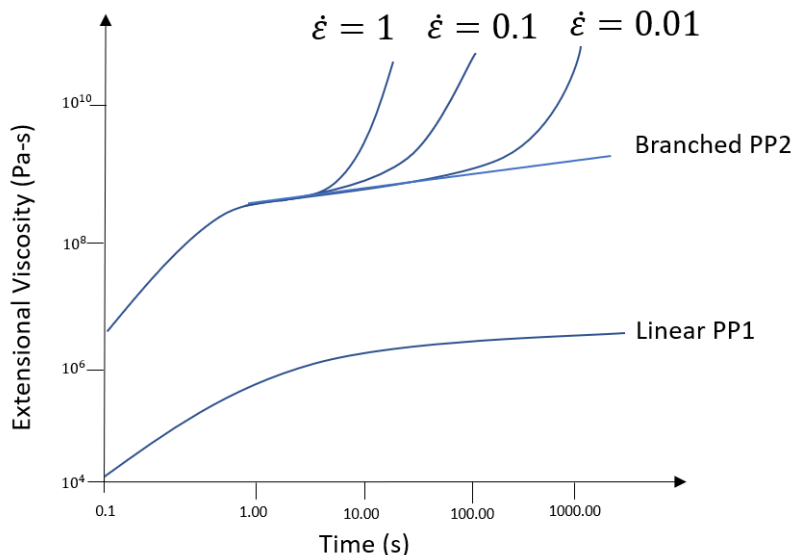
Figure 11: Comparison of extensional viscosity of linear and branched PP at different extensional rates

Finally, the addition of more LCBs per PP chain makes the MWD shift towards higher values as the longer branches have higher average lengths. Moreover, the CCD curve also becomes narrower as a result of these longer chains. The equations resembling to influence of the amount of LCBs per chain on the molar and mass fractions are discussed by [22], in combination with the expression for the long chain branch distribution in a simplified way using figures. The LCB distribution can be measured using a SEC, while the overall average LCB for the full polymer can be measured using rheology and NMR measurements. A SEC measures the intrinsic viscosity as a function of the molecular weight. By comparing the intrinsic viscosity of the branched molecule to the one of a linear molecule of the same MW, the relationship between the viscosity branching index and the MW is found, ultimately giving the LCB content via the Zimmer-Stockmayer equation [34].

Given the fact that adding (extra) LCBs to the recipe was not within the scope of this thesis, this route will not be further elaborated in order to obtain a better melt strength and elongational properties and improve the overall expansion process.

2.2.2 Degradation mechanisms

Like mentioned above, the main degradation mechanism of polypropylene is the β-chain scission initiated by thermal oxidation. The mechanism causes a modification in chemical structure and molecular weight of the polymer resulting in a change in mechanical and rheological properties. Beta-chain scission is the more dominant degrading reaction in PP-extrusion due to the fact that the PP-backbone contains a tertiary carbon which is prone to hydrogen atom transfer (HAT). HAT results in the formation of a PP-macroradical at the tertiary carbon, which precedes the scission (see 2.2.2.1). Furthermore, chain degradation by shear generated in the extruder and UV radiation are also discussed [35].

2.2.2.1 Beta Chain scission by Thermal Oxidation

During the chemical ageing mechanism, the polymer chain bonds are broken and shortened. Different scission mechanisms exist, of which the β-scission is the one most applicable for PP. Chain scission is a radical mechanism initiated by a free radical, which can originate from different sources. Generally, the free radical is passed on to the main chain by means of breaking the tertiary carbon-hydrogen bond, also known as the HAT mechanism. Subsequently, the chain is broken in two parts following the β-scission mechanism. The amount of scissions of the main chain increases by increasing the number of reprocessing cycles, following [36] and figure 12. As the chains get shorter and their entanglement reduces, the viscosity of the polymer matrix decreases in combination with a reduction in flexibility.
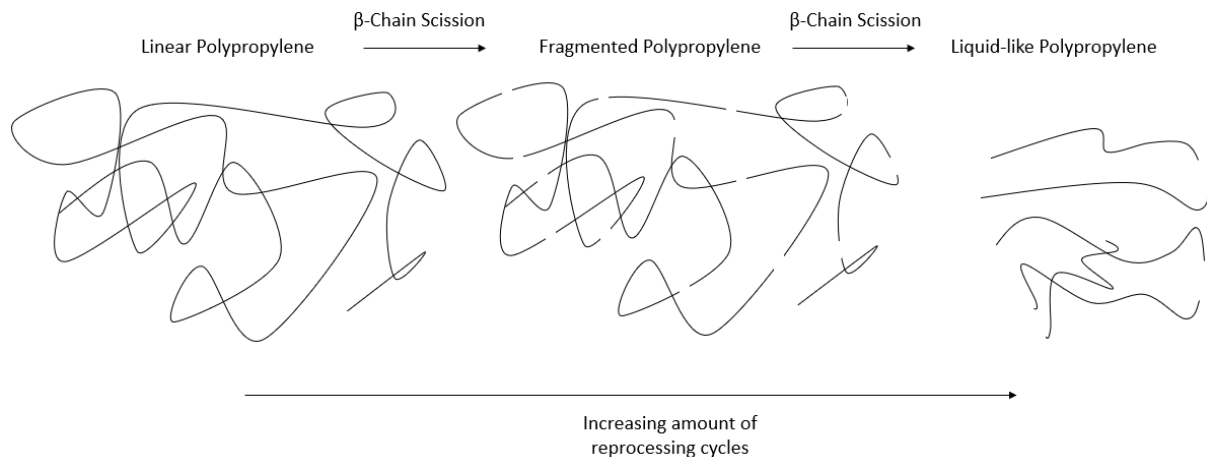
Figure 12: Influence of reprocessing cycles on linear PP

A common PP degradation mechanism caused by chain scission is the thermal oxidation process. If molecular oxygen is in a notable concentration present during the life cycle of the PP, it is subjected to a specific autooxidation cycle resulting in a structural change of the polymer. In addition, this change by oxidation could result in a change of: viscosity during processing, appearance and loss of mechanical properties such as elongation, impact strength, tensile strength and flexibility [37]. Ultimately, oxidation results in a degradation of the polymer and its properties [38], [39].

First, the autoxidation reaction is initiated by (often a combination) of light, heat, a reaction with impurities or a mechanical trigger creating a free alkyl radical by means of a homolytic scission of a C-H bond, which corresponds to the HAT mechanism. In step 2, the propagation takes place during which the alkyl radical reacts with oxygen to form a peroxyl radical. This radical is then in its turn abstracting a hydrogen from another C-H bond resulting in an ongoing degradation of the polymer. Another alkyl radical and a hydroperoxide are formed at the end of step 3. The O-O double bonds of the latter have a low bond energy, resulting in again a homolytic scission providing an alkoxyl radical and a hydroxyl radical rounding off step 5. The following and final two steps are based on the alkoxyl radical. During step 6, this radical abstracts a hydrogen from the polymer chain providing an alcohol and an alkyl radical. In the final step, this alkyl radical can in its turn react with oxygen making the circle round and resulting in the formation of another peroxyl radical [35]. A schematic overview of the thermal oxidation mechanism is depicted in figure 13.
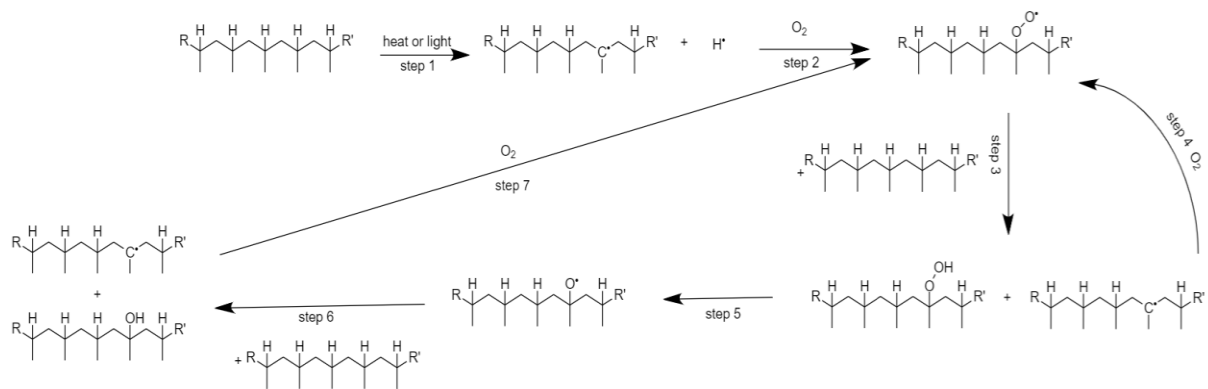
Figure 13: Thermal oxidation mechanism of PP

Finally, the chain scission mechanism causes the molecular weight distribution (MWD) curve of PP to shift away from its original position according to the extent of the degradation. As mentioned, is chain scission resulting in a fragmentation of polymer chains, which makes the MWD-curve shift towards lower values [40]. These lower values correspond to an easier processing of the material, but reduce the mechanical properties.

2.2.2.2 Mechanical Degradation by Shear

A second form of degradation occurs according to the amount of shear stress put upon the polymer matrix as a cause of the used screw and heat during the extrusion process. Following shear stress, mechanical degradation of the polymer takes place resulting in shortening the polymer main chains [41].

Generally speaking, the shear rate (γ) and shear stress (τ) are directly related to the shear viscosity, which is in its turn related to the flow behaviour of fluids [42]. Figure 14 depicts four possible models providing the flow behaviour of fluids. It is known that PP experiences a shear thinning effect caused by a disentanglement of its chains under flow resulting in a drop in viscosity [33]. Sufficiently high shear rates cause a full disentanglement of the polymer, resulting in an independency of viscosity regarding shear rate. The same goes for sufficiently low shear rates as they are not mobile enough to disentangle. The typical dependency of the viscosity to shear rate is depicted in figure 15, including the zero-shear viscosity and infinite-shear viscosity [43].
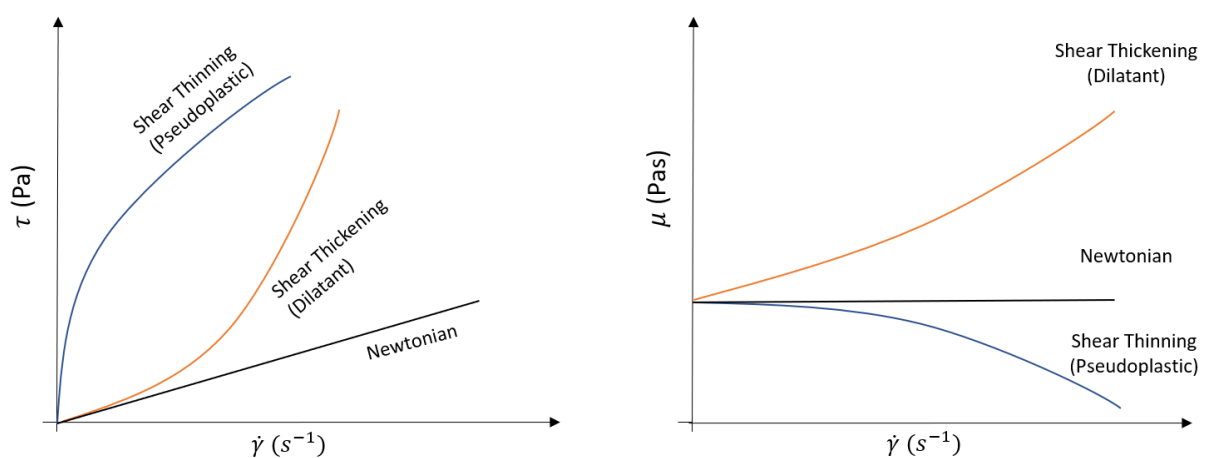
Figure 14: Correlation between shear rate, shear stress and viscosity in different fluids

The shear rate is expressed in reciprocal seconds (s^{-1}) and is calculated based on the velocity and shear gap. The shear stress on the other hand is calculated based on the shear force and shear area, expressed in Pascal (Pa). It is the force acting tangentially on a surface and actively present during extrusion [42]. Next to shear stress are perpendicular forces on surfaces also applied during extrusion, when forcing the extrudate through a die. These stresses are the so called normal stresses and are applicable when viscoelastic materials are deformed. Moreover, there is always a state of three-dimensional deformation, which can be explained using a three-dimensional Cartesian coordinate system [44]. During high shear rate extrusions, the ratio of these stresses could reach a value of 10 or higher, resulting in a fracture of the melt and a deterioration of the polymer. On top of the shear rate, the molecular weight, pressure, use of additives and fillers and temperature also influence the progress of the viscosity.
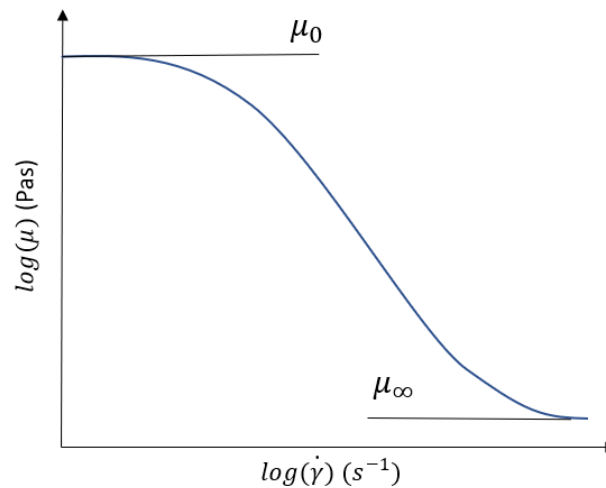
Figure 15: Correlation between shear rate and viscosity in polymer melts

Applying this knowledge to the extrusion process, an increase in rate of shearing (i.e. a faster extrusion through a die) corresponds to a lower viscosity due to a disentanglement of the chains. Thus, higher shear rates facilitate polymer flow through the extrusion die. Using a single screw extrusion setup, shear rates of 200 s^{-1} are found at the wall and shear rates of up to 1000 s^{-1} are found near the die. One can see that by increasing the shear rate, the extrudates become more and more distorted and their surface quality changes from smooth to sharkskin and finally the melt fracture state. This last melt fracture phase corresponds to a degradation of the polymer matrix. A combination of the shear stress at the wall and at the die results in a faster degradation process and a lower final viscosity at equilibrium [45].

2.2.2.3 Degradation by Light and UV radiation

A final degradation mechanism can be found in photodegradation [46]. Continuous exposure to sunlight or UV-radiation causes the chemical bonds in the PP to break. This breakage causes cracking, colour changing and ultimately a loss in mechanical properties [47]. Next to the effect of UV-radiation, environmental factors like contaminants, precipitations and the temperature also influence the weathering of polyolefins. In addition, a polyolefin matrix only absorbs UV-radiation because of the present impurities, the formed oxidation products or the additives and pigments present in the recipe.

2.2.3 Degradation Measurements

Many methods are currently available to measure the amount of degradation experienced by a polymer matrix in case it is going through different processing steps, based on the discussed

parameters in section 2.2.1 and 2.2.2. The briefly mentioned quantification methods are elaborated in the following paragraphs in combination with ways to prevent (further) degradation of the polymer chains.

2.2.3.1 GPC Measurement for MWD

A first measuring technique is based on measuring the MWD of the sample. This MWD curve can be constructed using gel permeation chromatography (GPC), a type of size exclusion chromatography. In terms of polymers, a high-temperature SEC is used as the solubility of PP in solvent is low at room temperature due to it still being in its solid semi-crystalline state. Heating the polymer matrix up to its melting temperature breaks up the crystalline bonds and makes dissolution possible. The macromolecules are separated based on their molecular size, after being dissolved in an organic solvent. Currently, 1,2,4-trichlorobenzene or o-dichlorobenzene at 130°C to 150°C are used as solvents for PP analysis. As for the gels and specifications on the equipment, [48] gives an up-to-date overview. Furthermore, the possibilities of coupling GPC to rheological measurements are also discussed in this review. The macromolecules are moved towards the gel, allowing only the part of the macromolecules smaller than the gel's pores to penetrate into these pores. The larger molecules are excluded from the pores, passing directly through the column. The separation is completed as the larger molecules elute first. Consequently, the smallest molecules will elute last. Keeping the total weight of each measurement constant, the area under de MWD-curve is also kept at a constant value. Now, the formed fragments of chains by chain scission will be excluded from their original higher MW side and reduce the weight fraction of this higher MW-side resulting in a MWD-curve shift towards lower values [36], [49], [48]. If one is to obtain the MWD of a long-chain branched polymer matrix, the SEC-MALS method is to be explored, which has also the possibility to both quantify the LCB content and form the LCB distribution across its molecular weight distribution using again the Zimm-Stockmayer approach (section 2.2.1.3). This technique is specified in [34].

2.2.3.2 Discoloration

Polymer degradation, being a physical phenomenon, usually generates some form of discoloration in the polymer as a result of a change in chemical structure of the polymer. This discoloration can be measured by taking an infrared spectrum via Fourier transform infrared spectroscopy. Both the spectrums before and after applying heat and oxygen have to be measured to indicate changes, which can be directly related to the degradation of the polymer. Applying the oxygen and heat resulted in absorption peaks resembling to chemical structures such as -OH, C=O and C-O-C all being different from the original spectrum, as described in [50]. A more in-depth review of the thermal oxidation mechanism can be found in section 2.2.2.1.

2.2.3.3 Dissolved Gas Analysis

Like mentioned in section 2.2.2, the concentration of oxygen in a molten polymer is directly related to polymer degradation. Using a pressure reducing chamber, desorbing the amount of dissolved gas, combined to a gas chromatograph, which tracks the amount of dissolved gas, gives a quantitative analysis of the amount of dissolved oxygen in the polymer. If the volume ratio of the gasses N_2/O_2 lies around 4, the dissolved oxygen from air is not consumed by the oxidizing reaction during the extrusion process and thus degradation has not taken place. If on the other hand this ratio is greater than four, which corresponds to an increase in O_2-consumption, the oxidizing reactions progress which results in a degradation of the polymer. The N_2/O_2-ratio is related to the applied extrusion pressure. Finding the optimum is thus essential to prevent degradation [51].

34

2.2.4 Preventing Polymer Degradation during Extrusion

There are different solutions regarding a diminution of the amount of polymer degradation. A combination of techniques gives the most favourable result in terms of degradation diminution.

2.2.4.1 Decrease of Dissolved Oxygen

A first possibility for reducing the polymer degradation is reducing the amount of oxygen dissolved in the molten polymer given this reduces the amount of radicals formed by oxidation (section 2.2.2). A change in screw-type influences the amount of entrained air in the polymer. A full flight screw (depicted in figure 16) causes break-ups of the polymer. During a break-up, the solid polymer collapses and entrains an amount of air present during the plasticizing step of the polymer extrusion (step during the extrusion where in the temperature is lowered again to increase the toughness, elongation to break and chain flexibility). Thus, using a UB-screw instead of a full-flight screw decreases the amount of entrained air (N_2) in the polymer, leading to a reduction in the amount of dissolved oxygen and ultimately to a reduction in polymer degradation [51]. The change in morphology of a polymer matrix during the extrusion process using a twin-screw extruder and the different flow fields in the extruder are given in [52]. Furthermore, [53] gives a more detailed mechanism of the solid bed break-ups.
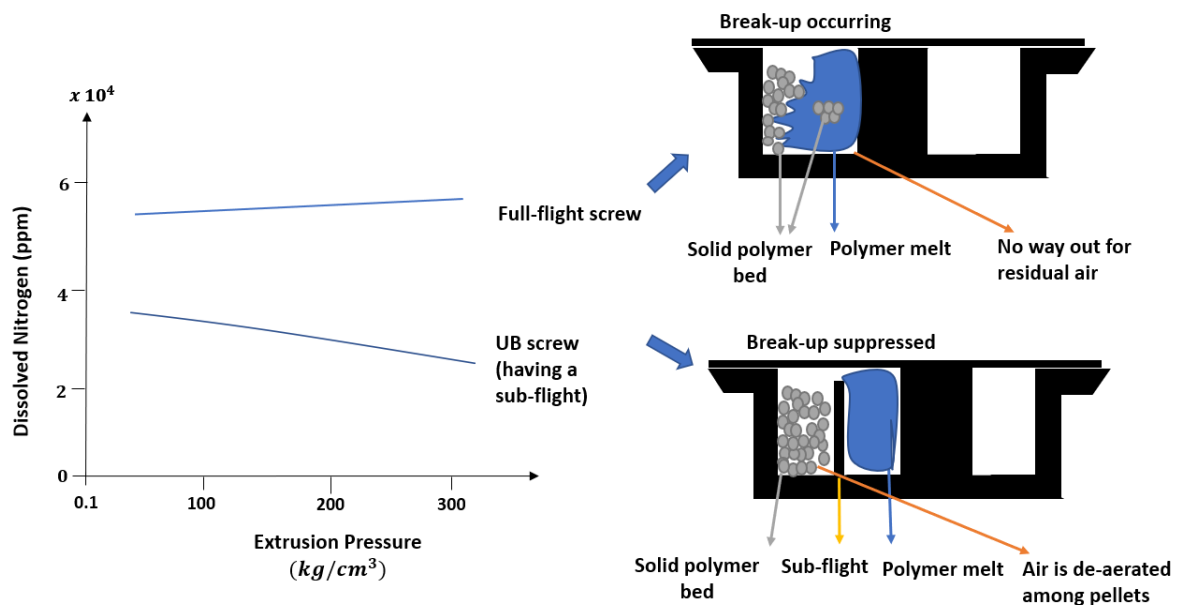
Figure 16: Amount of dissolved nitrogen related to screw type

2.2.4.2 Reducing Shear Heat

The already mentioned break-up of the polymer could also result in a pressure fluctuation within the screw channel. This fluctuation results in a decrease in screw clearance and ultimately to a local temperature increase due to the developed shear heat. Reducing the heat history, or time in the extruder, reduces the amount of break-ups and thus the amount of polymer degradation. Again, choosing the right screw type could prevent this problem [51].

2.2.4.3 Addition of Stabilizers

The addition of the correct stabilizers is often the most effective way of preventing polymer degradation during extrusion processes. A more in dept review of the useful stabilizers is done in section 2.4.

2.3 Acknowledged Info Around Reprocessing PP

Polypropylene is a widely used compound having many applications and processing ways. General PP-extrusion and the addition of a reprocessed fraction of PP to the polymer matrix has already been examined over the course of the last decade. The following paragraphs contain a brief summary of what has already been discovered and what has to be proven by experimental work.

2.3.1 Degradation

The researched PP was submitted to multiple extrusion cycles, studying the grade of degradation in the material. One could conclude that under the condition of lower temperatures (240°C) in the die zone and a small amount of extrusion cycles (five), the PP still maintained several entanglement points, and the mechanical chain breaking (or chain scission) did not reach a level of extensive degradation. In contrast, a die zone at a higher temperature (270°C) and more processing cycles (nineteen cycles) resulted in a massive increase in chain scissions. Moreover, material started behaving as a liquid due to a decrease in viscosity, achieved through a considerable reduction of molar mass, long chains and entanglements all mainly caused by chain scission [40].

Further research showed that the degradation process reduced the break properties of PP, for example strain at break, stress at break, and energy to break. Yield stress and yield modulus on the other hand were just slightly affected, having even the possibility to rise due to crystallization. Next to chain scission are high shear forces and every heating deteriorating the material [40].

In many operations, recycled PP is pelletized first in reprocessing plants by means of a heating cycle. The extruded pellets are then delivered to PP manufacturing plants for the production of end-products. The combination of the double heating and reprocessing causes the degradation to rise even further. If both processes could be blended into only one heating cycle, the deterioration would be minimized by decreasing the residence time in the extruder, which results in a lower overall heating of the PP. Finally, cold processes, such as shredding and crumbing, are recommended to prevent the degradation during hot processes, such as pelletizing [40].

2.3.2 Crystallization Behaviour & Mechanical Properties

In the past, the recycling process was associated with a continuous deterioration of the mechanical properties of the PP. However, [40] mimicked the procedure of PP reprocessing using repetitive cycles of injection moulding and proved that going through a smaller amount of reprocessing cycles resulted in an increase in Young's modulus and yield stress of the recycled material. This increase is a consequence of an augmentation of the crystallinity of the PP matrix. The crystallinity rose from 44.5% (in cycle 1) to 48.5% (in cycle 6). Furthermore, the crystallinity remained at 48.5% until the tenth cycle. In combination with the rise in crystallinity, the Young's modulus grew from 1700 MPa to 2000 MPa following the ASTM D638M norm. In addition, the yield stress rose from 34.8 MPa to 36.4 MPa. On the contrary, the elongation at break and fracture toughness both decreased by a larger margin due to the decrease in molecular weight and density. Like mentioned are the reprocessing cycles resulting

in a breakage of the molecular chain causing the entangled macromolecules to unbundle. These freed macromolecules can now rearrange themselves resulting in an augmentation of the total crystallinity. Furthermore, the developed crystalline segments will now hinder any further movement and rotations of the polymer chains, which increases the overall stiffness of the recycled blend.

2.3.3 Processability

Next to the degradation, crystallization, and mechanical properties of the recycled materials is the processability another important factor to determine whether the PP waste in suitable for re-use. In contrast to PE, the MFI of PP keeps at a constant value for over four reprocessing cycles after which a slight increase follows. This slow augmentation of MFI indicates that PP has good thermal stability during its lower reprocessing cycles, only really starting to degrade by cycle 5. Figure 17 depicts the augmentation of MFI for the common polyolefins following multiple reprocessing cycles.
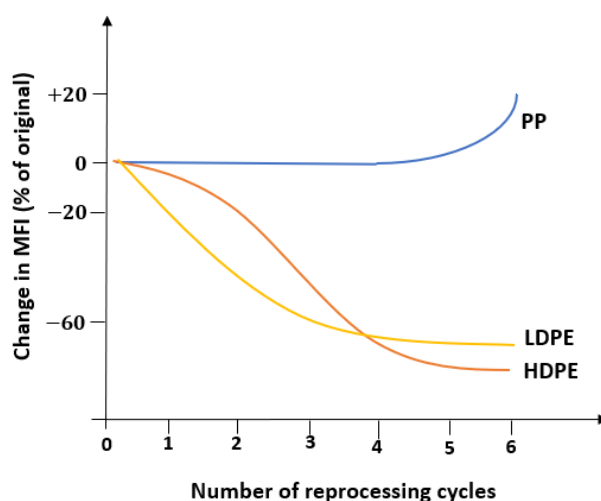
Figure 17: Change in MFI of common polyolefins following multiple reprocessing cycles

2.4 Stabilizers

To compensate for the occurring losses during mechanical and oxidative degradation, so called stabilizers are added to limit or decrease the amount of degradation taking place. Different types of stabilizers exist, each having their own use and implementation method.

2.4.1 Antioxidants

A first form of stabilizer protects polymers against the earlier described polymer oxidation. These so called antioxidants (AOs) protect the polymer chains by controlling molecular weight changes that lead to a loss of physical, mechanical and optical properties. There are two common types of antioxidants used in polymer chemistry. The first, or primary AOs, react with the formed alkoxy and peroxyl radicals and in doing so "scavenging" the formed radicals and interrupting the radical chain reactions. The majority of primary antioxidants for polymers are sterically hindered phenols and react with the peroxyl radicals to form hydroperoxides. Next to these primary AOs are there also secondary AOs available, for example phosphites and thiosynergists. These focus on reacting with hydroperoxides yielding inactive products like alcohols. By doing so, they protect both the polymer and primary antioxidant [39]. The stabilization mechanism countering the autoxidation of a polymer is depicted in figure 18.
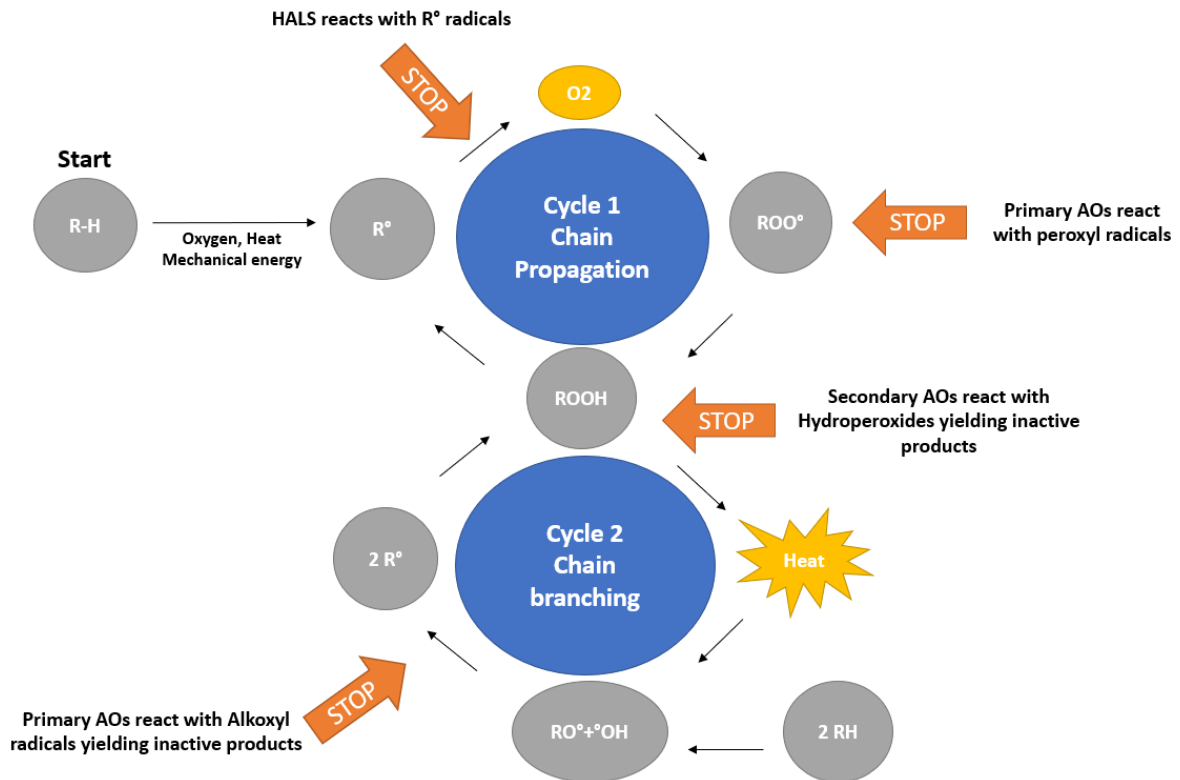
Figure 18: Schematic overview of the mechanism of AOs and HALS

2.4.2 Light and UV-stabilizers

To prevent a large degradation of the polymer by exposure to light and UV radiation, two types of stabilizers were designed to counteract the damaging effects.

2.4.2.1 Ultraviolet Light Absorbers (UVAs)

A first form of stabilizers absorbs the harmful UV radiation and dissipates it as thermal energy. The higher the concentration of absorbers, the more effective the photodegradation will be delayed. The UVAs protect: the polymer bulk, the additives in the recipe and other UV absorbing materials [54].

2.4.2.2 Hindered Amine Light Stabilizers (HALS)

The HALS, a second type of stabilizer, inhibit the polymer degradation but do not absorb UV radiation. This type of stabilizer is the more effective in polyolefin protection and can be regenerated. In the first step of the mechanism is the stabilizer used as a radical scavenger and thus preventing a further degradation of the polymer matrix. Secondly, the HALS are regenerated by reacting with a peroxyl group and transforming them back to the active form [54]. The HALS regeneration mechanism is depicted in figure 19.
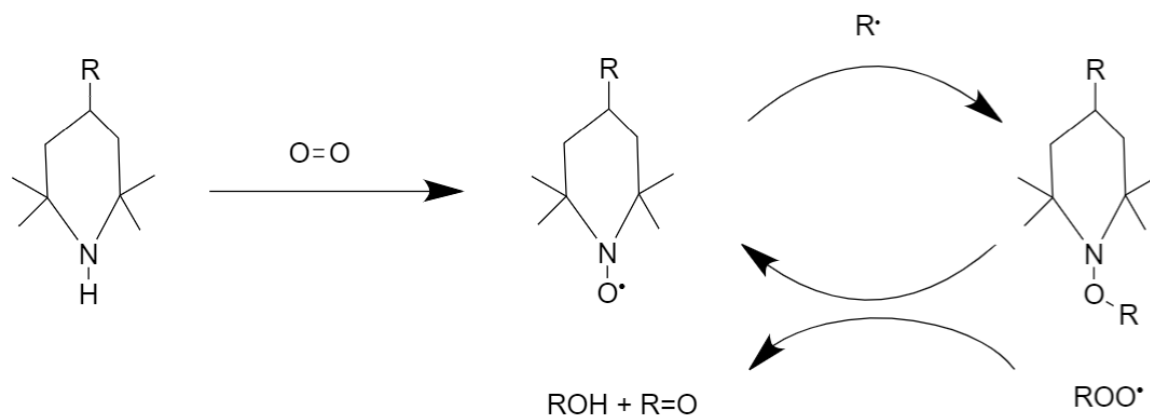
Figure 19: HALS Regeneration Mechanism

2.4.3 Loss of Stabilizers

There can be concluded from the examples of given stabilizers that most of these processing agents do not form chemical bonds with the polymers. Thus, regeneration is possible, giving no loss of stabilizer. The additives migrate in between the polymer chain. To improve their migration rate, these stabilizers need to have the correct size, diffusivity and solubility. Furthermore, additives like AOs should remain in the polymer matrix at a high enough concentration to provide a long-term stabilisation. A low rate of diffusion, a low volatility and a high equilibrium concentration ensure this stabilisation, resulting in a need for compatibility between both the polymer and additive [55].

Normally, the additive concentration in the environment is neglectable. This uneven amount of stabilizer results in a difference in the chemical potential of both the environment and the polymer solution leading to a system that is thermodynamically not in equilibrium. Hence, part of the additives tries to migrate outside of the polymer, restoring the equilibrium phase. The migration mechanism consists of a two-step process. First, the additives are passing into a medium close to the polymer surface, crossing the polymer-medium interface barrier. Dependent on which type of medium this is, an evaporation (in case of a gaseous medium) or dissolution (in case of an aqueous medium) takes place. Secondly, the molecular exchange of additives between both phases leads to the formation of a gradient of additive concentration. This gradient is the driving force of the diffusion of additive molecules. In order to minimize these losses by migration, one could increase the mass of the stabilizers by adding a long chain to the additives (see section 2.2.1.3). By doing so, the compatibility between the polymer and additive is improved resulting in a reduction in additive losses by evaporation and diffusion [56].

Chapter 3

Materials & Methods

A more in-depth overview of the different process steps is given in the following paragraphs, combined with the different parameter characterization methods. The settings of each process step did not vary as the polypropylene blend changed in composition during the multiple extrusion cycles. An overview of the different components in the recipe in combination with the different test compositions is given in section 3.1. Section 3.2 elaborates on the first two processing steps, being the extrusion and pelletizing. Furthermore, the last main processing step done on site at KB, being the expansion process, is discussed in section 3.3. Section 3.4 explains the lab-scale moulding process done at KB, being representative for the actual moulding process done by the customer for making the final products. The produced moulded test planks are then used for further characterization of the mechanical properties. Sections 3.5 to 3.7 cover these characterization techniques and the needed equipment. Finally, section 3.8 elaborates on the use of the rotational rheometer used for a further rheological characterization of the samples. Given this technique was done on campus at the Cel Kunststoffen, the whole procedure is open for public and will be thoroughly discussed.

3.1   Polymer Recipe

The main component of the polymer mixture is polypropylene. However, the raw polypropylene particles are part of a special grade to meet KB's exact standards for the foaming process. On top of the polypropylene, stabilizers are needed to limit the amount of thermal and mechanical degradation and facilitate processing. Furthermore, colour and other additives (for example a flame retardant or dissipative effect) are added in the recipe to the customer's specifications. A short overview of the general starting recipe components and an indication of their quantities is given by table 1.

Table 1: Different polymer recipes

Recipe component	Recipe A- Standard-non stabilized	Recipe B- Standard- stabilized	Recipe C- Recycled- Stabilized	Recipe D- Recycled- Recycling Stabilizer
Polypropylene grade	H	H	H	H
Colour pigment	L	L	L	L
Antioxidant	X	VL	VL	X
UV stabilizer	X	VL	VL	X
Special recycling stabilizer	X	X	X	VL
Externally recycled EPP	X	X	M	M
Expansion aid	VL	VL	VL	VL
Others	VL	VL	VL	VL

The letters used in the table give an indication of the amount of component present in the recipe. H stands for high amount, M stands for medium amount, L stands for a low amount and VL stands for a very low amount. Furthermore, if an X is appointed to the component, it is not present in the recipe. Table 1 indicates that in the recipes C and D, a medium amount of recycled EPP material is added to the starting recipe. This medium amount corresponds to 25 % of the total weight of the mixture. An overview of the total amount of external recycled fraction present in the sample after each extrusion stage is given by table 2. There should be

noted that this external recycled material is not thoroughly investigated in terms of differences in molecular structure in comparison to the standard EPP material, as it would deviate too far from the main goal of this thesis. However, a future analysis on this topic could indicate the collected differences in properties and rheology.

Table 2: Percentage of recycled material present in the blend after each extrusion

Extrusion cycle	1	2	3	4	5
Total % of recycled fraction present in the polymer blend	25.00	43.75	57.81	68.36	76.27

Furthermore, should it pointed out that the starting recipe of A does not include any stabilisation. Moreover, recipe D replaces the antioxidants and UV-stabilizers by a newly made recycling stabilizer to compare its effect on degradation to that of the standard stabilizers. Finally, a small amount of expansion aid was added to each recipe, which enhanced the solubility of inorganic compounds in the blend [57]. The exact amount of each component, as well as the supplier of the components and component types are confidential. An analytical balance was used to weigh all recipe components, followed by mixing all ingredients by hand to form a uniform blend. There is an extra condition regarding the timing of the addition of stabilizers, which will be further discussed in section 3.2.

3.2   Extrusion & Pelletizing

To portray the influence of multiple extrusion cycles on the mechanical and degradation properties of the material, it is important to fully understand this processing step. A schematic overview of the extrusion and pelletizing process is given by figure 20, adapted from [58].
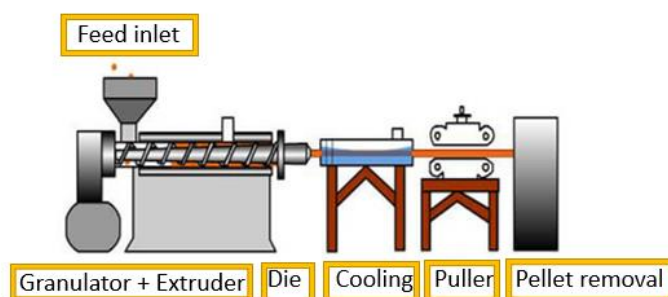
Figure 20: Extrusion process

First, a mixture of components, according to the defined recipes, is introduced via the feed-inlet of the extruder and the extrusion process starts. The whole mixture is molten during its movement through a twin-screw extruder, which gradually decreases the temperature until the melt reaches the die. The polymer matrix is pushed through this die, forming long polymer strands in the process. The strands are cooled in a water bath at room temperature before being cut into pellets of a specific size. A rotational cutter was used during this process to provide the correct length of pellets. The same strand pulling speed was used for all recipes and blends, resulting in representable pellets. The first part of the research, being the effect of multiple extrusion cycles on non-recycled material, uses recipe A end B as a starting point for characterization. The produced amounts of pellets of these two recipes before each extrusion step are portrayed by table 3. Moreover, this figure also indicates at which point an (additional) amount of stabilizer was added by means of indicating it with a yellow colour.

Extrusion cycle number	1	2	3	4	5
Recipe A: Non Stabilized (kg)	120	80	48	24	8
Stabilization at cycle 5 (kg)					8
Stabilization at cycle 4 (kg)				16	8
Stabilization at cycle 3 (kg)			24	16	8
Stabilization at cycle 2 (kg)		32	24	16	8
Recipe B: Stabilization at cycle 1 (kg)	40	32	24	16	8

First, 120 kg of recipe A was made (red), which does not contain stabilizer. This large amount was necessary given it needed to fulfil three roles. 8/120 kg of extruded pellets was kept aside for further testing and expansion. Every red arrow in the scheme represents a quantity of 8 kg kept aside for testing. In addition, 80/120 kg was processed by the extruder a second time still following the "Non Stabilized" line. The remaining 32 kg was stabilized (stabilizer was added before extruding it a second time) and is the starting point for the "Stabilization at cycle 2" line. After adding the stabilizer, the second extrusion cycle starts. Extrusion produces roughly 32 kg of stabilized pellets, of which 8 kg is kept aside for testing and 24 kg is processed once more by the extruder for cycle 3. This trend keeps going on until the end of cycle 5 is reached for every line given in table 3. All the obtained material after cycle 5 was subjected to the extrusion process and its subsequent degradation 5 times.

Secondly, 40 kg of recipe B (green) was made which includes stabilizers from the start. This recipe followed the same pattern as recipe A. Again, the recipe was put 5 times through the extruder, keeping 8 kg aside for testing after every extrusion cycle. Third, this pattern of extrusion for recipe B was repeated in combination with adding an additional amount of stabilizer after each extrusion cycle. In concrete words, a proportional amount of stabilizer was added to the 32 kg of pellets formed after cycle 1 before extruding them a second time. After cycle 2, another proportional amount was added to the 24 kg of pellets. This trend goes on until the end of cycle 5 is reached.

Recipe C follows the same pattern of extrusion as recipe B. A schematic overview of their extrusion amounts and stabilizer addition is depicted in table 4.

Extrusion cycle number	1	2	3	4	5
Recipe C: Addition of		24	18	12	6

standard Stabilizer at cycle 1 (kg)	30				
	=	=	=	=	=
Amount of standard material (kg)	22.5	18	13.5	9	4.5
	+	+	+	+	+
Amount of fresh recycled material added (kg)	7.5	6	4.5	3	1.5

The starting amount for this recipe is 30 kg. This 30 kg consists of 22.5 kg of standard stabilized material, which is in essence equal to the base recipe B. Furthermore, a fraction (7.5 kg) of external recycled EPP material is added to this fresh amount resulting in 30 kg of material. This amount is put through the first extrusion cycle. After the extrusion, 6 kg is kept aside for further testing and expansion, again represented by the red arrow. Similar to recipe B, this pattern was repeated once more in combination with adding an additional amount of stabilizer after each extrusion cycle.

Finally, the extrusion trajectory applied to recipe D is identical to the one of recipe C. The only difference is the type of stabilizer used in the recipe, which is again proportionally added to the recipe amount. Table 5 gives a schematic overview of the extrusion trajectory of recipe D.

Table 5: Recipe amount and stabilizer addition of recipe D

Extrusion cycle number	1	2	3	4	5
Recipe D: Addition of standard Stabilizer at cycle 1 (kg)	30	24	18	12	6
	=	=	=	=	=
Amount of standard material (kg)	22.5	18	13.5	9	4.5
	+	+	+	+	+
Amount of fresh recycled material added (kg)	7.5	6	4.5	3	1.5

Implementation of the different extrusion trajectories provides the samples needed to determine the impact of this processing step on the degradation and flow behaviour of the pellets.

44

3.3   Physical Expansion

Being a time consuming step, there was no possibility to expand every test batch (8 kg kept aside during extrusion) of pellets for further mechanical, rheological and DSC measurements. Based on the MFI results (see section 4.1 Melt flow analysis), the most beneficial pellets were chosen for expansion. A 20L autoclave reactor, CO_2, N_2, water, dispersants and wash water were used to expand the pellets into foamed particles under high pressure and temperature. A schematic of the autoclave reactor is given in figure 21 [59].
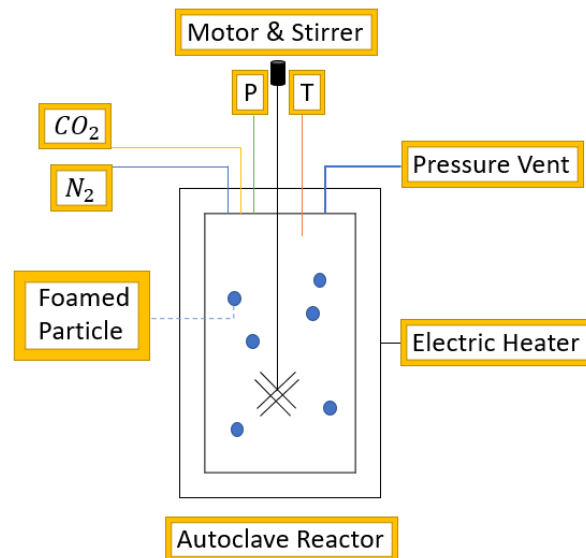
Figure 21: Schematic diagram of the batch autoclave reactor system used during expansion

The exact settings of the expansion process are confidential, however a general example of the process scheme following the physical expansion of propylene into foamed particles is depicted in figure 22.
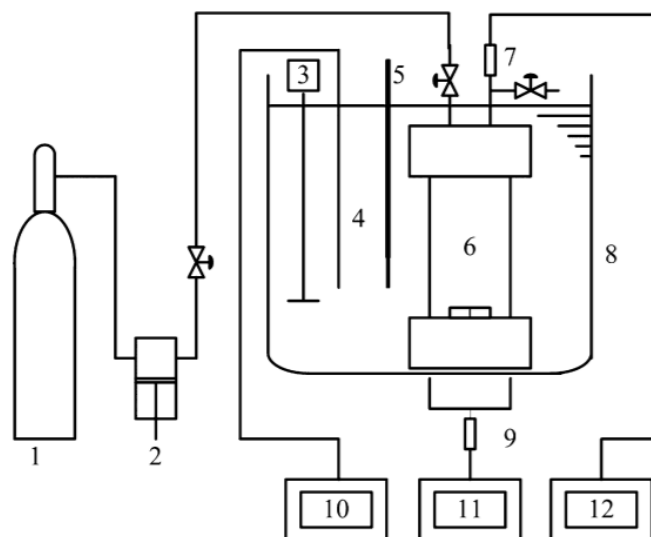
Figure 22: Expansion process equipment

In figure 22, the following components are present: (1) CO2 cylinder; (2) high-pressure liquid pump; (3) Stirrer; (4) Beckmann's thermometer; (5) mercury thermometer; (6) high-pressure

vessel with a magnetic stirring bar; (7) pressure transducer; (8) constant temperature oil-bath; (9) magnetic stirrer; (10) temperature controller; (11) stirring controller; (12) digital multimeter.

Generally, a stainless-steel high-pressure vessel, i.e. an autoclave reactor of 20 l, is used for a physical expansion. Multiple heating facilities are possible during this type of foaming process. [5] uses an electronically controlled oil bath, of which the temperature can be measured using a mercury thermometer. Using this setup, the temperature can be controlled to an accuracy of ±0.2 °C and measured to an accuracy of ±0.02 °C. The pressure monitoring in the reactor is done using a pressure transducer with an accuracy of ±0.01 MPa. For the expansion of propylene, temperatures above 140 °C and pressures around 40 bar are used. These values are obtained in the reactor following a well-controlled scheme during which the rise in both temperature and pressure happens quickly at the beginning and progresses more slowly until the desired pressure and temperature are reached. The CO_2 is loaded using a syringe high-pressure liquid pump. After reaching a temperature and pressure equilibrium (by absorption of the CO_2 in the pellets as described in section 2.1), the depressurization takes place. The CO_2 is released from the vessel using the pressure vent, causing the pressure to drop to the ambient pressure. The depressurization itself takes place in a time span of 5 to 20 seconds, in combination with a fast start of the pressure decrease after which the pressure will slowly reach the ambient pressure. Afterwards, the formed particles are dried in an oven at 80 °C and stabilized before further examination.

3.4   Moulding process

To be able to perform tensile, elongation, compression and rheological tests, the produced foamed particles first have to be moulded into test planks. Particle foam steam chest moulding is used in order to provide the needed test samples. Before the moulding process starts, the produced particles are dried at 80°C to remove any excess water, which could hinder the moulding process. The foamed particles of expanded polypropylene are first injected into a mould by means of a pressure filling. Next, steam is passed through the cavity from different angles, melting the surface of the particles and forming one larger component. An extra autoclave step is added to reach the fully molten state. Now, the cooling step takes place. Both water and air cooling are used to lower the temperature of the cavity and cool down the produced piece. The formed sample is ejected from the cavity and collected. Finally, the produced test planks are kept at a temperature of 80 °C for 24 hrs to reduce shrinkage and remove any excess water from the cooling step. Figure 23 is an example of a moulded test plank, which can be cut into the desired form for further testing.

Figure 23: Moulded test plank

3.5   Melt Flow Index

The melt flow index of the produced pellets is measured using the Instron MF20, of whom its schematic is given in the figures 24 and 25. A melt flow apparatus consists of a standard weight (2.16 kg), a piston, a die and a heater to warmup the material above its melting point. First, the heater is adjusted to the melting temperature (230°C) of standard polypropylene. Second, a small quantity of pellets (4 g) is poured into the feed inlet. Next, the piston is placed on top of the pellets. Subsequently, the weight is positioned and the test starts. The MFI is expressed as the weight of the amount of polymer flowing through a specific die geometry during 10 minutes, following the ASTM D1238 and ISO 1133 standards [60], [61].
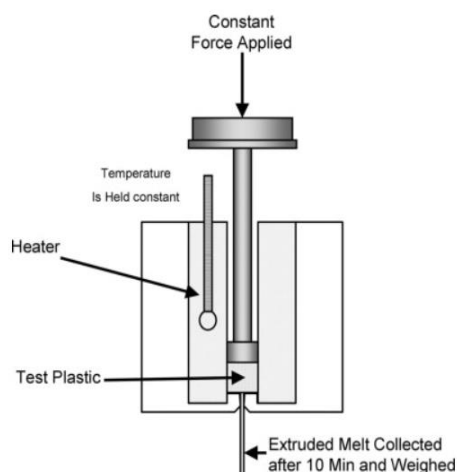
Figure 24: Schematic of a melt flow apparatus

Figure 25: Intron MF20

3.6   Differential Scanning Calorimetry

After expansion, a DSC-scan is done on the collected foamed particles. Approximately 5 mg of sample is needed per scan. The used apparatus was Mettler-Toledo equipment from the USA, of which an example is given by 26. During a DSC-scan, the energy needed to increase the temperature of a sample is compared to the needed energy for the reference sample to increase its temperature. The temperature of both the reference and sample are kept at the same level, which is compensated by a heat flux between both materials during the analysis. This heat flux

can be correlated to ongoing thermal phenomena. Furthermore, endothermic processes like melting are portrayed by downward peaks, exothermic processes on the other hand, like crystallization for instance, are portrayed by upward peaks. In conclusion, a DSC-scan provides useful information in terms of the ongoing thermal events, oxidation, thermal degradation and possible water loss. Moreover, the glass transition temperature can be determined by performing a DSC-scan [62], [63].

Figure 26: DSC-apparatus

3.7 Mechanical Tests

Once the moulded planks are produced, they are cut into the wanted samples for further testing. Both compression, tensile tests are performed to evaluate their changes throughout all the samples.

3.7.1 Tensile tests

In order to start the tensile tests, a sample in the shape of a dog bone is cut out of the moulded planks. Next, these samples are clamped between two points and a stress is put upon the sample. Following the ISO1926 norm for tensile testing, the behaviour of the polymer samples is determined after subjecting them to a tensile stress [64]. At first, the sample's dimensions are noted in the test programme followed by its weight. Secondly, the sample is fixed between the two provided clamps. Next, the test starts and the sample is tested upon breakage. The elongation at break, the tensile strength and the moulded foam density of each sample are collected from the test results. Figure 27 depicts the remains of a sample after the tensile testing.

Figure 27: Sample remains after the tensile test

3.7.2 Compression test

The compression tests followed the same line of action as the tensile tests. However, these tests follow the ISO844 norm for compression tests. The norm specifies the methods for the determination of the compressive strength and compressive stress at a certain percentage of relative deformation [65]. Furthermore, instead of using a dog bone shaped sample, cube shaped samples were used with a length of 50 mm. At first, the sample's exact dimensions are noted in the test programme followed by its weight. Secondly, the sample is fixed between two compression plates. Next, the test starts and the sample is compressed until a relative deformation of 75% is reached. The different compression stresses resembling to different percentages of deformation are collected from the test results. In addition, the moulded foam densities are also calculated by the test.

3.7.3 Density

The bulk densities of the produced foamed particles are measured using an ethanol solution, a graduated cylinder and an analytical balance. After airdrying the particles, roughly 4 g of particles are weighed on the analytical balance. Next, they are immersed in the ethanol solution, by which their volume is calculated. Dividing their mass by the volume gives the desired density.

3.8   Rotational Rheometer

The execution of a more in-depth rheological analysis of the profound samples gives a better insight on their change in viscoelastic properties, which can be linked to a form of polymer degradation. The rheological measurements were done using a Modular Compact Rheometer (MCR 302e) provided by Anton Paar and located at the lab of Cel Kunststoffen in Diepenbeek. Figure 28 portrays the used rheometer. This type of rheometric analysis is based upon correlating operational parameters, for example the present angular displacement or torque, to an imposed stress or strain in order to measure the desired rheological properties like the elastic modulus and complex viscosity. The exact technical possibilities and specifications of the rheometer are elaborated in-depth by [66]. Although this apparatus has many different characterization methods to define the polymer properties, with respect to their molecular structure and processing behaviour, there was opted to compare the samples using the Frequency Sweeps mode.

Figure 28: schematic of the Modular Compact Rheometer

By operating the apparatus in the Frequency Sweep mode, the long-and short-term rheological behaviour of the samples is investigated. Using an actively heated hood, which combines radiation and convection (using N_2) heating, the samples are first heated to 230°C, i.e. the melting temperature of standard isotactic polypropylene. Next, the measuring system moves backwards and forwards at the set amplitude (or strain γ) percentage of 1%. The angular frequency (ω), however, logarithmically decreases between high (100 rad/s) and low frequencies (0.1 rad/s). In doing so, 16 measuring points were collected and used to provide the plots of both the storage and loss moduli (G' and G") in combination with the curve representing the complex viscosity (η*). All collected data and curves are investigated in section 4.5. Furthermore, this section elaborates on the importance of these three parameters in terms of the degradation happening in the samples during the extrusion process.

A full mechanical model for the oscillatory measurements, in combination with a more detailed explanation of the used equipment and calculation methods is given by [67], [68].

Chapter 4

Results & Discussion

This chapter provides a systematic analysis of the different methods indicating a degradation of the produced samples caused by multiple extrusion cycles. Furthermore, the impact of adding an amount of stabilizer and the choice of stabilizer will be elaborated. Multiple characterization methods are used, focussing on rheology, DSC and mechanical analysis. The samples containing purely re-extruded material are first discussed in every section, after which the results of the blends with recycled material are explained. A basic rheological analysis is done at first by taking an MFI of the gathered samples and plotting the results. Section 4.2 gives an overview of the results obtained from the DSC scans, in particular the degradation temperature and crystallinity are more thoroughly discussed. Moreover, the increase or decrease in enthalpy beneath the curves is linked to the deterioration of the polymer chain. In section 4.3, the change in mechanical properties during the reprocessing is discussed, as well as the impact of adding stabilizer and/or a recycled fraction on these properties. Furthermore, an analysis of the bulk density of the produced foamed particles is done in section 4.4 to mark changes on this physical parameter. Finally, section 4.5 supplements section 4.1 with a more in in-depth rheological analysis, focussing on the change in complex viscosity and storage/loss moduli by means of an rotational rheometer.

4.1 Melt Flow Analysis

One of the most robust ways of getting an indication of the viscoelastic behaviour of a polymer or a polymer blend is by measuring its melt flow index, as explained in section 3.5. All recipes and compositions were subjected to this analysis, starting with the reprocessed products in section 4.1.1. Secondly, section 4.1.2 addresses the different trends in the blends containing the externally recycled fraction. Finally, an intermediate conclusion in terms of the rheology of the samples is given in section 4.1.3.

4.1.1 Reprocessed material

A schematic overview of the measured melt flow indices of the recipes A and B containing the reprocessed material is given in figure 29.
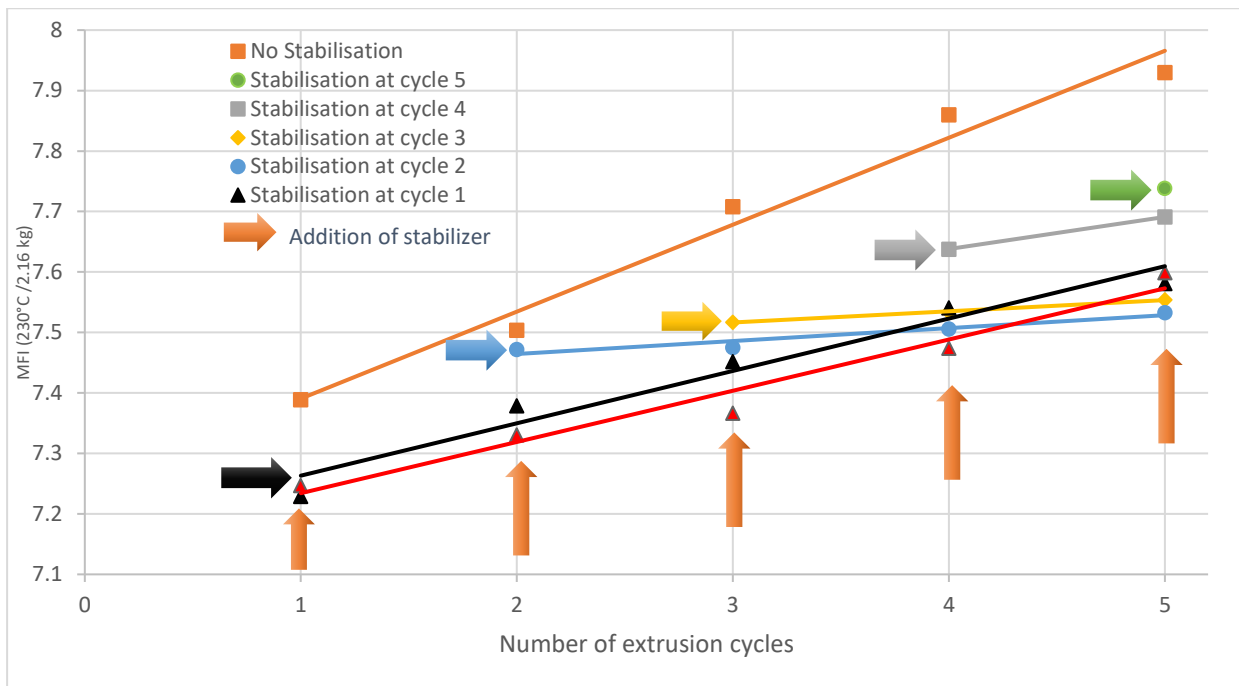
Figure 29: MFI of Reprocessed EPP with addition of stabilizer in function of the number of extrusion cycles

Like mentioned in section 3.1, the base recipe for the "stabilisation at cycle 1" and "stabilisation at each cycle" is the recipe B at which the stabilizer is added from the beginning. The other curves are based on the recipe A, adding a proportional amount of stabilizer before a certain extrusion cycle. This addition is once more indicated by the yellow colour. The exact MFI data are given by table 6.

Table 6: MFI of Reprocessed EPP with addition of stabilizer in function of the number of extrusion cycles

Extrusion cycle number	1	2	3	4	5
Recipe A: Non Stabilized MFI (g/10 min)	7.39	7.50	7.71	7.86	7.93
Standard deviation (g/10min)	0.03	0.03	0.04	0.06	0.07
Stabilization at cycle 5 MFI (g/10min)					7.74
Standard deviation (g/10min)					0.04
Stabilization at cycle 4 MFI (g/10min)				7.64	7.69
Standard deviation (g/10min)				0.07	0.03
Stabilization at cycle 3 MFI (g/10min)			7.52	7.53	7.55
Standard deviation (g/10min)			0.01	0.06	0.01

52

Stabilization at cycle 2 MFI (g/10min)		7.47	7.48	7.51	7.53
Standard deviation (g/10min)		0.04	0.05	0.06	0.04
Recipe B: Stabilization at cycle 1 MFI (g/10min)	7.23	7.38	7.45	7.54	7.58
Standard deviation (g/10min)	0.03	0.03	0.03	0.04	0.05
Recipe B: Stabilization at each cycle MFI (g/10min)	7.25	7.33	7.37	7.47	7.60
Standard deviation (g/10min)	0.01	0.03	0.03	0.03	0.04

A first influencing factor is the impact of adding an amount of stabilizer to the recipe. When comparing the MFI values in table 5 of recipe A "non stabilized" to recipe B "stabilization at cycle 1", there can be concluded that adding an amount of stabilizer before going through the first extrusion step, has a significant impact on the MFI. When excluded, the MFI rose from a value of 7.23 to a value of 7.39 g/10 min. In addition, adding the stabilizer at a later cycle instead of at the beginning resulted generally in a higher MFI after 5 extrusion cycles. For example, comparing the values from "stabilization at cycle 3" to those of "stabilization at cycle 5", an increase of MFI of 0.18 g/10 min is seen.

Secondly, the MFI values did not increase at a constant rate, but this rate fluctuated. Looking at the values of recipe A "non stabilized" and recipe B "stabilization at cycle 1", there can be concluded that the rate was high at the first two cycles, but decreased after cycle 3. However, this trend is not seen in the curve of recipe B "stabilization at each cycle", which has an almost linear increase of the MFI.

Third, adding extra stabilizer before every extrusion cycle did not have significant impact on the MFI values. A slight decrease in MFI is seen when comparing both curves of recipe B. However, this difference is nullified by cycle 5.

Section 2.2 established that a decrease in viscosity can be directly related to a decrease in chain length following the β-chain scission degradation mechanism for polypropylene, which lowers the MW of the main chain thereby lowering the viscosity. Following the established viscosity trends, there can be concluded that the addition of stabilizer minimizes this degradation, while adding extra stabilizer at each cycle might not be viable or cost-efficient. Furthermore, this degradation is at its highest rate during the first few cycles, flattening out towards cycle 5.

4.1.2 Recycled fraction

A schematic overview of the measured melt flow indices of the recipes C and D is given in figure 30. In each of these recipes, 25% of fresh recycled material got injected before each extrusion cycle started to elaborate its effect on the MFI.
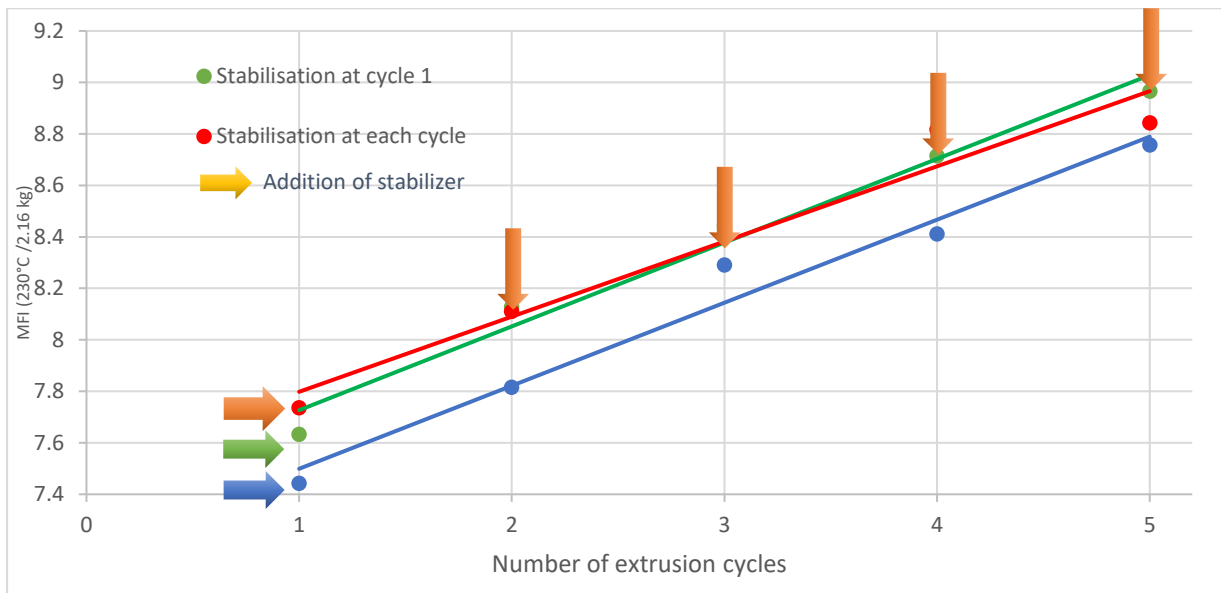
Figure 30: MFI of Reprocessed EPP with addition of 25% of recycled material at each cycle

Like mentioned in section 3.1, the starting point for making both curves of recipe C, which go by the name of "stabilisation at cycle 1" and "stabilisation at each cycle", is recipe B. However, at the start of each extrusion step 25% of fresh recycled material is added to the recipe before running it through the extruder. Furthermore, recipe D and its corresponding curve "stabilisation at cycle 1 with Recycle stabilizer" is completely analogously constructed as the "stabilisation at cycle 1" curve of recipe C, only swapping out the standard stabilizer for a new type of recycling stabilizer. The exact MFI data and their corresponding standard deviations are given in table 7.

Table 7: MFI of Reprocessed EPP with addition of 25% of recycled material at each cycle

Extrusion cycle number	1	2	3	4	5
Recipe C: Addition of standard Stabilizer at cycle 1 to recycled blend (g/10min)	7.74	8.11	8.40	8.82	8.84
Standard deviation (g/10min)	0.03	0.02	0.07	0.06	0.02
Recipe C: Addition of standard Stabilizer at each cycle to recycled blend (g/10min)	7.63	8.13	8.44	8.72	8.97
Standard deviation (g/10min)	0.05	0.03	0.03	0.06	0.07
Recipe D: Addition of Recycle Stabilizer at cycle 1 to recycled blend (g/10min)	7.44	7.82	8.29	8.41	8.76
Standard deviation (g/10min)	0.06	0.06	0.03	0.04	0.01

At first, after comparing the MFI results of both recycled recipes of C, a similar trend as before can be seen in terms of adding a supplementary amount of stabilizer at each cycle. The extra addition does not have a significant impact, as it only results in a slight decrease of 0.10 g/10 min. Moreover, an increase is seen at the end of cycle 5.

Second, based on the plots of recipes C and D, one should notice that the addition of a fresh recycled fraction causes the MFI to rise at a constant rate of approximately 0.4 g/10 min until it reaches the value of around 9 g/10 min, which is the value of the externally recycled material's MFI. The fact that the recycled material's value is reached is logical, as by cycle 5 76% of the blend's composition can be attributed to the external recycled material (following table 2).

Thirdly, adding the recycling stabilizer decreases the MFI value almost linearly by 0.3 g/10 min every cycle in comparison to the recycled blend with the regular stabilizers. However, the continuous addition of a supplementary percentage of recycled fraction before each cycle causes the MFI to increase in the long run to the value of 9 g/10 min. Both remarks could indicate that the stabilizer prevents some form of PP degradation, as it caused a decrease in MFI, specifically looking at the first 4 cycles.

Once more, the decrease in viscosity can be directly related to a decrease in chain length following the β-chain scission degradation mechanism for polypropylene as elaborated in section 2.2. Following the established viscosity trends, there can be concluded that the addition of the recycling stabilizer minimizes this degradation significantly better than the standard stabilizer, with a MFI reduction of 0.3 g/10 min. Moreover, adding extra standard stabilizer at each cycle does not cause a significant decrease in MFI. Furthermore, the rate of the degradation is not really measurable throughout the 5 cycles as the rise in MFI is mostly caused by the addition of fresh recycled material. However, the presence of degradation could be confirmed by comparing the MFI values of the recipes C and D, which indicates that recycling stabilizer works more effectively than the standard stabilizers.

4.1.3 Preliminary Conclusion in terms of Rheology

Based on the performed MFI analysis, there can be concluded that the addition of stabilizers decreases the amount of deterioration of the PP during extrusion. In addition, swapping out the standard stabilizers by the recycling stabilizer minimizes this degradation. Furthermore, repeatedly adding more stabilizers to the mixture after each extrusion cycle does not affect the MFI significantly. Finally, the addition of 25% recycled material causes a large increase of the MFI, which can be attributed to the fact that the recycled material has a MFI of 9 g/10 min and resembles to 76% of the blend composition after 5 extrusion cycles.

One should be aware of the fact that an MFI is a single point measurement and solemnly gives an indication of the melt's viscosity, rather than an exact value. While for example a capillary rheometer would give a full depiction of the relationship between the shear rate and shear viscosity, the MFI only depicts one point of that curve. Hence, section 4.5 gives a better indication of the trends in viscosity.

4.2 Degradation Temperature & Crystallinity

After expansion and the drying step, the produced foamed particles were analysed using the available DSc- apparatus. A DSC-scan was taken of a small fraction (roughly 5 mg) of these particles, which provided a schematic of their thermal history. This history ran through their first melt peak, followed by a crystallization peak and ended at the point at which the material started degrading. These graphs provided the desired final degradation temperature of the material and the enthalpy value corresponding to the height of its crystallization peak. The latter gives an indication whether the polymer chain length will have decreased after reprocessing the material.

4.2.1 Degradation temperature

An overview of the retrieved values from the scans is depicted in table 8. The non-stabilized pellets were not expanded into foamed particles, which is why these values cannot be retrieved in the table. Furthermore, only certain pellet samples were chosen for the expansion process as this was the most time-consuming step of the process.

Table 8: Degradation temperature values of the non-recycled blends

Extrusion cycle number	1	2	3	4	5	Increase or Decrease in T (°C)
Recipe A: Non Stabilized Temperature (°C)	x	x	x	x	x	/
Stabilization at cycle 5 Temperature (°C)					255.2	/
Stabilization at cycle 4 Temperature (°C)				243.5	252.8	+9.3
Stabilization at cycle 3 Temperature (°C)			247.9	x	248.2	+0.3
Stabilization at cycle 2 Temperature (°C)		249.1	x	x	x	/
Recipe B: Stabilization at cycle 1 Temperature (°C)	249.1	x	252.7	x	249.4	+0.3
Recipe B: Stabilization at each cycle Temperature (°C)	252.3	x	271.0	x	257.4	+5.1

A first noticeable trend is that the degradation temperature does not change massively over the course of the cycles. Furthermore, this change is mostly a small increase. Secondly, the addition of an extra amount of stabilizer before each extrusion cycle causes a slight overall degradation temperature increase, in comparison to only adding it before the first cycle (5.1 °C increase in comparison to 0.3 °C).

The same analysis was done considering the recycled blends. The gathered data from the scans is depicted in table 9.

Table 9: Degradation temperature values of the recycled blends

Extrusion cycle number	1	2	3	4	5	Increase or Decrease in T (°C)
Recipe C: Addition of standard Stabilizer at cycle 1 to recycled blend Temperature (°C)	249.7	x	x	240.6	241.4	-8.3

Recipe C: Addition of standard Stabilizer at each cycle to recycled blend Temperature (°C)	247.9	x	263.9	x	255.3	+7.4
Recipe D: Recycled material addition of recycling stab at start of 1st cycle-Temperature (°C)	240.9	x	242.8	x	242.1	+1.2

Once more, there can be concluded that a slight rise in degradation temperature is occurring in both the recipes of C and D. However, a decrease is found in the first recipe of C. This decrease may be caused by the continuous addition of the fresh recycled fraction, which changes the overall structure of the blend and is, when the last cycle is reached, the more dominant component in the mixture.

Generally, there can be concluded that a slight increase in degradation temperature is seen in the blends containing an extra amount of stabilizer and that its addition leads to an overall higher degradation temperature. Furthermore the addition of the recycled fraction does not change the degradation temperature significantly. The implementation of the recycling stabilizer instead of the standard ones lowers the initial degradation temperature and keeps the value constant over the different extrusion cycles.

The degradation temperature can be linked to the thermal stability of the polymer blend. A higher degradation temperature indicates a higher thermal stability, which in its turn can be linked to the point to which the PP material is able to resist the heat and maintain its mechanical properties like fracture toughness and elasticity [69].

4.2.2 Crystallinity

Next to the degradation temperature, the DSC-scans also unveiled the crystallization enthalpies of the produced particles. These can be directly related to the amount of crystallization taking place in the sample, which is in its turn relatable to the amount of degradation in the samples. The collected enthalpy values of both the recycled and non-recycled samples are given by table 10.

Table 10: Crystallization enthalpy values of foamed particles

Extrusion cycle number	**1**	**2**	**3**	**4**	**5**	**Percentual Increase or Decrease (%)**
Recipe A: Non Stabilized (MJ)	x	x	x	x	x	/
Stabilization at cycle 5 (MJ)					357.2	/

Stabilization at cycle 4 (MJ)				363.8	388.5	6.8
Stabilization at cycle 3 (MJ)			350.4	x	419.3	19.7
Stabilization at cycle 2 (MJ)		391.7	x	x	x	/
Recipe B: Stabilization at start of cycle 1 (MJ)	368.9	x	377.9	x	387.9	5.2
Recipe B: Stabilization at each cycle (MJ)	374.5	x	324.5	x	398.3	6.4
Recipe C Recycled material - stabilized at start of 1st cycle (MJ)	358.4	x	x	362.3	420.0	17.2
Recipe C Recycled material- stabilized at every cycle (MJ)	310.5	x	303.2	x	389.5	25.4
Recipe D Recycled material- addition of recycling stab at start of 1st cycle (MJ)	338.0	x	423.9	x	393.2	16.3

First, one can generally conclude that, as the recipe progressed through the extrusion cycles, its crystallinity increased. Secondly, this increase was much more significant for the recycled blends, which had an average increase of around 19% in comparison to the non-recycled blends, which only increased by an average of 6%. Third, the extra addition of stabilizer did not reduce this increase. In contrary, both the values of the non-recycled and recycled fraction saw a larger increase caused by this supplementary addition of stabilizer. Finally, the recycling stabilizer caused only a slight decrease in crystallinity increase, which can be neglected.

Following the reasoning of section 2.3, it is to be expected that a certain amount of reprocessing cycles results in the β-chain scission mechanism taking place, which breaks the molecular chains and untangles the macromolecules. However, these freed macromolecules now get the opportunity to rearrange themselves resulting in a possible augmentation of the overall crystallinity, as was also found by [70]. Furthermore, the greater increase in crystallinity of the recycled blends could indicate that a larger amount of degradation is taking place, as more macromolecules are freed from their entanglements and by doing so augment the crystallinity. However, the recycled material itself could be of a higher crystallinity or could be more prone to degradation. A structural analysis is to be done to prove these findings.

4.3 Mechanical Properties

Both compression and tensile tests were performed on the produced foamed particles following the procedures described in section 3.7. As a result, a comparison between the different samples, being samples of the non-recycled and recycled blends, can be made

regarding both mechanical properties in order to detect a change. A change in properties could indicate the presence of a form of degradation in the material. In addition, if this change is significant, it should be compared to the company's standards in order to determine if the resultant properties are still satisfactory for further processing. All produced samples were kept in an acclimated room before testing in order to reproduce the same conditions. Section 4.3.1 gives an overview of the gathered data in terms of the performed tensile tests. Section 4.3.2 on the other hand, gives an overview of the collected data from the compression tests. Finally, section 4.3.3 gives a conclusion in terms of the mechanical property analysis. All the exact data corresponding to the plots and tables are to be found in the Appendix A.

4.3.1 Tensile tests

The performed tensile tests resulted in the ultimate tensile stress and the elongation upon breakage of the samples. First, the non-recycled blends were examined. Taking into account the already established trends in the sections 4.1 and 4.2, there was chosen to only evaluate the lines "Recipe B: Stabilization at each cycle" and "Recipe B Stabilisation at cycle 1" of the non-recycled blends, as these were the most likely to indicate a specific trend. A schematic overview of the collected data in terms of the tensile stresses is given in figure 31. Figure 32 depicts the data of the elongation at break.
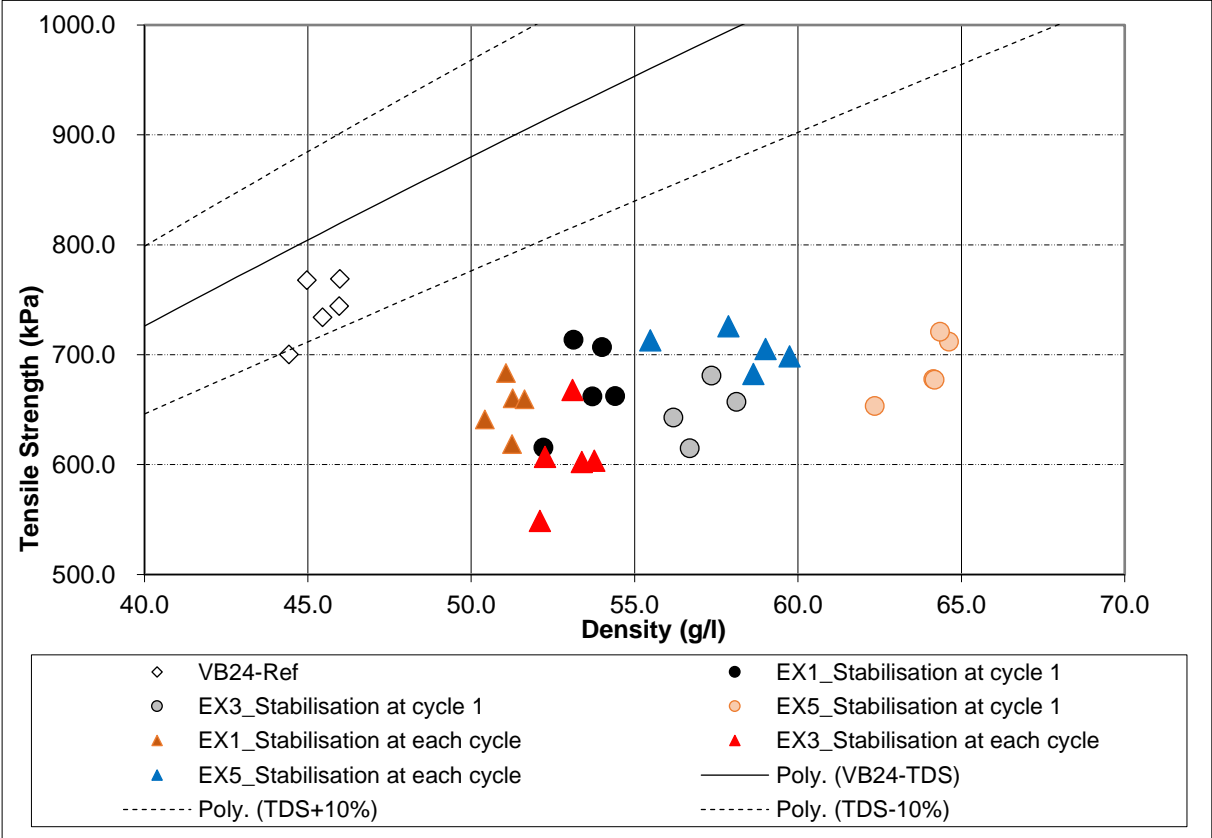
Figure 31: Non-recycled test materials vs Regular VB24 - Tensile strength (kPa)
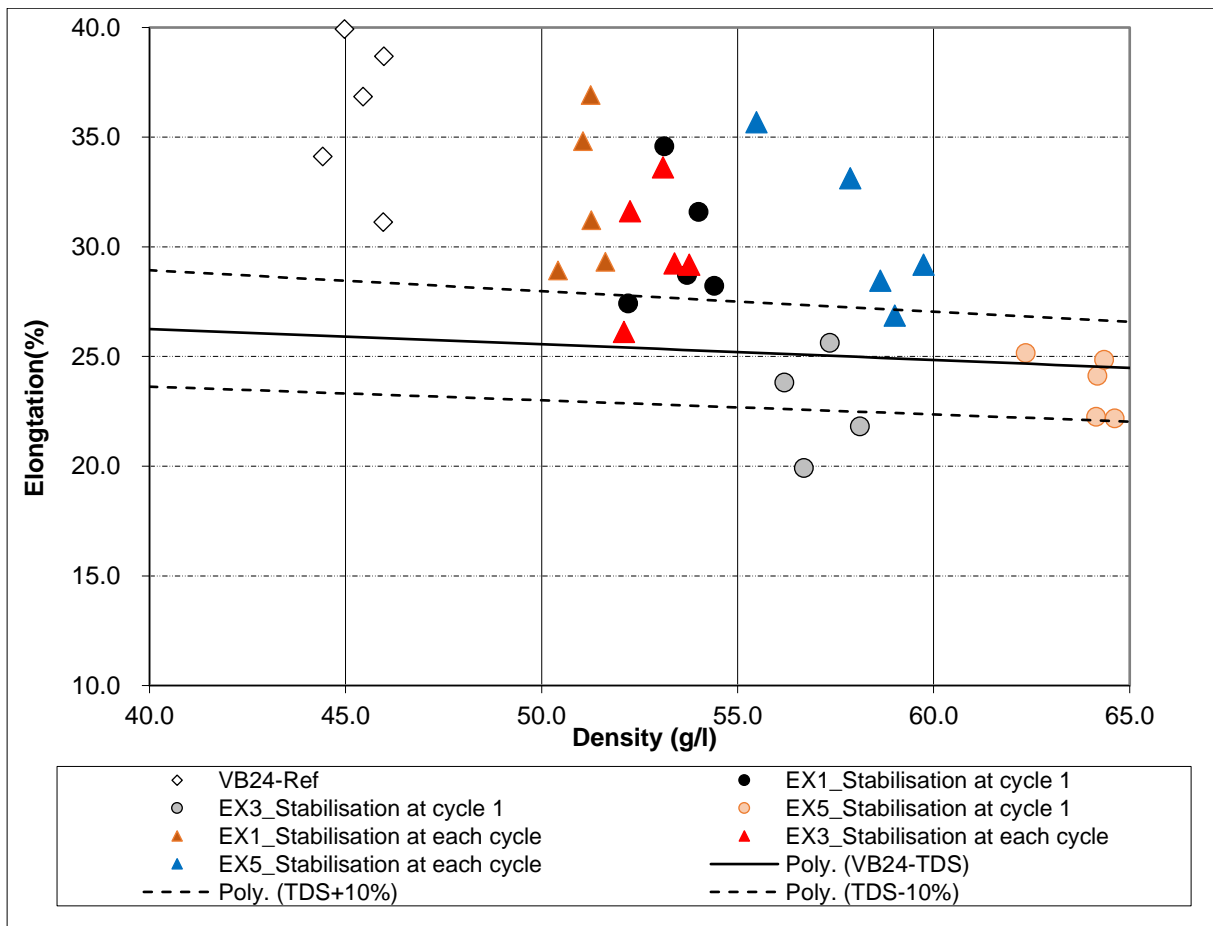
Figure 32: Non-recycled test materials vs Regular VB24 - Elongation (%)

In addition to the test samples are the values of the product grade, on which the test samples are based, also added to both plots. These originate straight from the technical data sheet (TDS) of KB. Furthermore, a 10% safety margin was added around the properties of the reference sample all in order to be able to judge the produced samples correctly.

Based on the data in figure 31, it can be concluded that, as the amount of extrusion cycles increased, the tensile stress stayed relatively identical for both sample types, with an average of 670 kPa for the "stabilization at cycle 1" samples and an average of 650 kPa for the "stabilization at each cycle" samples. When comparing all samples to the values needed to reach the safety margin of 10% of the reference sample, one can conclude that none of the produced samples reach this margin. However, the samples produced after the first extrusion of the recipe come closest to the desired values. Moreover, as the recipe content progresses through more extrusion cycles, the distance to the safety margin increases. This could indicate a form of degradation taking place in the material.

As can be seen in figure 32, one can conclude that the elongation percentage drops from an average of 30.8% to an average of 23.7% for the "stabilisation at cycle 1" samples when progressing through the different extrusion cycles. In addition, the "stabilisation at each cycle" samples also decrease in elongation at break%. When comparing the test values to those of the reference values, an overshoot is seen for the samples of the first extrusion, but as the recipes progress through the cycles, they meet the requirements of the 10% margin. Generally, there can be concluded that the elongation at break decreases as the amount of extrusion cycles increases. This could be a result of the ongoing degradation in the polymer chains, which lowers the MW and density thereby lowering the elongation at break.

60

Furthermore, the density increased with an increasing amount of extrusion cycles. However, these moulding densities were tweaked during the moulding process and cannot be linked to the exact molecular weight of the foamed particles. Normally, one would expect a decrease in density and molecular weight following an ongoing degradation in the polymer (see section 2.2.1). An analysis of the actual density of the foamed particles after the expansion is done in section 4.4.
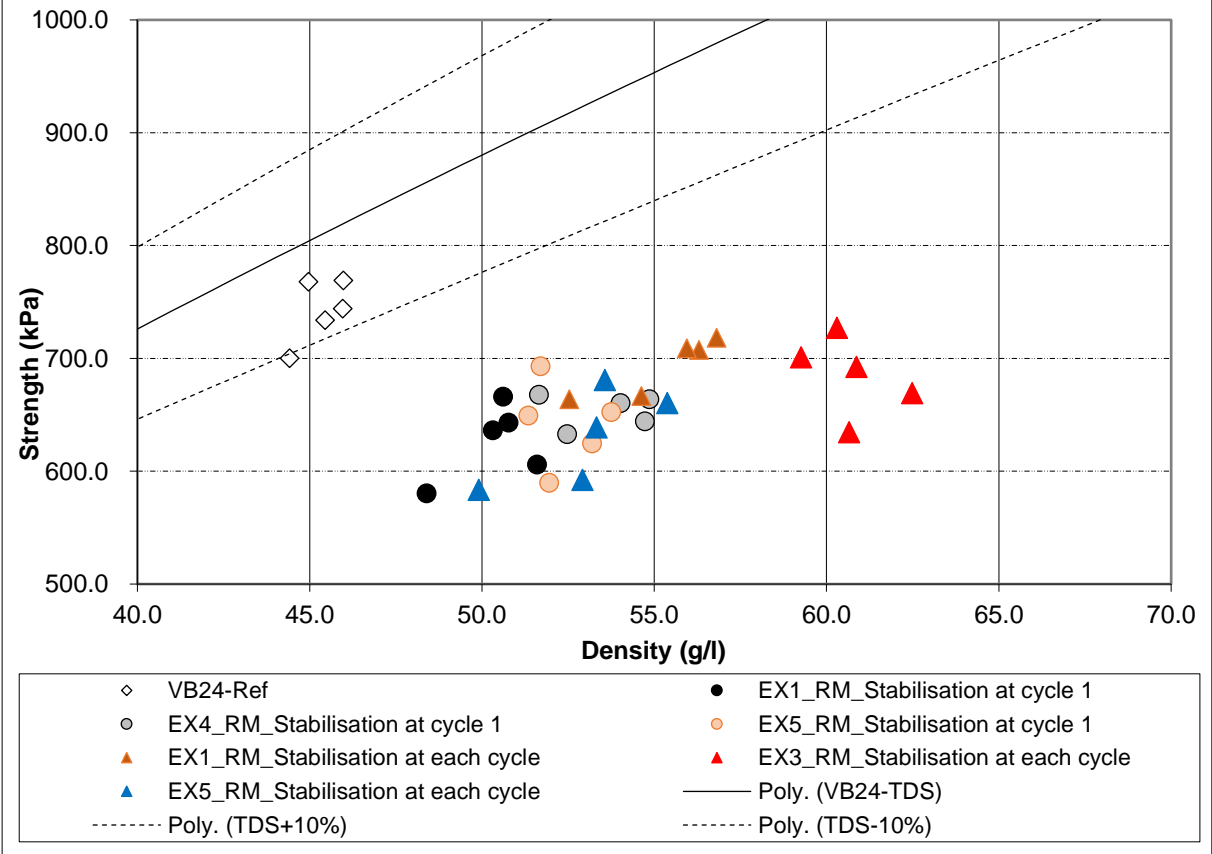
Figure 33: Recycled test materials of Recipe C vs Regular VB24 - Tensile strength (kPa)

Regarding the recycled blends, all samples of both recipe C and D were evaluated. Figure 33 and 34 give the tensile strength and elongation at break plots of both lines of recipe C (being the "stabilisation at cycle 1" and "stabilization at each cycle" line.

There can be concluded from figure 33 that the tensile stresses of the "stabilization at cycle 1" samples stayed relatively constant with an average of 640 kPa. However, the tensile strength values of the "stabilization at each cycle" samples decreased, going from 693 kPa after the first extrusion cycle to 631 kPa after the last. This decrease could again be a sign of degradation taking place. It is known that the mechanical properties of a polymer, like elongation and tensile strength, are directly linked to the polymer's entanglement density and MW [71]. Both physical parameters are in their turn related to the amount of degradation in a polymer, following the reasoning of section 2.2. A lower tensile strength indicates a lower MW and entanglement degree, which indicates that the chain scission mechanism has taken place. Again, none of the samples meet the requirements of the reference sample in terms of tensile strength, with the samples corresponding to the first extrusions approaching the desired values the most.
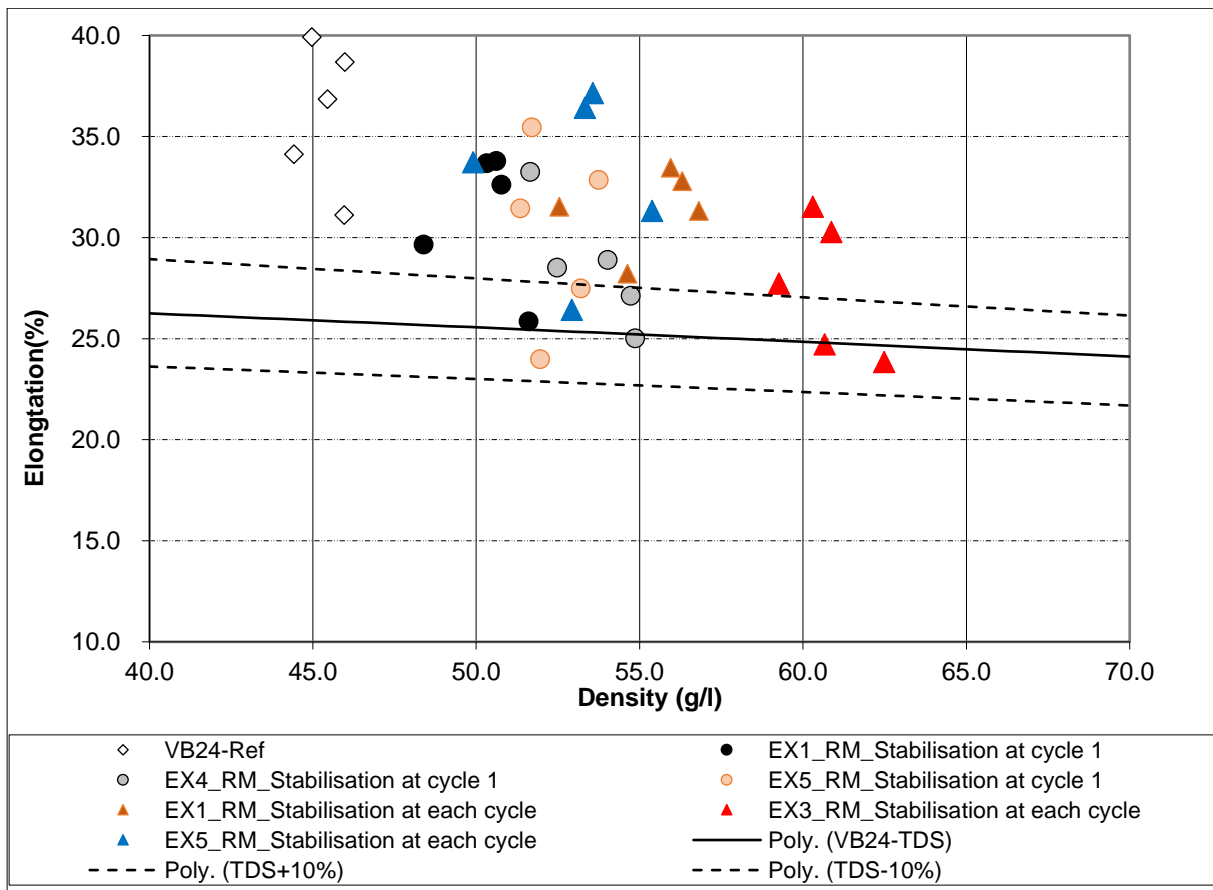
Figure 34: Recycled test materials of Recipe C vs Regular VB24 - Elongation (%)

As can be seen figure 34, the average elongation at break % of the "stabilisation at cycle 1" samples decreases from 31.1% to 30.3% when going to multiple extrusion cycles. However, this value rises slightly from 31.5% to 33.0% regarding the "stabilization at each cycle" samples. In the first case, one can apply the same reasoning as done for the non-recycled blends. However, an increase in elongation at break would indicate an increase in ductility of the material, which is a result of a higher amount of entanglements. This small rise could be the due to the effect of the standard stabilizer on the recycled material, or the recycled material having a slightly other stereo tacticity resulting in other mechanical properties. However, this small difference could also be appointed to the measurement precision of the used apparatus and may be negligible. Finally, all samples reach above the opposed 10% margin of the reference sample, which makes them suitable for further processing.
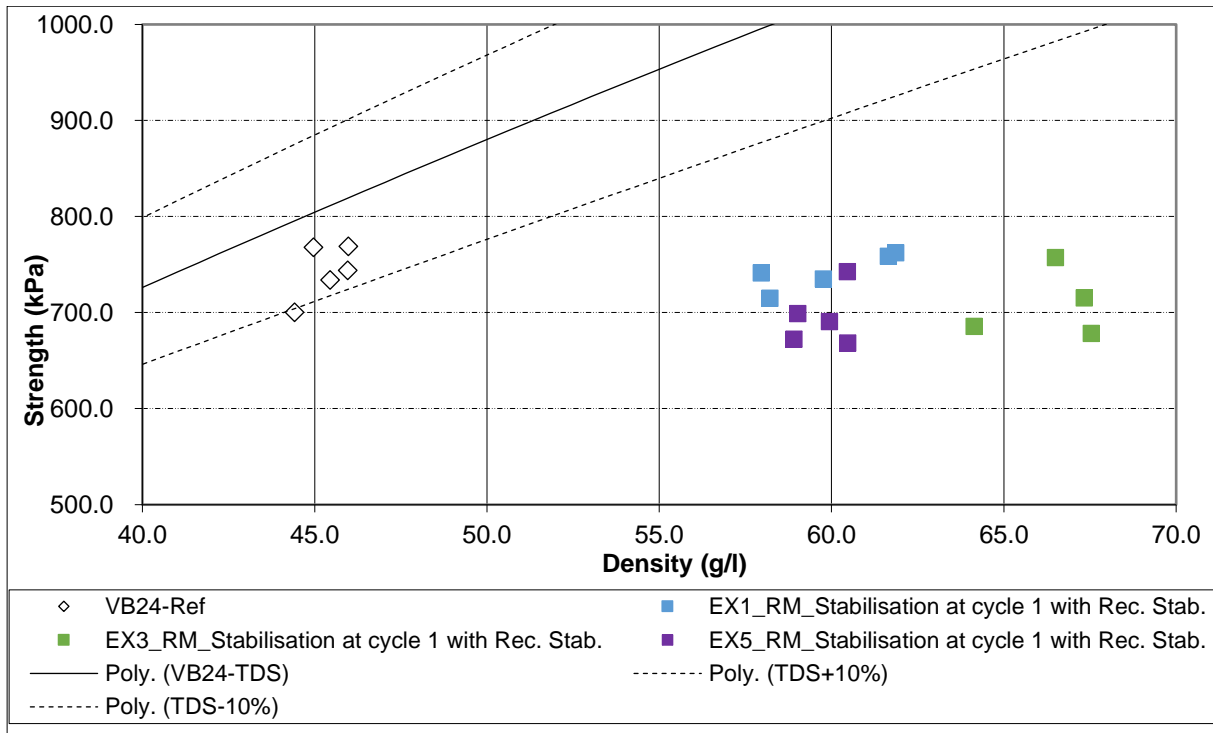
Figure 35: Recycled test materials of Recipe D vs Regular VB24 - Tensile strength (kPa)

From the plotted data in figure 35, one can conclude that the tensile strength decreases as the amount of extrusion cycles increases, which can be appointed to a MW and density decrease due to a form of degradation taking place. Moreover, an increase in elongation at break is seen in figure 36, which could indicate that the added recycled material is a more ductile material, with a lower tensile strength but more entanglements. One can notice that the elongation results of the third extrusion sample do not meet the 10% safety margin of the reference, however those of the first and fifth sample do. Furthermore, none of the samples meet the safety margin of the tensile strength plot, nor are these tensile strength values higher than the uses found with the standard stabilizer. The "Rec. Stab." corresponds to the new recycle stabilizer.
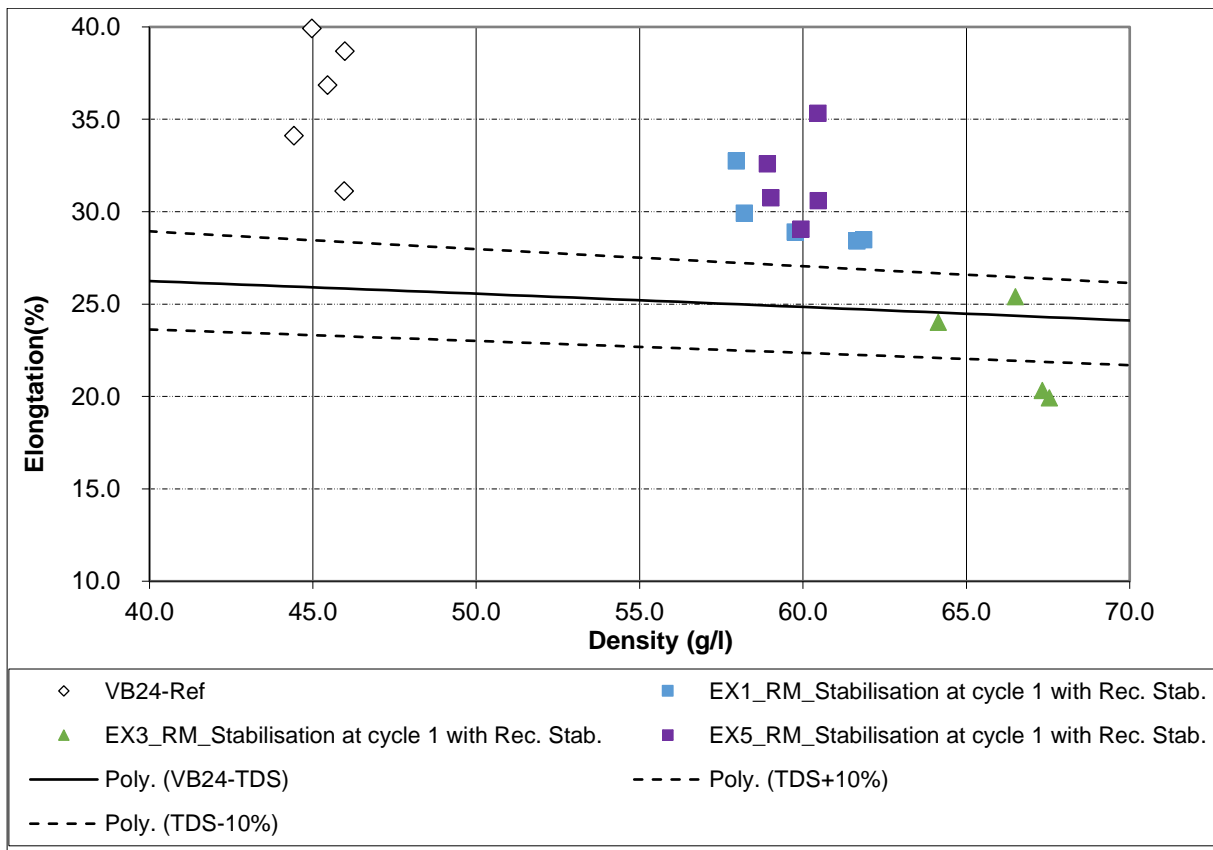
Figure 36: Recycled test materials of Recipe D vs Regular VB24 - Elongation (%)

Finally, there should be noted that after expansion, the foamed particles are normally washed in an industrial way to remove all excess dispersants (section 2.1.1.6). However, the above elaborated experimental samples were washed by hand, which does not remove the dispersants as efficient. The remaining dispersants could hinder the formation of a uniform melt during the moulding process and in doing so downgrade the mechanical properties of the formed test planks by lowering the density and increase the space between the foamed particles.

4.3.2 Compression tests

The compression strength of the samples was tested at different points of strain 75% of the samples. Figures 37 to 39 plot the values of the non-recycled blends, while figures 40 to 42 plot those of the recycled blends. Given the fact that it is hard to compare the different compression strengths as the moulded densities change as well for each line, the values are solemnly compared to the reference compression strength margins.

Based on the gathered data from figures 37 to 39, there can be concluded that only the samples of "stabilisation at each cycle" from the first extrusion lack in compression strength throughout all strain% values. Secondly, one can conclude that as the strain% increases, more samples approach the lower limit of the 10% margin. However, none of the sample averages, apart from the one mentioned, reach out of bounce. Thus, the effect of the multiple extrusion cycles on the compression strength is not significant.
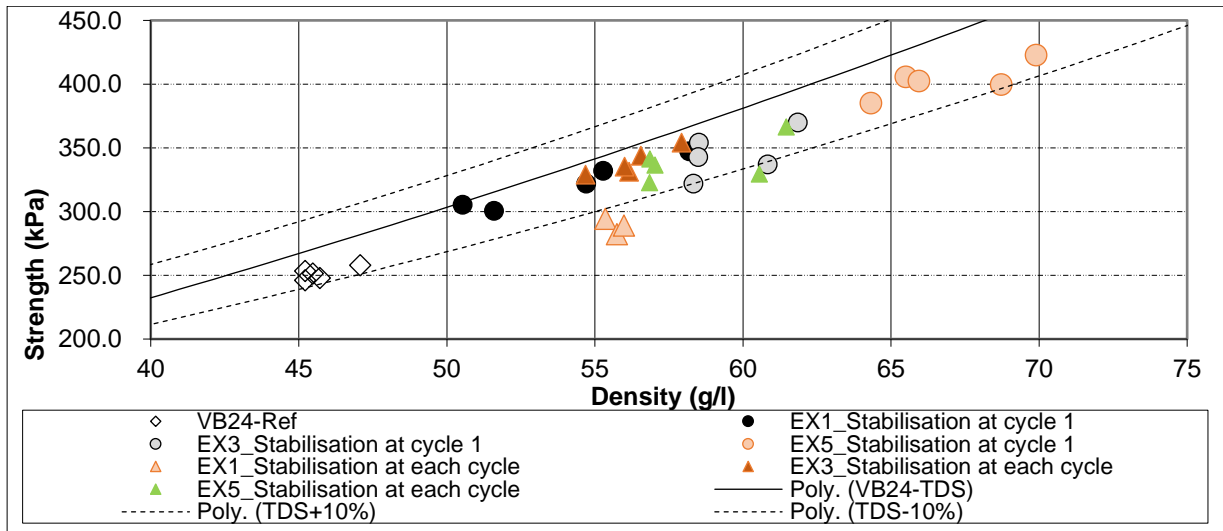
Figure 37: Non-recycled VB24 Test materials vs Regular VB24- Compression at 25% strain
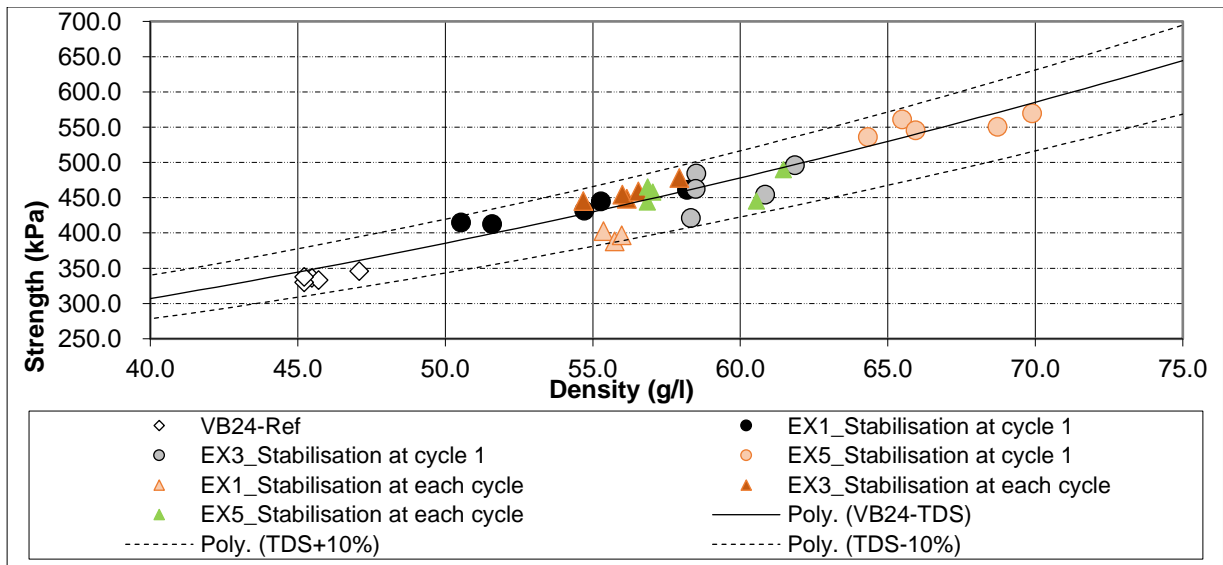
Figure 38: Non-recycled VB24 Test materials vs Regular VB24- Compression at 50% strain
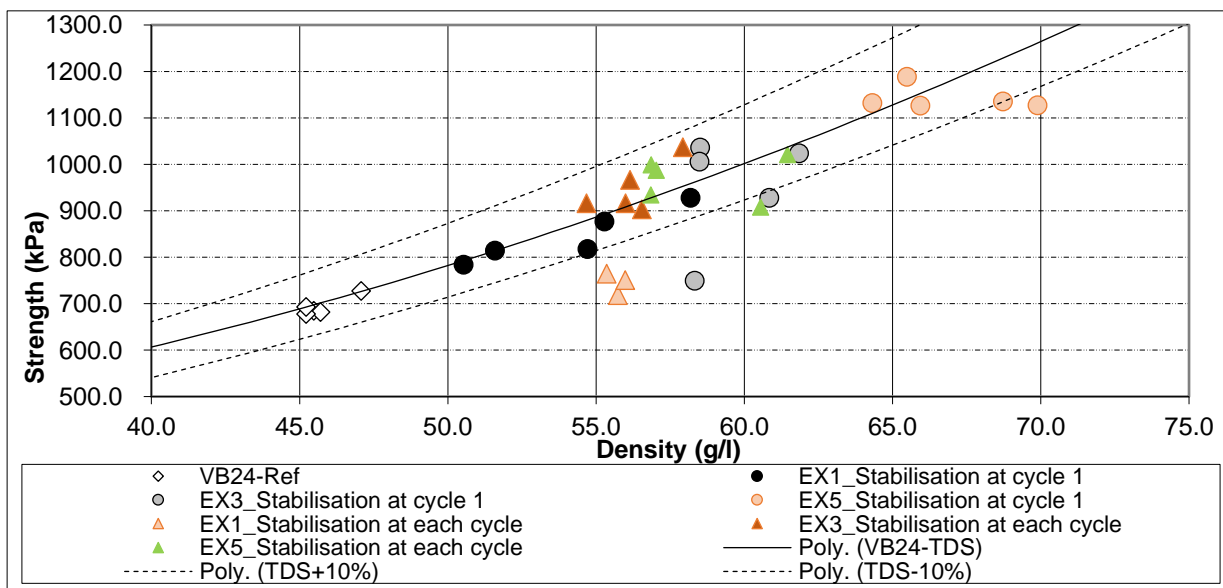
Figure 39: Non-recycled VB24 Test materials vs Regular VB24- Compression at 75% strain
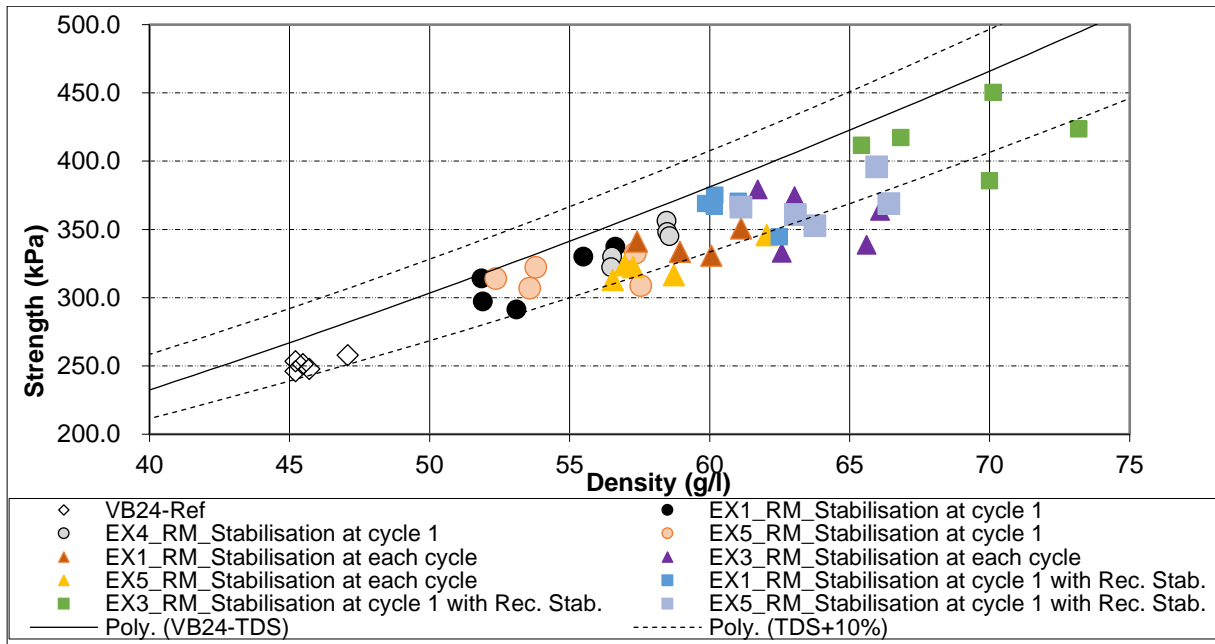
Figure 40: Recycled VB24 Test materials vs Regular VB24- Compression at 25% strain
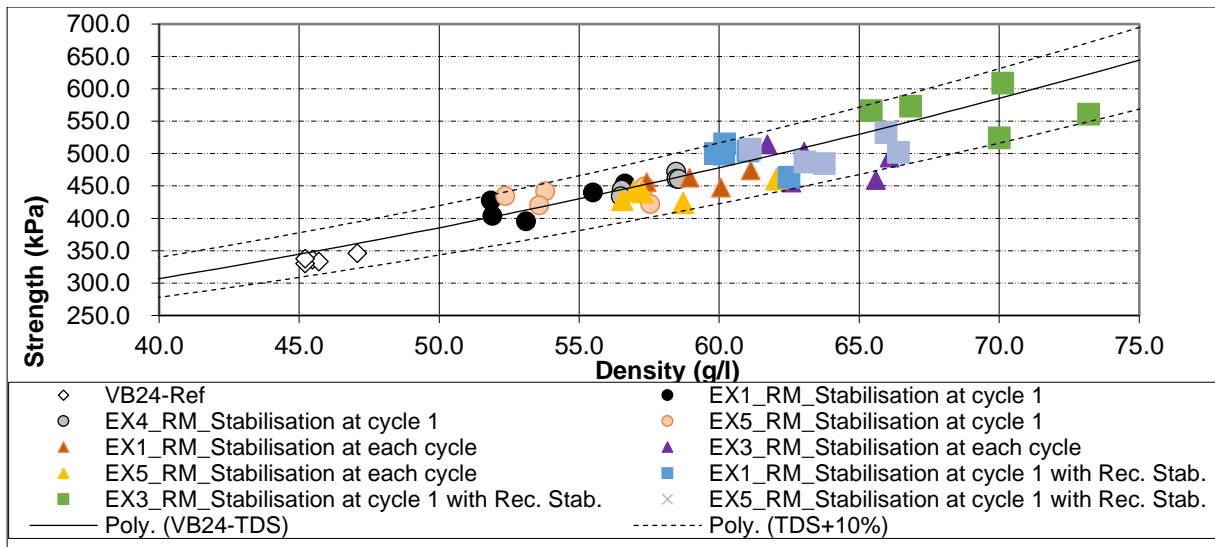
Figure 41: Recycled VB24 Test materials vs Regular VB24- Compression at 50% strain
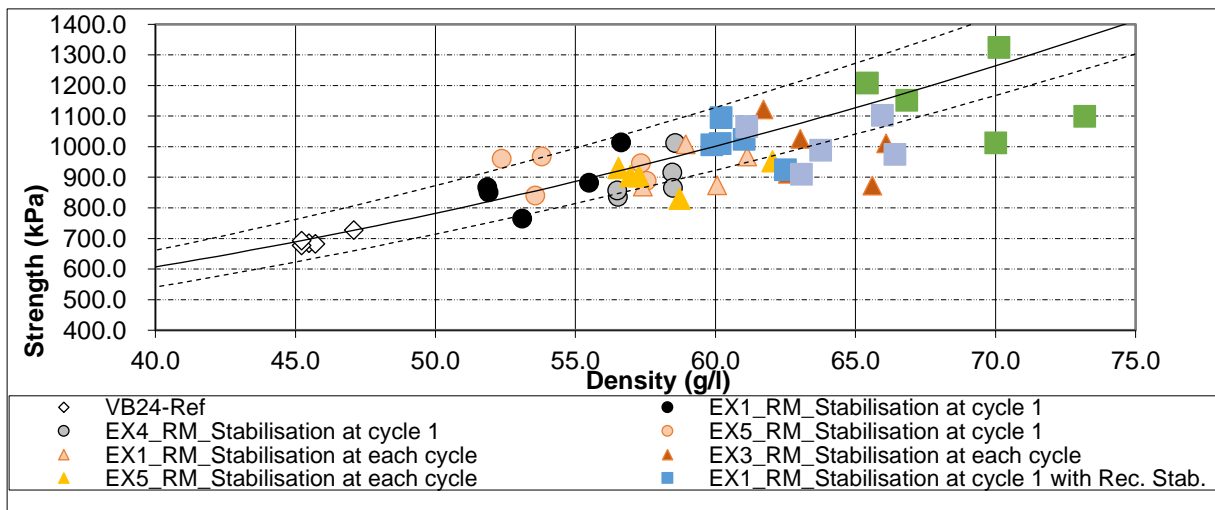
Figure 42: Recycled VB24 Test materials vs Regular VB24- Compression at 75% strain

Based on figures 40 to 42, which resemble to the plots of the recycled blends, one can conclude an overall decrease in compression strength in comparison to the non-recycled blends. At 25% strain, the values approach already closer to the 10% safety margin than the non-recycled samples, indicating that the added recycled material has a lower compression strength in comparison to the standard material. Furthermore, both the samples of the type "stabilisation at each cycle" and "stabilisation at cycle 1 with Rec. Stab." do not meet the safety margin after 5 extrusion cycles at 75% strain. Moreover, the values of the "stabilisation at cycle 1 with Rec. Stab." samples do not meet the requirements after 3 extrusion cycles at 75% strain. Thus, a change in stabilizer resulted in a worsened compression strength.

4.3.3 Intermediate Conclusion in terms of Mechanical properties

Table 11 gives a brief summary of the demonstrated changes in compression strength, elongation at break and tensile strength for all the samples over the course of the extrusion cycles. A relative percentage of increase or decrease in property was made, referring to the value of the first cycle as the starting point. Furthermore, the values were ranked "acceptable" and "not acceptable" after comparing them to the values of the reference grade, found in the technical data sheets.

Table 11: Summary of mechanical properties recycled & non recycled samples

Sample type	Tensile Strength	Elongation at break	Compression strength
Recipe B: Stabilization at start of cycle 1	± Constant +0.3 % Not acceptable	Big decrease -23% Acceptable	Small decrease Acceptable
Recipe B: Stabilization at each cycle	± Constant -2 % Not acceptable	Small decrease -5 % Acceptable	Small decrease Acceptable
Recipe C Recycled material - stabilized at start of 1st cycle	± Constant -2 % Not acceptable	Small decrease -3 % Acceptable	Larger decrease Acceptable
Recipe C Recycled material- stabilized at every cycle	Larger decrease -9 % Not acceptable	Small increase +4.9 % Acceptable	Larger decrease Not acceptable
Recipe D Recycled material- addition of recycling stab at start of 1st cycle	Small decrease -6.6 % Not acceptable	Small increase +6.7 % Acceptable	Larger decrease Not acceptable

Once can conclude from table 11 that the properties of the first three sample types are acceptable according to KB's standards, apart from the tensile strength. However, this lack in tensile strength could be due to the fact that there are still dispersants present between the

particles as these were produced in an experimental way. Furthermore, the addition of the recycled fraction generally increased the ductility of the samples, but caused a larger drop in compression strength and tensile strength, resulting in the non-usability of these samples after 5 cycles. In addition, this drop in tensile and compression strength could also indicate a drop in MW as both mechanical properties are directly related to the MW following section 2.3.2 and [72]. This drop in MW is in its turn relatable to the presence of polymer degradation.

4.4   Density of the foamed particles

After expansion, each batch of foamed particles got measured upon their bulk density. It is known that the density is inversely proportional to the specific volume. Moreover, this specific volume is influenced by many parameters such as the molecular weight and morphology, shear rate and average temperature and pressure during flow [73].

Given that the stereoregularity of the produced foamed particles is identical (all isotactic PP), the shear rate, temperature and pressure during processing stay the same for each sample and that the molecular weight is sufficiently high, a relative linearity can be expected between the bulk density of the foam particles and the molecular weight. Like mentioned in section 2.1.1 and 2.2.1, both parameters give an indication whether the polymer matrix is exposed to some form of degradation during processing. In addition, the processing of the polymer is also influenced by the density as higher densities cause a more difficult processing. Again, only the densities of the already discussed samples in section 4.3 are further elaborated as these are most likely to portray a trend. Table 12 gives a summary of the collected particle bulk densities after expansion.

Table 12: Summary of the collected densities

Sample type	Density after 1 Extrusion cycle (g/l)	Density after 3 Extrusion cycles (g/l)	Density after 5 Extrusion cycles (g/l)
Recipe B: Stabilization at start of cycle 1	49.4	43.7	47.8
Recipe B: Stabilization at each cycle	45.6	46.2	44.1
Recipe C Recycled material - stabilized at start of 1st cycle	41.6	40.2	39.0
Recipe C Recycled material- stabilized at every cycle	43.5	44.7	38.2
Recipe D Recycled material- addition of recycling stab at start of 1st cycle	44.9	45.5	39.9

The column "density after 1 extrusion cycle" gives the measured density of expanded foamed particles, which only experienced the whole extrusion process once. The same reasoning goes for the third and fourth column. Globally, there can be concluded that the bulk density of the particles drops after 5 extrusion cycles, which could again be an indication of polymer degradation taking place following section 2.2.1. Furthermore, the overall densities of the samples containing a recycled fraction are lower in comparison to the non-recycled samples.

This could indicate a difference in morphology of the added recycled fraction in comparison to the standard material. Following [74], it is expected that a higher stereoregularity, shorter side chains and a more regular copolymer configuration increase the degree of crystallinity and thereby increase the stiffness and density of the material. However, like mentioned in section 3.1, the external recycled material was not further examined during this thesis.

4.5   Rheology: Rotational Rheometer

The performed oscillatory tests gathered data of the samples in terms of both the storage and loss moduli (G' and G") in combination with the curve representing the complex viscosity (η*). All three parameters are part of the basic concepts of rheology and will first be shortly elaborated in section 4.5.1 in order to specify their importance. Section 4.5.2 discusses the course of the η*-curves, as well as linking the changes in η* to the degradation. Next, section 4.5.3 portrays the profiles of the collected storage and loss moduli, linking them to a change in mechanical properties.

4.5.1 Basic concepts of the Storage & Loss modulus

The examined EPP samples are all viscoelastic polymers, making their deformations both plastic and elastic. Accordingly, this behaviour is translated by a combination of the Hookean (elastic behaviour) and Newtonian (plastic) equations for material response following the Maxwell or Kelvin-Voight model. A summary of all equations and models is given by [75], [44] and [76]. Like mentioned in section 3.8, an oscillatory frequency is applied to the sample while measuring the respective stress response and keeping the strain constant at 1%. The small amplitude or strain is compulsory to guarantee that the measurements are still performed in the linear viscoelastic region of the PP samples. If this condition is fulfilled, G is independent of the applied stress or strain, making it possible to draw conclusions about the molecular structure from the linear viscoelastic response. Applying the knowledge above, this G should be divided into an elastic part and a plastic part. This term is defined as the complex modulus G*, which is a combination of the storage modulus G', representing the elastic energy stored, and the loss modulus G", which represents the viscous energy dissipated. These two moduli are directly linked to the molecular parameters of the chains in unimodal compositions or to blend composition in case of a polymer mixture, according to [77] and [78]. Furthermore, the calculation of η* is based on both moduli values in combination with the ω following the equation given by [79] and [80]: $\eta^* = \frac{G^*}{\omega} = \frac{\sqrt{G'^2 + G''^2}}{\omega}$.

4.5.2 Complex Viscosity

Figures 43 to 47 give a schematic overview of the collected complex viscosity data after performing the rheometric tests. All tests were performed following the protocol given in section 3.8. The exact data are added to the Appendix B.
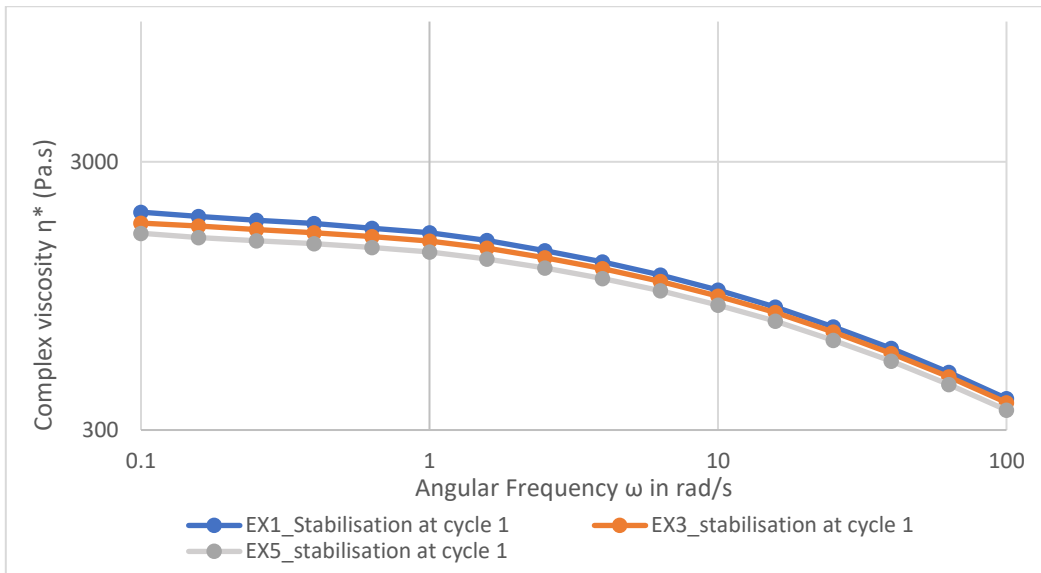
Figure 43: Schematic overview of the change in η* of the non-recycled samples with stabilization at the 1st cycle
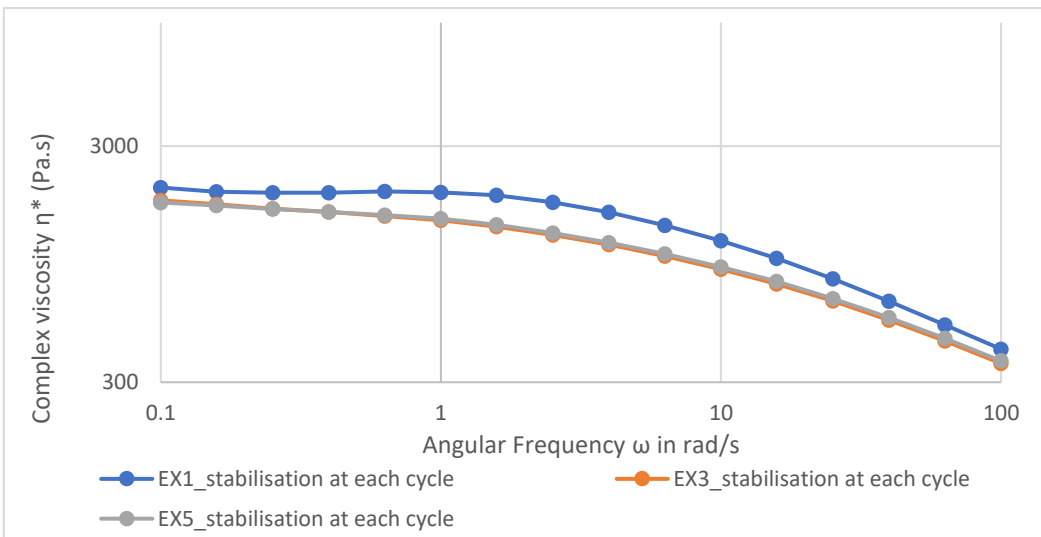
Figure 44: Schematic overview of the change in η* of the non-recycled samples with stabilization at each cycle
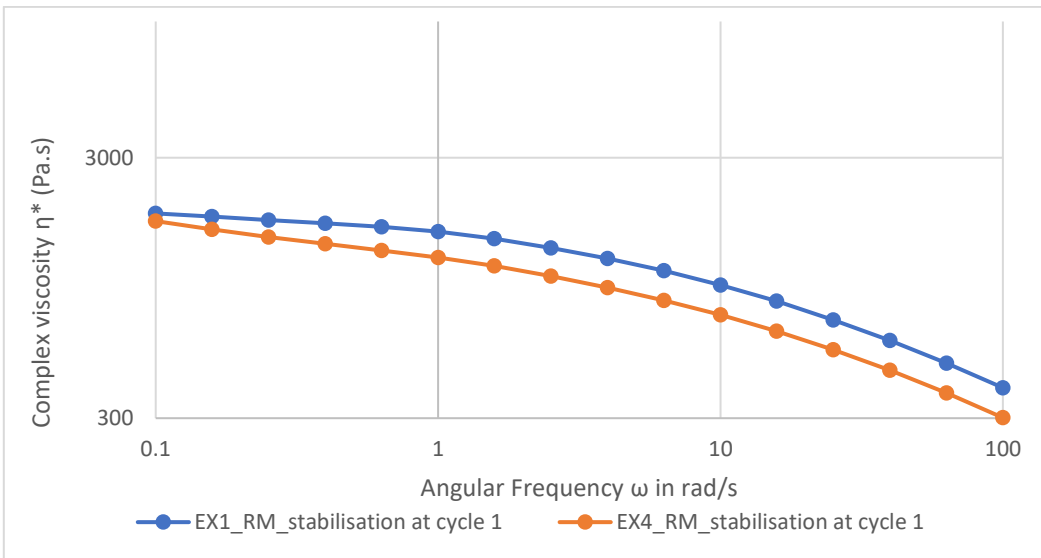
Figure 45: Schematic overview of the change in η* of the recycled samples with stabilization at the 1st cycle
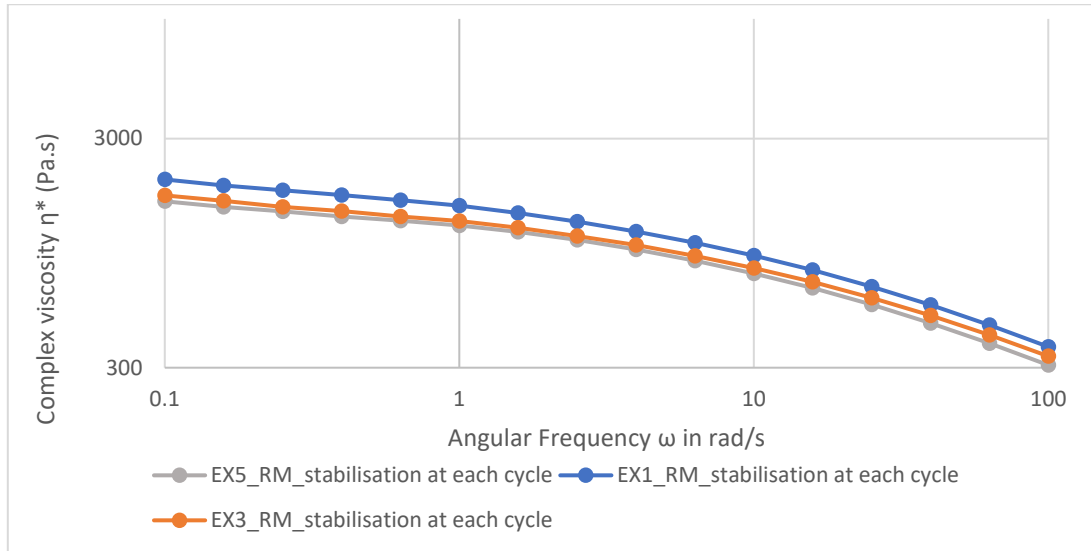
Figure 46: Schematic overview of the change in η* of the recycled samples with stabilization at each cycle
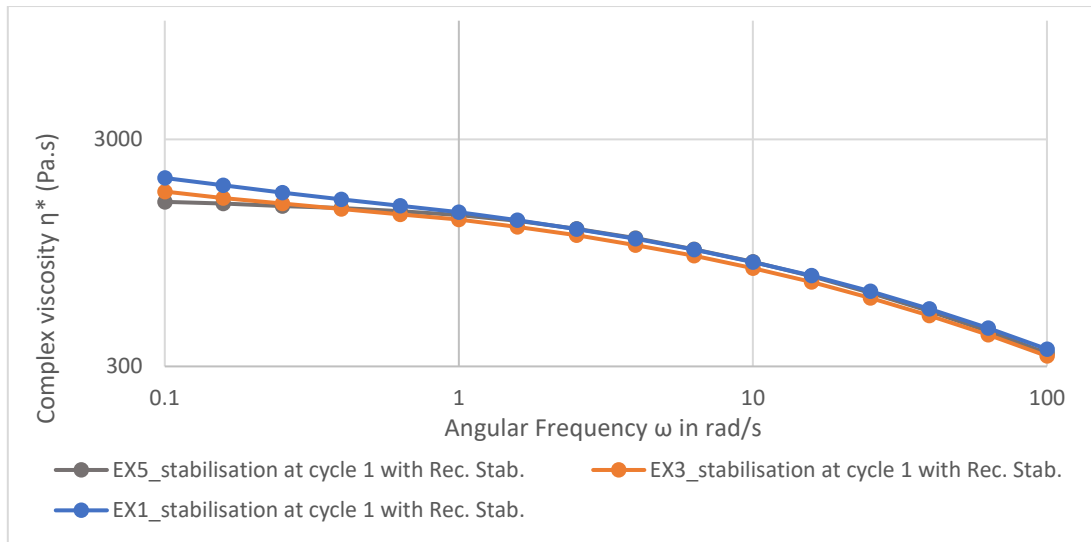
Figure 47: Schematic overview of the change in η* of the recycled samples with stabilization at the 1ˢᵗ cycle with Rec Stab.

In order to draw conclusions in terms of degradation of the samples, one should calculate a change in molecular weight of the polymer, as was concluded in section 2.2.1 and 2.3.1. However, in order to relate the viscosity to the MW, this molecular weight should be above the critical molecular weight, which is guaranteed with our polypropylene samples. Furthermore, this empirical relationship is only valid for the zero shear viscosity $\eta_0 \sim Mw^{3.4}$ following [81], [80]. This viscosity is found in the Newtonian regime at very low shear rates and angular frequencies. In order to estimate the zero shear viscosity, the Carreau-Yasuda regression can be applied, as described in [68], resulting in the corresponding MWs of the samples. This regression was not executed in this thesis, however, one can visually extrapolate and examine the above figures and draw similar conclusions around a change in molecular weight of the samples. Table 13 gives a summary of the calculated η* at the lowest ω and indicates the increase or decrease in viscosity.

Table 13: Change in complex viscosity over the course of the extrusion cycles

Sample type	η* after 1 Extrusion cycle	η* after 3 Extrusion cycles	η* after 5 Extrusion cycles	Increase Decrease

	(Pa.s)	(Pa.s)	(Pa.s)	(%)
Recipe B: Stabilization at start of cycle 1	1947.43	1772.86	1624.84	-16.6 %
Recipe B: Stabilization at each cycle	2003.38	1768.41	1732.0	-13.5 %
Recipe C Recycled material - stabilized at start of 1st cycle	1833.45	1712.65*	/	-6.6 %
Recipe C Recycled material- stabilized at every cycle	1990.48	1695.31	1598.03	-19.7 %
Recipe D Recycled material- addition of recycling stab at start of 1st cycle	2028.26	1767.72	1592.23	-21.4 %

First, there can be concluded that the η* of all recipes drops over the course of the extrusion cycles, which indicates that the β-chain scission mechanism influences the MW and leads to a degradation of the PP chains, which was also concluded from the gathered MFI data. Secondly, the addition of extra stabilizer at each cycle of recipe B does not lead to a significant decrease in degradation, as the % of decrease is still large at 13.5 %. Third, the addition of recycled material causes an even greater decrease in η* at around 20%. One can notice that the addition of the recycling stabilizer hinders this decrease at the first cycles, but as more recycled material gets added these η* values approach the same limit. This could indicate that this recycled material is generally more prone to further degradation, or has a different molecular weight and structure in comparison to the original EPP material. Finally, the drop in η* is the most significant after the first few extrusion cycles and diminishes slightly approaching the fifth cycle.

4.5.3 Storage & Loss modulus

Following [76], a close inspection of the G' and G" can indicate changes in the structural strength and flexibility of the polymer structure. In figure 48, a comparison is made between the moduli of two samples of Recipe B which endured a different amount of extrusion cycles (1 and 5 cycles). The comparison was made to indicate the influence of going through multiple extrusion cycles on both moduli. The exact values of both moduli can be found in Appendix B.
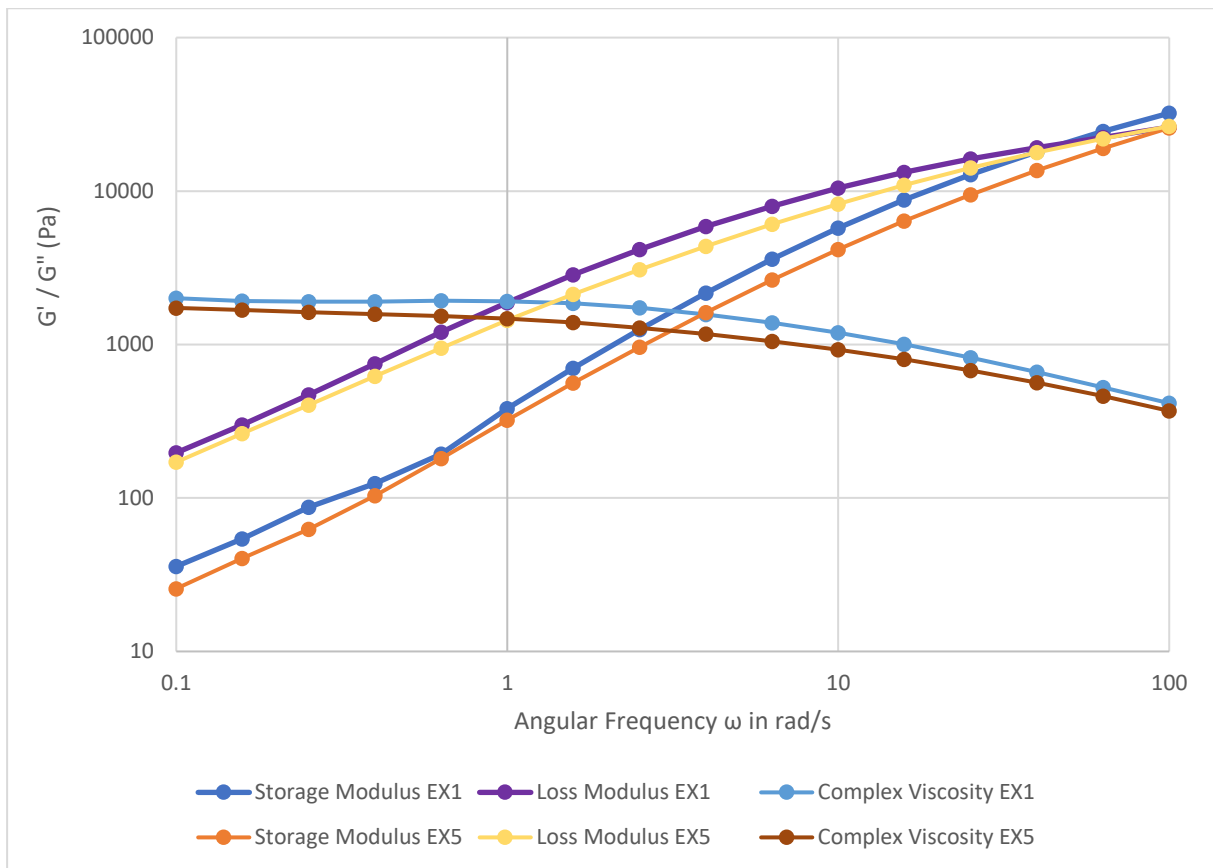
Figure 48: Schematic overview of the influence of multiple extrusion cycles on both shear moduli (G' & G")

There can be concluded that both moduli decrease after going through more extrusion cycles. A decrease in G' indicates a decrease in elastic behaviour in the high ω range as a cause of a decrease in the amount of deformation energy that can be stored, ultimately resulting in a less rigid structure. In addition, a decrease in G" indicates a decrease in viscous behaviour as this parameter has the upper hand in the low ω region where the deformation energy is lost. A higher G" stands for more entanglements and flexibility. However, the G" after 5 cycles is lower than its value after 1 cycle, thereby indicating a lower increase in flexibility [76]. The same conclusion was found for all samples regarding the influence of the extrusion process.

Secondly, the influence of adding a recycled fraction to the blend was examined in terms of a change in both moduli. Figure 46 gives a schematic overview of both sample types of the lines "EX1_stabilisation at each cycle" regarding their changes in loss and storage moduli.
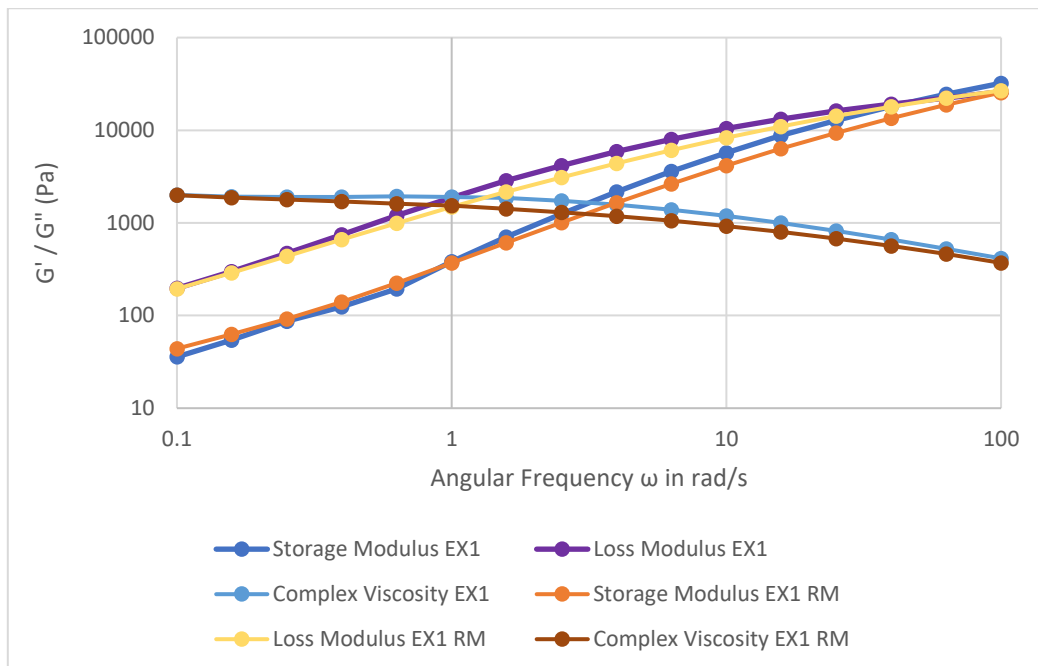
Figure 49: Schematic overview of the influence of the recycled fraction on both shear moduli (G' & G")

From figure 49, there can be concluded that an overall decrease in G" is seen by adding the recycled fraction, which corresponds again to a decrease in entanglements and flexibility. However, at frequencies below 1 rad/s, an increase in G' is to be seen for the recycled samples in comparison to the G' of the non-recycled samples, which indicates it being a more rigid structure at low ω. This fact is also confirmed by the loss factor, which correlates both moduli. The same comparison can be made between the recycled samples using the standard stabilizer and the samples using the recycling stabilizer. These moduli did not differ significantly. The exact values can be found in Appendix B.

Finally, there should be noted that the progressions of both the storage moduli of the recycled and non-recycled samples do not resemble to the expected progression of a normal isotactic PP homopolymer. A certain kink in the curve is seen in comparison to the G' curve of standard PP. Following figure 50 and comparing these trends to figure 49, there can be concluded that the kink corresponds to a form of cross-linkage or addition of a LCB, as is elaborated in [82]. Like assumed in section 2.1 and 2.2.1, this is added to the standard recipe in order to improve the structural strength of the polymer. However, due to confidentiality reasons of the recipe and it not being the core goal of this thesis, this fact will not be discussed any further but might give some possibilities for the future.
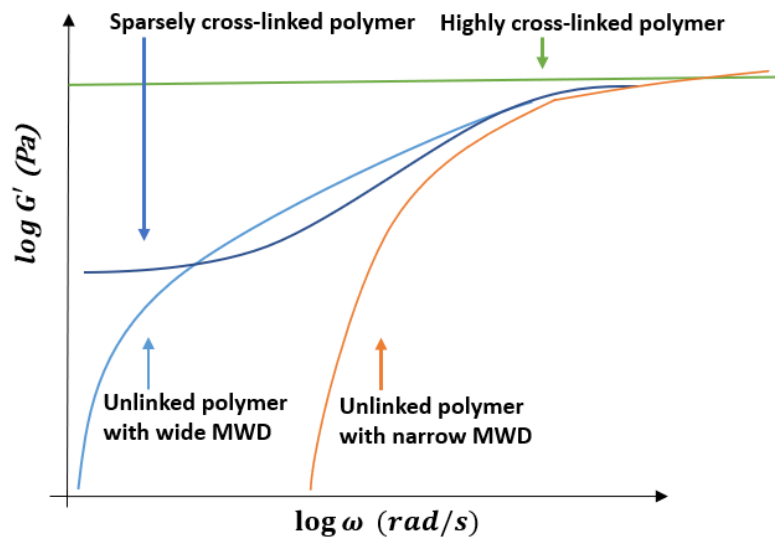
Figure 50: Comparison of structures using G'-curves resulting from frequency sweeps

Chapter 5

Conclusions

The effect of going through multiple extrusion cycles and the introduction of external recycled product was investigated on expanded polypropylene particles. Four different recipe types were made (A-D) in order to demonstrate the influence of the different compositions on final properties. The aim of this thesis was to report on the change in rheological and mechanical properties of these four recipes and form a conclusion around their stability and the potential degradation they experience during processing. The most common degradation mechanisms in EPP processing are the β-chain scission and the melt fracture by shear. In order to report on the change in properties, two recipes were constructed only consisting of non-recycled material. Next, two were constructed at which 25 % of recycled material was added before every new extrusion cycle, i.e. two recycled blends. Furthermore, the amount of stabilizer added was varied in both the recycled and non-recycled recipes from not including it in the recipe to an addition after each cycle in order to demonstrate its use. Moreover, the type of stabilizer was varied in the recycled recipes to compare the performance of a new type of stabilizer to the standard one. All blends were prepared using an experimental extrusion and expansion setup, providing the needed foamed particle samples. In addition, a foamed particle moulder was used to construct test planks needed for the mechanical tests.

Two types of rheological tests were performed in order to indicate the influence of the recycled material, stabilizer and going through multiple extrusion cycles on the amount of degradation taking place in the EPP chains. First, a standard melt flow analysis was done on all produced recipe pellets after extrusion. A rise in MFI indicates a decrease in viscosity, which in its turn indicates a decrease in MW and entanglement, i.e. polymer degradation taking place. These MFIs indicated that the addition of stabilizer, in comparison to excluding it from the recipe, resulted in the lowest decrease in viscosity. In addition, swapping out the standard stabilizers by the recycling stabilizer in the recycled samples resulted in lower MFI values, thus minimizing the degradation. Furthermore, repeatedly adding more stabilizers to the mixture after each extrusion cycle did not affect the MFI significantly. Finally, the recycled blends experienced a larger increase in MFI in comparison to the non-recycled samples. This increase can be attributed to the fact that the recycled material has a MFI of 9 g/10 min and resembles to 76% of the blend composition after 5 extrusion cycles.

One should be aware of the fact that an MFI is a one point measurement and solemnly gives an indication of the melt's viscosity, rather than an exact value. In order to get a more exact measurement of the change in MW by degradation, the rheological analysis was elaborated by means of an rotational rheometer. The performed oscillatory tests gathered data of the samples in terms of both the storage and loss moduli (G' and G") in combination with the curve representing the complex viscosity (η^*). However, in order to link the η^* to the MW, this first had to be converted to the zero shear viscosity (η_0) following the Carreau-Yasuda regression as the following correlation is valid: $\eta_0 \sim Mw$. The Carreau-Yasuda regression was not performed, however, an approximation of the zero shear viscosity was made by taking the η^* at the lowest angular frequency (0.1 rad/s) in the linear region. The resulting viscosities indicated a drop in η^* of all recipes over the course of the extrusion cycles, which again indicated a decrease in MW weight following the β-chain scission mechanism. Secondly, the addition of extra stabilizer at each cycle of recipe B did not lead to a significant decrease in degradation, as the % of decrease was still large at 13.5 %. Third, the samples containing recycled material saw an even greater decrease in η^* at around 20%. One could notice that the addition of the recycling stabilizer hindered this decrease at the first cycles, but as more recycled material got added these η^* values approached the same viscosity limit. This could

indicate that the recycled material is generally more prone to further degradation, or has a different molecular weight and structure in comparison to the original EPP material. Finally, the drop in η* was the most significant after the first few extrusion cycles, diminishing slightly when approaching the fifth cycle.

In terms of both moduli, there could be concluded for all recipes (recycled and non-recycled) that both decreased after going through more extrusion cycles. The decrease in G' indicated a decrease in elastic behaviour in the high ω range, ultimately resulting in a less rigid structure. In addition, the decrease in G" indicated a decrease in viscous behaviour resulting in a lower amount of entanglements thereby decreasing the flexibility. Furthermore, the recycled blends saw a lower G" over the whole course of the curve in comparison to the non-recycled samples, but a slightly higher G' was found at the low frequency range. This could indicate it being a more rigid structure at low ω. Finally, the recycled samples using the standard stabilizer and the samples using the recycling stabilizer were compared, which did not give any significant changes in moduli.

There should be noted that the progressions of both the storage moduli of the recycled and non-recycled samples do not resemble to the expected progression of a normal isotactic PP homopolymer. A certain kink in the curve is seen in comparison to the G' curve of standard PP. However, due to confidentiality reasons of the recipe and it not being the core goal of this thesis, this fact was not elaborated on any further.

Secondly, the mechanical properties were evaluated by means of tensile and compression tests. The tensile tests gave the elongation at break and tensile strength of the samples. These indicated that both properties of the non-recycled samples decreased over the course of multiple extrusion cycles, which indicates again a loss in MW weight of the samples. However, the elongation at break of all samples still matched KB's standards, with the elongation at break of the extra stabilized samples decreasing the least. Furthermore, the tensile strength of these samples decreased only slightly over the course of the extrusion cycles, but did not meet the standards. The recycled blends on the other hand saw a slightly larger decrease in tensile strength, still not matching KB's standards. The lack in tensile strength could be due to the fact that there are still dispersants present between the particles as these were produced in an experimental way, leading to a worsened cohesion and density. Moreover, the elongation at break increased slightly for the recycled samples, resulting in an increased ductility. This increase was the largest for the samples containing the recycling stabilizer. In addition, these samples also saw the smallest decrease in tensile strength. Finally, the compression strength decreased for all samples, with the recycled samples demonstrating a larger decrease. Again, this decrease could be appointed to the amount of degradation taking place.

In terms of the density analysis, one could conclude that the density dropped as a cause of a loss in MW for all samples. Furthermore, the overall densities of the samples containing a recycled fraction were lower in comparison to the non-recycled samples. This could indicate a difference in morphology of the added recycled fraction in comparison to the standard material. A higher stereoregularity, shorter side chains and a more regular copolymer configuration increase the degree of crystallinity and thereby increases the stiffness and density of the material. However, like mentioned in section 3.1, the external recycled material was not further examined during this thesis.

The DSC-scans demonstrated a rise in crystallinity for all samples after going through multiple extrusion cycles, which could be due to the fact that degradation is happening and thereby cutting the chains/macromolecules. However, these freed macromolecules now get the opportunity to rearrange themselves resulting in an augmentation of the overall crystallinity. There should be noted that the rise in crystallinity is more profound with the recycled blends,

which could again indicate that the added external recycled material is of a higher crystallinity itself.

In summary, there can be concluded from both rheological tests that the non-recycled sample containing extra stabilizer is the most stabile sample as it decreased the least in MW. Furthermore, all recycled samples saw the largest decrease in MW, with the new recycling stabilizer not being as effective as the MFI results indicated. The mechanical tests confirmed this statement, with the non-recycled sample containing extra stabilizer having the lowest decrease in tensile strength, elongation at break and compression strength after 5 extrusion cycles. Furthermore, the recycled blends were deemed less stabile as they decreased most in all mechanical properties except from the elongation at break, with the sample containing the recycling stabilizer staying more stable thereby minimizing the amount of deterioration of the polymer chain. However, these recycled samples did not meet the standards, making them unusable.

Chapter 6

Outlook

This thesis investigated the effects of multiple extrusion cycles and an external recycled fraction on the properties of the produced foamed particles. Different recipes were constructed in order to indicate the essence of different recipe components in terms of degradation (prevention). However, the expansion of recipe A, which did not incorporate any stabilizer, did not take place. This recipe should be elaborated further in the future as it could provide valuable information about the exact influence of (not) adding stabilizer in terms of the mechanical properties. In addition, recipe D was constructed to study the influence of the new recycling stabilizer. However, similarly to the standard stabilizer, an additional amount of this stabilizer was not added before every extrusion cycle. One could verify if an additional amount of recycling stabilizer would have as insignificant of an impact as the standard stabilizer, or that it actually decreased the degradation further on, resulting in an overall higher MW. Moreover, in terms of recipe components, the added externally recycled material could be further investigated. Examining a sample of pure recycled material on the ODR and putting it through a SEC at high temperature would give a better indication of its molecular weight (distribution), molecular structure and complex viscosity, making its introduction in the virgin material more predictable in terms of final properties. Finally, the progressions of both the storage moduli of the recycled and non-recycled samples did not resemble to the expected progression of a normal isotactic PP homopolymer. A certain kink in the curve is seen in comparison to the G' curve of standard PP. This kink corresponds to a form of cross-linkage or addition of a LCB, which is added to the standard PP in order to improve its structural strength. However, due to confidentiality reasons of the recipe and it not being the core goal of this thesis, this fact was not discussed any further but might give some possibilities for the future.

Next to the used methods in terms of the PP-degradation analysis could the dissolved gas analysis, measuring discoloration via an IR-scan and the SEC at high temperature also give (an even better) indication of the amount of degradation taking place and the change in MW. Furthermore, the ODR analysis could be extended to the actual implementation of the Carreau-Yasuda regression model rather than implementing the estimation used in this work. In doing so, the exact molecular weight can be calculated corresponding to the gathered complex viscosity data.

The received tensile results were all sub-standard. However, as the foamed particles were produced in an experimental way, the produced particles were not as greatly cleaned after expansion. This resulted in a certain amount of dispersants still remaining between the particles, causing the tensile strength to decrease. A small industrial particle washer would prevent this from happening.

The DSC-scans indicated a rise in crystallinity for all samples. Keeping track of the melt temperatures could have confirmed this statement as these rise as well with a rising crystallinity.

Finally, the cell-sizes were not evaluated. Given that the cell size is a relatively important foaming property (section 2.1.1) as the foam morphology can be directly linked to the melt strength and density, a measurement of these sizes would indicate whether the provided cell size is favourable in terms of the following moulding processes.

Bibliography

[1] Kaneka Belgium NV, "Eperan PP," 2021. [Online]. Available: http://www.kaneka.be/products/eperan/eperan-pp. [Accessed 12 03 2021].

[2] European Commission, *A European Strategy For Plastics in a Circular Economy,* 2018, pp. 5-6.

[3] F. Jin, M. Zhao, M. Park and S. Park, "Recent Trends of Foaming in Polymer Processing: A," *Polymers,* vol. 2019, no. 11, 2019.

[4] D. Zimnyakov, R. Zdrajevsky, N. Minaev, E. Epifanov, V. Popov and O. Ushakova, "Extreme Foaming Modes for SCF-Plasticized Polylactides: Quasi-Adiabatic and Quasi-Isothermal Foam Expansion," *Polymers,* vol. 12, no. 5, 2020.

[5] Z. Xu, X. Jiang, T. Liu, G. Hu, L. Zhao, Z. Zhu and W. Yuan, "Foaming of polypropylene with supercritical carbon dioxide," *Journal of Supercritical Fluids ,* no. 41, pp. 299-310, 2006.

[6] N. Weingart, D. Raps, M. Lu, L. Endner and V. Altstädt, "Comparison of the Foamability of Linear and Long-Chain Branched Polypropylene—The Legend of Strain-Hardening as a Requirement for Good Foamability," *Polymers (Basel) ,* vol. 12, no. 3, p. 725, 2020.

[7] M. Liang and C. Wang, "Production of Engineering Plastics Foams by Supercritical CO2," *Industrial & Engineering Chemistry Research ,* vol. 39, no. 12, pp. 4622-4626, 2000.

[8] C. Maya, M. Fernandez-Ponce, L. Casas and C. Mantell, "A comparative analysis on the impregnation efficiency of a natural insecticide into polypropylene films by means of batch against semi-continuous techniques using CO2 as solvent," *The Journal of Supercritical Fluids,* vol. 169, no. 105127, 2021.

[9] C. Cejudo Bastante, L. Casas Cardoso, C. Mantell Serrano and E. Martínez de la Ossa, "Supercritical impregnation of food packaging films to provide antioxidant properties," *The Journal of Supercritical Fluids,* vol. 128, pp. 200-207, 2017.

[10] D. Markovic, S. Milovanovic, M. Radetic, B. Jokic and I. Zizovic, "Impregnation of corona modified polypropylene non-woven material with thymol in supercritical carbon dioxide for antimicrobial application," *The Journal of Supercritical Fluids,* vol. 101, pp. 215-221, 2015.

[11] B. Wenclawiak, "SFC and SFE: An Introduction for Novices," in *Analysis with Supercritical Fluids: Extraction and Chromatography ,* Heidelberg, Springer-Verlag, 1992, pp. 1-5.

[12] M. Abate, A. Ferri, J. Guan, G. Chen and V. Nierstrasz, "Impregnation of Materials in Supercritical CO2 to Impart Various Functionalities," in *Advanced Supercritical Fluids Technologies*, IntechOpen, 2019.

[13] B. Wenclawiak, "Fluid Properties in SFE," in *Analysis with Supercritical Fluids: Extraction and Chromatography ,* Heidelberg, Springer-Verlag, 1992, pp. 34-37.

[14] J. Karger-Kocsis, "Polypropylene Foaming," in *Polypropylene: An A-Z Reference ,* Dordrecht, Kluwer Publishers, 1999, pp. 635-642.

[15] C. DeArmitt and R. Rothon, "Dispersants and Coupling Agents," in *Applied Plastics Engineering Handbook ,* William Andrew Applied Science Publishers , 2011, pp. 441-454.

[16] S. Patermann and V. Altstädt, "PP/EPDM-Blends by Dynamic Vulcanization: Influence of increasing peroxide concentration on mechanical, morphological and rheological characteristics," May 2014. [Online]. Available: https://www.researchgate.net/publication/278188682_PPEPDM-Blends_by_Dynamic_Vulcanization_Influence_of_increasing_peroxide_concentratio

n_on_mechanical_morphological_and_rheological_characteristics. [Accessed 25 03 2021].

[17] C. Tzoganakis, J. Vlachopoulos and A. Hamielec, "Modelling of the Peroxide Degradation of Polypropylene," *International Polymer Processing Journal,* vol. III, pp. 141-150, 1988.

[18] A. Hogt, J. Meijer and J. Jelenic, "Modifications of PP by organic peroxides," in *Reactive Modifiers for Polymers*, Birmingham, Chapman & Hall, 1997, pp. 92-101.

[19] D. Auhl, J. Stange, H. Münstedt, B. Krause, D. Voigt, A. Lederer, U. Lappan and K. Lunkwitz, "Long-Chain Branched Polypropylenes by Electron Beam Irradiation and Their Rheological Properties," *Macromolecules,* vol. 37, no. 25, pp. 9465-9472, 2004.

[20] C. Yang, Q. Zhao, Z. Xing, W. Zhang, M. Zhang, H. Tan, J. Wang and G. Wu, "Improving the Supercritical CO_2 Foaming of Polypropylene by the Addition of Fluoroelastomer as a Nucleation Agent," *Polymers,* vol. 11, no. 226, 2019.

[21] V. Shrinivas, R. Narasimhan and T. Argumam, "Failure analysis of AISI 440C strand dies used in twin screw extruders during polymer compounding," *Materialstoday: Proceedings,* 2011.

[22] J. B. P. Soares, "An Overview of Important Microstructural Distributions for Polyolefin Analysis," *Macromolecular Symposia ,* vol. 257, pp. 1-12, 2007.

[23] D. Rosato and D. Rosato, "Overview," in *Plastics Engineered Product Design*, Elsevier B.V., 2003, pp. 1-45.

[24] B. Monrabal and P. del Hierro, "Characterization of polypropylene–polyethylene blends by temperature rising elution and crystallization analysis fractionation," *Analytical and Bioanalytical Chemistry,* vol. 399, p. 1557–1561, 2011.

[25] G. W. Coates, "Precise Control of Polyolefin Stereochemistry Using Single-Site Metal Catalysts," *Chemistry Reviews ,* vol. 100, pp. 1223-1252, 2000.

[26] Y. Jahani, M. Ghetmiri and M. Vaseghi, "The Effects of Long Chain Branching of Polypropylene and Chain Extension of Poly(ethylene Terephthalate) on Thermal Behavior, Rheology and Morphology of Their Blends," 2012.

[27] R. G. Larson, "Rheology of entangled polymers," in *The structure and rheology of complex fluids*, Oxford, Oxford University Press, 1999, pp. 149-158.

[28] E. Sackmann, J. Käs and H. Strey, "The observation of polymer reptation," *Advanced materials,* vol. 6, no. 6, pp. 507-509, 1994.

[29] T. C. B. Mcleish, "Present puzzles of entangled polymers," *Rheology Reviews,* pp. 197-233, 2003.

[30] M. Doi and S. F. Edwards, "Dynamics of concentrated polymer systems. Part 1.— Brownian motion in the equilibrium state," *Journal of the Chemical Society, Faraday Transactions 2: Molecular and Chemical Physics,* vol. 74, pp. 1789-1801, 1978.

[31] M. Wagner, H. Bastian, P. Hachmann and J. Meissner, "The strain-hardening behaviour of linear and long-chain-branched polyolefin melts in extensional flows," *Rheologica Acta,* vol. 39, pp. 97-109, 2000.

[32] P. Spitael and C. Macosko, "Strain Hardening in Polypropylenesand Its Role in Extrusion Foaming," *Polymer Engineering and Science ,* vol. 44, no. 11, pp. 2090-2100, 2004.

[33] M. Gahleitner, "Melt rheology of polyolefins," *Progress in Polymer Science,* vol. 26, pp. 895-944, 2001.

[34] Y. Yu, P. J. DesLauriers and D. C. Rohlfing, "SEC-MALS method for the determination of long-chain branching and long-chain branching distribution in polyethylene," *Polymer,* vol. 46, pp. 5165-5182, 2005.

84

[35] W. Waldman and M. De Paoli, "Thermo-mechanical degradation of polypropylene, low-density polyethylene and their 1:1 blend," *Polymer Degradation and Stability,* vol. 60, pp. 301-308, 1998.

[36] S. Canevarolo, "Chain scission distribution function for polypropylene degradation during multiple extrusions," *Polymer Degradation and Stability,* vol. 70, no. 1, pp. 71-76, 2000.

[37] B. Fayolle, L. Audoin and J. Verdu, "Oxidation induced embrittlement in polypropylene - a tensile testing study," *Polymer Degradation and Stability ,* vol. 70, no. 3, pp. 333-340, 2000.

[38] G. Gryn'ova, J. Hodgson and M. Coote, "Revising the mechanism of polymer autooxidation," *Organic & Biomolecular Chemistry,* vol. 21, no. 2, 2011.

[39] BASF, "Antioxidants to prevent Polymer Oxidation," SpecialChem, 2021. [Online]. Available: https://polymer-additives.specialchem.com/centers/antioxidants-to-prevent-polymer-oxidation. [Accessed 22 03 2021].

[40] S. Yin, R. Tuladhar, F. Shi, R. Shanks, M. Combe and T. Collister, "Mechanical Reprocessing of Polyolefin Waste: A Review," *Polymer Engineering and Science ,* pp. 2899-2909, 2015.

[41] Polymer Database, "Flow Properties Of Polymers," Polymerdatabase.com, 2021. [Online]. Available: https://polymerdatabase.com/polymer%20physics/Viscosity2.html . [Accessed 18 04 2021].

[42] T. G. Mezger, "Flow behavior and viscosity," in *The Rheology Handbook Second Edition*, Hannover , Vincentz Network , 2006, pp. 19-26.

[43] T. G. Mezger, "Rotational Tests," in *The Rheology Handbook Second Edition*, Hannover, Vincentz Network, 2006, pp. 29-73.

[44] T. G. Mezger, "Viscoelastic behavior," in *The Rheology Handbook Second Edition*, Hannover, Vincentz Network , 2006, pp. 80-89.

[45] J. Vlachopoulos and D. Strutt, "The Role of Rheology in Polymer Extrusion," [Online]. Available: http://www.polydynamics.com/Rheology.pdf. [Accessed 23 04 2021].

[46] R. Rennie and J. Law, "Grotthuss−Draper law," in *A Dictionary of Chemistry*, Oxford University Press, 2016.

[47] G. Wypych, "Absorption, reflection and refraction," in *Handbook of UV Degradation and Stabilization ,* ChemTec Publishing, 2015, pp. 37-65.

[48] A. M. Striegel, W. Yau, J. Kirkland and D. Bly, "High-Temperature SEC and Rheological Connections," in *Modern Size-Exclusion Liquid Chromatography*, Hoboken, John Wiley & Sons, 2009, pp. 434-456.

[49] G. Gellerstedt, "Gel Permeation Chromatography," in *Methods in Lignin Chemistry ,* Heidelberg, Springer, 1992, pp. 487-497.

[50] J. Almond, P. Sugumaar, M. Wenzel, G. Hill and C. Wallis, "Determination of the carbonyl index of polyethylene and polypropylene using specified area under band methodology with ATR-FTIR spectroscopy," *E-Polymers,* vol. 20, no. 1, pp. 369-381, 2020.

[51] H. Kometani, T. Matsumura, T. Suga and T. Kanai, "Quantitative Analysis for Polymer Degradation in the Extrusion Process," *International Polymer Processing Journal of the Polymer Processing Society,* vol. 21, no. 1, pp. 24-31, 2006.

[52] H. Li and U. Sundararaj, "Morphology Development of Polymer Blends in Extruder: The Effects of Compatibilization and Rotation Rate," *Macromolecular Chemistry and Physics ,* vol. 210, pp. 852-863, 2009.

[53] G. Campbell and M. Spalding, "A mechanism for solid bed breakup in single-screw extruders," *Spe Antec Technical Papers* , vol. 60, pp. 1152-1160, 2014.

[54] BASF, "Light stabilizers and UV absorbers to prevent polymer degradation," SpecialChem, 2021. [Online]. Available: https://polymer-additives.specialchem.com/centers/light-stabilizers-and-uv-absorbers. [Accessed 30 03 2021].

[55] J. Bart, "Mechanisms of Physical Loss of Additives from Polymers," in *Polymer Additive Analytics: Industrial Practice and Case Studies* , Firenze University Press, 2006, p. 126.

[56] K. Benzarti and X. Colin, "Understanding the durability of advanced fibre-reinforced polymer (FRP) composites for structural applications," in *Advanced Fibre-Reinforced Polymer (FRP) Composites for Structural Applications*, Woodhead Publishing, 2013, pp. 361-439.

[57] N. Zoratto, R. Matassa, M. E. and G. Familiari, "Glycerol as a green solvent for enhancing the formulation of dextran methacrylate and gellan-based semi-interpenetrating polymer networks," *Journal of Material Science,* vol. 55, p. 9562–9577, 2020.

[58] Golden Far East Machinery , "How to operate extruder machine？," 15 04 2020. [Online]. Available: https://www.jydjx.com/news/how-to-operate-extruder-machine.html. [Accessed 15 03 2021].

[59] M. Hossain, "Production of H2 from microalgae biomass in supercritical water using a Ni/La-γAl2O3 catalyst," *Energy Procedia,* no. 110, pp. 384-389, 2017.

[60] L. McKeen, "Introduction to Plastics and Elastomers," in *Effect of Temperature and other Factors on Plastics and Elastomers (Second Edition)*, William Andrew Applied Science Publishers , 2008, pp. 1-39.

[61] Illinois Tool Works, "Instron MF20 Melt Flow Tester," 2021. [Online]. Available: https://www.instron.us/en-us/products/testing-systems/rheology/melt-flow-index-testers#mf20. [Accessed 2021 04 04].

[62] M. Moraes, C. Silva and R. Vieira, "Characterization of biopolymer membranes and films: Physicochemical, mechanical, barrier, and biological properties," in *Biopolymer Membranes and Films*, Brzail, Elsevier , 2020, pp. 67-95.

[63] METTLER TOLEDO, "DSC 3 - Differential Scanning Calorimeter," 2021. [Online]. Available: https://www.mt.com/int/en/home/products/Laboratory_Analytics_Browse/TA_Family_Browse/DSC/DSC_3.html. [Accessed 07 05 2021].

[64] International Organization for Standardization, "ISO 1926:2009 Rigid cellular plastics — Determination of tensile properties," 12 2009. [Online]. Available: https://www.iso.org/standard/52864.html. [Accessed 27 04 2021].

[65] International Organization for Standardization, "ISO 844:2021 Rigid cellular plastics — Determination of compression properties," 03 2021. [Online]. Available: https://www.iso.org/standard/73560.html. [Accessed 28 04 2021].

[66] Anton Paar GmbH, "Modular Compact Rheometer: MCR 102e/302e/502e," 2021. [Online]. Available: https://www.anton-paar.com/no-en/products/details/rheometer-mcr-102-302-502/. [Accessed 05 10 2021].

[67] Anton Paar GmbH, "Oscillatory Measurements: Back and Forth to the Result!," 2021. [Online]. Available: https://www.anton-paar.com/corp-en/services-support/document-finder/application-reports/joe-flow-oscillatory-measurements/. [Accessed 15 05 2021].

[68] Anton Paar GmbH, "Calculation of the weight average molar mass Mw based on the zero-shear viscosity measurement using a frequency sweep," 2021. [Online]. Available: https://www.anton-paar.com/corp-en/services-support/document-

finder/application-reports/calculation-of-the-weight-average-molar-mass-mw-based-on-the-zero-shear-viscosity-measurement-using/. [Accessed 20 05 2021].

[69] R. Jones, J. Kahovec, R. Stepto, E. Wilks, M. Hess, T. Kitayama and W. Metanomski, "Definitions of Terms Relating to Degradation, Aging, and Related Chemical Transformations of Polymers," in *Compendium of Polymer Terminology and Nomenclature IUPAC Recommendations 2008*, Cambridge, RSC Publishing, 2009, pp. 251-255.

[70] H. Moreira Da Costa, M. G. Oliveira and V. D. Ramos, "Degradation of polypropylene (PP) during multiple extrusions: Thermal analysis, mechanical properties and analysis of variance," *Polymer Testing,* vol. 26, no. 5, pp. 676-684, 2007.

[71] K. Balani, V. Verma, A. Agarwal and R. Narayan, "Physical, thermal and mechanical properties of polymers," in *Biosurfaces: A Materials Science and Engineering Perspective*, John Wiley & Sons, 2015, pp. 329-344.

[72] H. F. Brinson and C. L. Brinson, "Molecular Weight," in *Polymer Engineering Science and Viscoelasticity: An Introduction*, Houston, Springer, 2008, pp. 131-138.

[73] M. H. van der Beek, "The influence of shear flow on specific volume," in *Specific volume of polymers : influence of the thermomechanical history*, Eindhoven, Universiteitsdrukkerij TU Eindhoven, 2005, pp. 61-84.

[74] L. J. Fetters, D. Lohse, D. Richter, T. Witten and A. Zirkel, "Connection between Polymer Molecular Weight, Density, Chain Dimensions, and Melt Viscoelastic Properties," *Macromolecules,* vol. 27, no. 17, pp. 4639-4647, 1994.

[75] H. F. Brinson and L. C. Brinson, "Differential Constitutive Equations," in *Polymer Engineering Science and Viscoelasticity: An Introduction*, Houston , Springer US, 2015, pp. 159-200.

[76] T. G. Mezger, "Oscillatory tests," in *The Rheology Handbook*, Hannover, Vincentz Network, 2006, pp. 114-141.

[77] P. Moldenaers, "Effect of multiwall carbon nanotubes on the phase separation of concentrated blends off poly[(a-methyl styrene)-co-acrylonitrile] and poly(methyl methacrylate) as studied by melt rheology and conductivity spectroscopy," *European Polymer Journal,* vol. 53, pp. 253-269, 2014.

[78] J. Allard, "Basic Concepts of Rheology," in *Effect of compatibilization on the phase separation of polymer blends: Effect of compatibilizer's structure and molecular weight*, 2018, pp. 16-18.

[79] C. W. Macosko, "Linear Viscoelasticity," in *RHEOLOGY Principles, Measurements and Applications*, New York, Wiley-VCH, 1994, p. 124.

[80] T. G. Mezger, "Zero-shear Viscosity," in *The Rheology Handbook*, Hannover , Vincentz Network , 2006, p. 96.

[81] A. Zahavich, B. Latto, E. Takacs and J. Vlachopoulos, "The Effect of Multiple Extrusion Passes During Recycling of High Density Polyethelene," *Advances in Polymer Technology,* vol. 16, no. 1, pp. 11-24, 1998.

[82] D. Lohse, "Well-Defined, Model Long Chain Branched Polyethylene. 2. Melt Rheological Behavior," *Macromolecules,* vol. 35, no. 8, pp. 3066-3075, 2002.

Appendix

A. Mechanical tests

Table 14: Tensile strength test results of the recycled fractions

Tensile Strength (ISO1926)-Intro Recyclate			
Sample Name :		**VB24-Ref**	
Lot No :		/	
Date :		04-mei-21	
No	Sample	Tensile strength	Elongation at Break
	Foam Density	kPa	%
Avg	45.4	743.2	36.15
1	44.4	700.4	34.1
2	45.5	734.1	36.9
3	46.0	744.3	31.1
4	45.0	768.0	39.9
5	46.0	769.1	38.7
Sample Name :	**EX1_RM_Stabilisation at cycle 1**		
Lot No :	?		
Date :	12-mei-21		
No	Sample	Tensile strength	Elongation at Break
	Foam Density	kPa	%
Avg	50.3	626.5	31.13
1	50.6	666.2	33.8
2	51.6	606.2	25.9
3	50.3	636.5	33.7
4	48.4	580.6	29.7
5	50.8	643.1	32.6
Sample Name :	**EX4_RM_Stabilisation at cycle 1**		
Lot No :	/		
Date :	12-mei-21		
No	Sample	Tensile strength	Elongation at Break
	Foam Density	kPa	%
1	53.55	654.0	28.57
2	54.02	660.66	28.90
3	54.86	663.94	25.03
4	52.47	633.0	28.53
5	54.73	644.45	27.13

No	Sample	Tensile strength	Elongation at Break
6	51.65	667.8	33.26

Sample Name :	**EX5_RM_Stabilisation at cycle 1**		
Lot No :	/		
Date :	12-mei-21		

No	Sample	Tensile strength	Elongation at Break
	Foam Density	kPa	%
1	52.39	642.0	30.26
2	51.95	589.83	24.00
3	53.20	624.79	27.50
4	51.35	649.5	31.46
5	53.75	652.57	32.86
6	51.70	693.3	35.46

Sample Name :	**EX1_RM_Stabilisation at each cycle**		
Lot No :	/		
Date :	12-mei-21		

No	Sample	Tensile strength	Elongation at Break
	Foam Density	kPa	%
1	55.25	693.2	31.47
2	56.30	707.56	32.80
3	56.81	718.42	31.33
4	54.63	666.9	28.23
5	52.54	664.05	31.53
6	55.95	709.0	33.46

Sample Name :	**EX3_RM_Stabilisation at each cycle**		
Lot No :	/		
Date :	12-mei-21		

No	Sample	Tensile strength	Elongation at Break
	Foam Density	kPa	%
1	60.72	685.0	27.63
2	59.26	701.21	27.73
3	60.66	634.58	24.73
4	60.87	692.5	30.29
5	62.49	669.26	23.86
6	60.30	727.2	31.53

Sample Name :	**EX5_RM_Stabilisation at each cycle**		
Lot No :	/		
Date :	12-mei-21		

No	Sample	Tensile strength	Elongation at Break

No	Sample	Tensile strength	Elongation at Break
	Foam Density	kPa	%
1	53.02	631.4	33.02
2	52.92	592.53	26.43
3	53.33	639.04	36.43
4	49.91	583.7	33.73
5	53.57	681.01	37.16
6	55.38	660.6	31.33
Sample Name :	**EX1_RM_Stabilisation at cycle 1 with Rec. Stab.**		
Lot No :	/		
Date :	12-mei-21		
No	Sample	Tensile strength	Elongation at Break
	Foam Density	kPa	%
1	59.89	742.7	29.70
2	59.76	735.14	28.90
3	61.65	758.97	28.43
4	58.21	715.3	29.93
5	57.96	741.6	32.76
6	61.86	762.5	28.50
Sample Name :	**EX3_RM_Stabilisation at cycle 1 with Rec. Stab.**		
Lot No :	/		
Date :	12-mei-21		
No	Sample	Tensile strength	Elongation at Break
	Foam Density	kPa	%
1	66.38	709.3	22.42
2	66.50	757.35	25.40
3	67.33	715.51	20.33
4	64.14	685.8	24.03
5	67.54	678.5	19.93
Sample Name :	**EX5_RM_Stabilisation at cycle 1 with Rec. Stab.**		
Lot No :			
Date :	12-mei-21		
No	Sample	Tensile strength	Elongation at Break
	Foam Density	kPa	%
1	59.76	694.7	31.67
2	60.46	742.97	35.33
3	59.94	690.81	29.06
4	59.02	699.2	30.76
5	58.91	672.33	32.60
6	60.47	668.4	30.60

Tensile Strength (ISO1926)-Multiple Extrusion cycles			
Sample Name :		**VB24-Ref**	
Lot No :		E1428	
Date :		04-mei-21	
No	Sample	Tensile strength	Elongation at Break
	Foam Density	kPa	%
Avg	45.4	743.2	36.15
1	44.4	700.4	34.1
2	45.5	734.1	36.9
3	46.0	744.3	31.1
4	45.0	768.0	39.9
5	46.0	769.1	38.7
Sample Name :	**EX1_Stabilisation at cycle 1**		
Lot No :	?		
Date :	12-mei-21		
No	Sample	Tensile strength	Elongation at Break
	Foam Density	kPa	%
Avg	53.8	686.4	30.79
1	53.1	713.8	34.6
2	53.7	662.0	28.7
3	54.4	662.5	28.2
4	54.0	707.1	31.6
Sample Name :	**EX3_Stabilisation at cycle 1**		
Lot No :			
Date :	12-mei-21		
No	Sample	Tensile strength	Elongation at Break
	Foam Density	kPa	%
1	57.09	649.1	22.81
2	56.19	642.98	23.83
3	56.69	615.08	19.93
4	57.35	681.0	25.63
5	58.12	657.18	21.83
Sample Name :	**EX5_Stabilisation at cycle 1**		
Lot No :			
Date :	12-mei-21		

No	Sample	Tensile strength	Elongation at Break
	Foam Density	kPa	%
1	63.93	688.3	23.72
2	62.35	653.51	25.16
3	64.14	677.89	22.26
4	64.62	712.0	22.19
5	64.18	677.18	24.13
6	64.35	721.0	24.86
Sample Name :	**EX1_Stabilisation at each cycle**		
Lot No :			
Date :	12-mei-21		
No	Sample	Tensile strength	Elongation at Break
	Foam Density	kPa	%
1	51.13	652.7	32.25
2	51.27	660.51	31.23
3	50.42	641.3	28.93
4	51.06	683.5	34.83
5	51.25	618.8	36.93
6	51.63	659.4	29.33
Sample Name :	**EX3_Stabilisation at each cycle**		
Lot No :			
Date :	12-mei-21		
No	Sample	Tensile strength	Elongation at Break
	Foam Density	kPa	%
1	52.92	606.0	29.97
2	53.10	667.97	33.63
3	53.77	603.48	29.19
4	52.26	607.1	31.63
5	53.39	602.4	29.26
6	52.10	548.9	26.13
Sample Name :	**EX5_Stabilisation at each cycle**		
Lot No :			
Date :	12-mei-21		
No	Sample	Tensile strength	Elongation at Break
	Foam Density	kPa	%
1	58.15	705.1	30.67
2	59.74	698.51	29.20
3	59.01	705.13	26.87
4	55.48	713.2	35.69
5	58.64	682.55	28.46
6	57.87	726.1	33.13

Table 16: Compression test results of the recycled material

Compressive Strength (ISO844)

Sample Name : **VB24-Ref**

Lot No :

Date : 04-mei-21

No	Molded Density (g/l)	Compression Stress (kPa)				
		5%	10%	25%	50%	75%
1	**45.5**		206.1	251.4	336.1	684.9
2	**45.7**		202.2	247.9	332.9	682.5
3	**45.2**		202.0	246.3	329.9	677.9
4	**47.1**		210.9	257.9	345.8	727.4
5	**45.2**		209.7	253.7	337.5	693.2

Sample Name : **EX1_RM_Stabilisation at cycle 1**

Lot No :

Date : 19-mei-21

No	Molded Density (g/l)	Compression Stress (kPa)				
		5%	10%	25%	50%	75%
1	**51.9**		248.9	314.4	427.6	868.3
2	**53.1**		231.8	291.5	395.3	765.3
3	**56.6**		278.6	337.5	453.8	1014.4
4	**51.9**		241.6	297.4	403.8	851.1
5	**55.5**		269.7	330.3	439.9	882.8

Sample Name : **EX4_RM_Stabilisation at cycle 1**

Lot No :

Date : 19-mei-21

No	Molded Density (g/l)	Compression Stress (kPa)				
		5%	10%	25%	50%	75%
1	58.5		286.2	356.5	472.1	916.2
2	58.5		281.5	348.4	461.2	866.0
3	56.5		256.9	330.3	444.5	837.1
4	58.6		286.1	345.1	460.6	1012.6
5	56.5		258.6	322.6	434.0	857.3

Sample Name : **EX5_RM_Stabilisation at cycle 1**

Lot No :

Date : 19-mei-21

No	Molded Density (g/l)	Compression Stress (kPa)				
		5%	10%	25%	50%	75%
1	53.8		256.0	322.5	441.9	968.1
2	57.5		251.0	309.1	422.1	889.4
3	53.6		241.2	307.2	420.0	841.1
4	57.3		268.4	332.9	449.3	946.5
5	52.4		251.2	314.3	434.5	961.6

Sample Name : **EX1_RM_Stabilisation at each cycle**

Lot No :

Date : 19-mei-21

No	Molded Density (g/l)	Compression Stress (kPa)				
		5%	10%	25%	50%	75%
1.0	57.4		271.6	341.3	455.7	869.7
2.0	61.1		283.2	350.8	474.0	968.6
3.0	58.9		266.1	333.7	462.3	1008.7
4.0	60.1		261.8	331.0	447.4	874.1

Sample Name : **EX3_RM_Stabilisation at each cycle**

Lot No :

Date : 19-mei-21

No	Molded Density (g/l)	Compression Stress (kPa)				
		5%	10%	25%	50%	75%
1.0	66.1		286.3	363.8	493.9	1011.0
2.0	61.7		309.5	379.5	514.0	1122.8
3.0	62.6		254.1	333.0	455.3	911.9
4.0	65.6		259.4	339.0	459.1	873.4
5.0	63.0		308.4	374.6	502.8	1025.7

Sample Name : **EX5_RM_Stabilisation at each cycle**

Lot No :

Date : 19-mei-21

No	Molded Density (g/l)	Compression Stress (kPa)				
		5%	10%	25%	50%	75%
1.0	57.0		260.3	323.8	442.3	904.4
2.0	62.0		283.2	345.9	460.0	953.0
3.0	58.7		255.7	316.6	423.4	830.3
4.0	56.5		257.3	313.1	428.6	931.2
5.0	57.3		258.1	322.4	440.3	903.7

Sample Name : **EX1_RM_Stabilisation at cycle 1 Rec. Stab.**

Lot No :

Date : 19-mei-21

No	Molded	Compression Stress (kPa)				

	Density (g/l)	5%	10%	25%	50%	75%
1.0	61.0		292.1	370.8	504.0	1025.2
2.0	62.5		280.8	344.7	463.6	925.8
3.0	60.2		285.8	367.4	499.4	1011.9
4.0	59.9		286.7	369.1	500.3	1007.5
5.0	60.2		297.3	375.2	514.9	1096.3

Sample
Name :   **EX3_RM_Stabilisation at cycle 1 with Rec. Stab.**

Lot No   :

Date   :   19-mei-21

No	Molded	Compression Stress (kPa)				
	Density (g/l)	5%	10%	25%	50%	75%
1.0	66.8		317.5	417.4	573.2	1153.0
2.0	73.2		338.0	423.8	561.0	1100.7
3.0	70.1		361.9	450.5	608.9	1325.8
4.0	70.0		304.5	385.7	524.3	1013.6
5.0	65.4		320.6	411.8	566.3	1208.9

Sample
Name :   **EX5_RM_Stabilisation at cycle 1 Rec. Stab.**

Lot No   :

Date   :   19-mei-21

No	Molded	Compression Stress (kPa)				
	Density (g/l)	5%	10%	25%	50%	75%
1.0	66.4		278.8	369.2	501.8	976.3
2.0	63.8		270.7	353.0	484.3	989.4
3.0	61.1		275.6	366.6	506.7	1067.4
4.0	66.0		321.5	396.0	532.4	1103.5
5.0	63.1		270.8	361.3	487.2	911.3

Table 17: Compression test results of the non-recycled blends

Compressive Strength (ISO844)

Sample
Name :   **VB24-Ref**

Lot No
:   E1428

Date
:   04-mei-21

No	Molded	Compression Stress (kPa)				
	Density (g/l)	5%	10%	25%	50%	75%
1	**45.5**		206.1	251.4	336.1	684.9
2	**45.7**		202.2	247.9	332.9	682.5
3	**45.2**		202.0	246.3	329.9	677.9
4	**47.1**		210.9	257.9	345.8	727.4
5	**45.2**		209.7	253.7	337.5	693.2

Sample Name :   **EX1_Stabilisation at cycle 1**

No	Molded	Compression Stress (kPa)				
	Density (g/l)	5%	10%	25%	50%	75%
1	**50.5**		241.4	305.6	414.6	784.3
2	**55.3**		268.0	332.1	444.6	877.2
3	**58.2**		282.4	347.4	461.1	928.3
4	**51.6**		238.0	300.8	412.6	814.4
5	**54.7**		257.7	322.0	431.7	817.8

EX3_Stabilisation at cycle

No	Molded	Compression Stress (kPa)				
	Density (g/l)	5%	10%	25%	50%	75%
1	61.9		294.0	370.1	495.9	1024.3
2	58.5		274.3	354.2	484.4	1036.5
3	58.5		281.0	343.0	462.6	1006.4
4	60.8		274.6	337.1	454.1	928.2
5	58.3		263.9	322.1	421.2	749.9

EX5_Stabilisation at cycle

No	Molded	Compression Stress (kPa)				
	Density (g/l)	5%	10%	25%	50%	75%
1	69.9		338.9	423.2	569.6	1127.6
2	64.3		297.4	385.4	536.0	1132.0
3	65.5		316.4	405.9	560.7	1188.8
4	65.9		318.0	402.6	545.5	1126.6
5	68.7		317.7	400.0	550.7	1135.7

No	Molded	Compression Stress (kPa)				
	Density (g/l)	5%	10%	25%	50%	75%
1.0	55.4		195.1	294.3	402.6	764.8
2.0	55.7		197.2	282.5	388.2	718.9
3.0	56.0		183.6	289.3	396.5	751.1

No	Molded	Compression Stress (kPa)				
	Density (g/l)	5%	10%	25%	50%	75%

1.0	56.2		265.9	331.5	448.4	967.1
2.0	56.0		266.2	335.5	454.0	916.2
3.0	54.7		267.0	329.0	445.1	916.5
4.0	56.6		279.4	344.0	458.8	903.1
5.0	57.9		291.3	354.2	478.0	1037.2

Sample Name : **EX5_Stabilisation at each cycle**

Lot No :

Date : 19-mei-21

No	**Molded**	Compression Stress (kPa)				
	Density (g/l)	5%	10%	25%	50%	75%
1.0	61.5		301.1	366.6	489.6	1021.2
2.0	57.0		277.9	336.5	457.8	987.8
3.0	56.9		260.3	323.0	443.6	934.4
4.0	56.9		281.0	341.4	465.0	999.3
5.0	60.6		272.5	329.7	445.0	908.0

B. Rheological tests

Table 18: Rheological test results non-recycled blend stabilisation at cycle 1

1	16	EX1C1						
Point No.	Angular Frequency	Storage Modulus	Loss Modulus	Loss Factor	Shear Strain	Shear Stress	Torque	Complex Viscosity
	[rad/s]	[Pa]	[Pa]	[1]	[%]	[Pa]	[mN·m]	Pa.s
1	100	27463	28156	1.025	1	395.1	1.8179	393.3162474
2	63.1	20342	23432	1.152	1	311.84	1.4348	491.757756
3	39.8	14656	19081	1.302	1	241.79	1.1125	604.522246
4	25.1	10230	15143	1.48	1.01	183.67	0.84512	728.0742681
5	15.8	6928.8	11729	1.693	1.01	136.92	0.62997	862.1956337
6	10	4547.3	8866.1	1.95	1.01	100.15	0.46081	996.4219312
7	6.31	2896.7	6547.7	2.26	1.01	71.958	0.33109	1134.680765
8	3.98	1791.1	4726.9	2.639	1.01	50.804	0.23376	1270.065655
9	2.51	1079.9	3343.7	3.096	1.01	35.315	0.16249	1399.90463
10	1.58	638.57	2324.8	3.641	1.01	24.232	0.11149	1525.889735
11	1	372.52	1587.9	4.262	1.01	16.393	0.075425	1631.011208
12	0.631	212.92	1049.8	4.93	1.01	10.766	0.049535	1697.582525
13	0.398	127.01	691.76	5.447	1.01	7.0685	0.032523	1767.143565
14	0.251	75.936	449.88	5.924	1.01	4.5856	0.021099	1817.703882
15	0.158	48.632	292.18	6.008	1.01	2.9769	0.013697	1874.681235
16	0.1	32.92	191.94	5.83	1.01	1.9573	0.0090057	1947.42625
1	16	EX3C1						
Point No.	Angular Frequency	Storage Modulus	Loss Modulus	Loss Factor	Shear Strain	Shear Stress	Torque	Complex Viscosity
	[rad/s]	[Pa]	[Pa]	[1]	[%]	[Pa]	[mN·m]	Pa.s
1	100.00	26429.00	27262.00	1.03	1.00	381.42	1.76	379.6983915
2	63.10	19468.00	22630.00	1.16	1.00	300.01	1.38	473.0844984
3	39.80	13939.00	18360.00	1.32	1.01	231.69	1.07	579.1908664
4	25.10	9693.50	14529.00	1.50	1.01	175.53	0.81	695.850446

5	15.80	6535.20	11226.00	1.72	1.01	130.56	0.60	822.1319587
6	10.00	4268.80	8461.90	1.98	1.01	95.26	0.44	947.7679307
7	6.31	2702.80	6228.20	2.30	1.01	68.24	0.31	1075.970567
8	3.98	1661.90	4481.20	2.70	1.01	48.03	0.22	1200.864804
9	2.51	994.08	3156.90	3.18	1.01	33.26	0.15	1318.61151
10	1.58	581.67	2181.60	3.75	1.01	22.69	0.10	1428.99543
11	1.00	337.30	1482.90	4.40	1.01	15.28	0.07	1520.777334
12	0.63	191.96	976.57	5.09	1.01	10.00	0.05	1577.270298
13	0.40	112.49	640.06	5.69	1.01	6.53	0.03	1632.838784
14	0.25	67.65	415.71	6.15	1.01	4.23	0.02	1677.999422
15	0.16	44.79	269.13	6.01	1.01	2.74	0.01	1726.780421
16	0.10	30.69	174.61	5.69	1.01	1.78	0.01	1772.857054

1	16	EX5C1						
Point No.	Angular Frequency	Storage Modulus	Loss Modulus	Loss Factor	Shear Strain	Shear Stress	Torque	Complex Viscosity
	[rad/s]	[Pa]	[Pa]	[1]	[%]	[Pa]	[mN·m]	Pa.s
1	100.00	24850	25503	1.026	1	357.65	1.6456	356.0794166
2	63.10	18276	21178	1.159	1	281.09	1.2934	443.3210213
3	39.80	13037	17151	1.316	1.01	216.51	0.99622	541.292674
4	25.10	9011.3	13551	1.504	1.01	163.57	0.75263	648.3543577
5	15.80	6037.3	10440	1.729	1.01	121.21	0.55773	763.2884924
6	10.00	3912.6	7847.3	2.006	1.01	88.134	0.40552	876.861198
7	6.31	2456	5752.9	2.342	1.01	62.87	0.28928	991.3187594
8	3.98	1495.1	4125.2	2.759	1.01	44.1	0.20291	1102.456878
9	2.51	885.73	2893.2	3.266	1.01	30.412	0.13993	1205.475508
10	1.58	510.94	1992.5	3.9	1.01	20.675	0.095129	1301.878263
11	1.00	292.14	1353.4	4.633	1.01	13.916	0.064031	1384.571175
12	0.63	163.67	891.37	5.446	1.01	9.1089	0.041912	1436.246709
13	0.40	94.408	583.77	6.183	1.01	5.9434	0.027347	1485.815621
14	0.25	57.351	378.23	6.595	1.01	3.8448	0.017691	1524.116956
15	0.16	36.638	244.82	6.682	1.01	2.4879	0.011447	1566.748796
16	0.10	24.015	160.7	6.691	1.01	1.633	0.0075138	1624.844923

Table 19: Rheological test results non-recycled blend stabilisation at each cycle

1	16	EX1EX						
Point No.	Angular Frequency	Storage Modulus	Loss Modulus	Loss Factor	Shear Strain	Shear Stress	Torque	Complex Viscosity
	[rad/s]	[Pa]	[Pa]	[1]	[%]	[Pa]	[mN·m]	Pa.s
1	100.00	32190	26100	0.694	1	393.29	1.8096	414.4159867
2	63.10	24506	22331	0.783	1	312.79	1.4392	525.4271099
3	39.80	18034	19192	0.897	1.01	243.46	1.1202	661.6957222
4	25.10	12799	16175	1.033	1.01	184.92	0.85085	821.765688
5	15.80	8746.8	13218	1.195	1	136.96	0.63017	1003.163627

Point No.	Angular Frequency	Storage Modulus	Loss Modulus	Loss Factor	Shear Strain	Shear Stress	Torque	Complex Viscosity
6	10.00	5732.2	10450	1.392	1	98.728	0.45426	1191.891844
7	6.31	3597.8	7978	1.633	1.01	69.241	0.31859	1386.960796
8	3.98	2162.3	5874.7	1.928	1.01	47.191	0.21714	1572.865152
9	2.51	1251.4	4167.9	2.281	1.01	31.322	0.14412	1733.749574
10	1.58	702.01	2854.2	2.694	1.01	20.277	0.0933	1860.293974
11	1.00	382.94	1871.5	3.167	1.01	12.781	0.058807	1910.276235
12	0.63	193.73	1202.6	3.545	1.01	7.9115	0.036402	1930.434699
13	0.40	124.08	747.61	3.785	1.01	4.8822	0.022464	1904.112468
14	0.25	87.263	469.66	3.741	1.01	3.0072	0.013837	1903.179148
15	0.16	54.164	299.07	3.463	1.01	1.8535	0.0085283	1923.640485
16	0.10	35.812	197.111	3.076	1.01	1.164	0.0053558	2003.378288
1	16	EX3EX						
Point No.	Angular Frequency	Storage Modulus	Loss Modulus	Loss Factor	Shear Strain	Shear Stress	Torque	Complex Viscosity
	[rad/s]	[Pa]	[Pa]	[1]	[%]	[Pa]	[mN·m]	Pa.s
1	100.00	25086	25861	1.031	1	361.92	1.6653	360.2913706
2	63.10	18506	21481	1.161	1.01	284.95	1.3111	449.3379638
3	39.80	13270	17434	1.314	1.01	220.19	1.0131	550.4962948
4	25.10	9238.9	13818	1.496	1.01	167.07	0.76871	662.235286
5	15.80	6236.2	10687	1.714	1.01	124.36	0.57222	783.1294771
6	10.00	4081.2	8066.9	1.977	1.01	90.864	0.41808	904.0523715
7	6.31	2588.7	5945.3	2.297	1.01	65.172	0.29987	1027.644979
8	3.98	1594	4283.5	2.687	1.01	45.936	0.21136	1148.359633
9	2.51	955.52	3018.2	3.159	1.01	31.819	0.1464	1261.291265
10	1.58	561.77	2087.8	3.717	1.01	21.73	0.099984	1368.391077
11	1.00	326.59	1421.6	4.353	1.01	14.66	0.067453	1458.632095
12	0.63	187.83	939.98	5.004	1.01	9.6338	0.044327	1519.116848
13	0.40	110.87	617.93	5.574	1.01	6.3096	0.029031	1577.380535
14	0.25	69.119	403.86	5.843	1.01	4.1181	0.018948	1632.398523
15	0.16	44.949	265.16	5.899	1.01	2.7029	0.012437	1702.169721
16	0.10	30.79	174.14	5.656	1.01	1.7773	0.0081777	1768.41069
1	16	EX5EX						
Point No.	Angular Frequency	Storage Modulus	Loss Modulus	Loss Factor	Shear Strain	Shear Stress	Torque	Complex Viscosity
	[rad/s]	[Pa]	[Pa]	[1]	[%]	[Pa]	[mN·m]	Pa.s
1	100.00	25791	26437	1.025	1	370.99	1.707	369.3359785
2	63.10	19013	21977	1.156	1.01	292.07	1.3439	460.5385813
3	39.80	13623	17843	1.31	1.01	225.62	1.0381	564.0458848
4	25.10	9474.6	14140	1.492	1.01	171.07	0.7871	678.1195366
5	15.80	6385.4	10934	1.712	1.01	127.28	0.58561	801.3910184
6	10.00	4168.2	8248.9	1.979	1.01	92.893	0.42742	924.2199005
7	6.31	2636.7	6075.1	2.304	1.01	66.561	0.30626	1049.542759
8	3.98	1616.8	4372.5	2.704	1.01	46.855	0.21559	1171.317831
9	2.51	963.22	3078.7	3.196	1.01	32.422	0.14918	1285.204034
10	1.58	561.45	2127.6	3.789	1.01	22.116	0.10176	1392.67947

11	1.00	321.58	1442.7	4.486	1.01	14.856	0.068355	1478.105878
12	0.63	180.79	950.34	5.257	1.01	9.7228	0.044736	1533.096128
13	0.40	103.57	619.86	5.985	1.01	6.3162	0.029062	1579.027621
14	0.25	62.595	403.6	6.448	1.01	4.1048	0.018887	1627.191788
15	0.16	40.392	262.64	6.502	1.01	2.6706	0.012288	1681.821752
16	0.10	25.649	171.29	6.678	1.01	1.7408	0.0080096	1731.996978

Table 20: Rheological test results recycled blend stabilisation at first cycle

1	16	EX1RMC1						
Point No.	Angular Frequency	Storage Modulus	Loss Modulus	Loss Factor	Shear Strain	Shear Stress	Torque	Complex Viscosity
	[rad/s]	[Pa]	[Pa]	[1]	[%]	[Pa]	[mN·m]	Pa.s
1	100.00	27166	28353	1.044	1	394.46	1.815	392.6683289
2	63.10	19949	23476	1.177	1	309.61	1.4246	488.2286221
3	39.80	14248	18989	1.333	1.01	238.6	1.0978	596.4824253
4	25.10	9885	15002	1.518	1.01	180.57	0.83085	715.7725382
5	15.80	6651.9	11560	1.738	1.01	134.06	0.61682	844.1276969
6	10.00	4342.8	8699.9	2.003	1.01	97.732	0.44968	972.3588425
7	6.31	2752.8	6397.7	2.324	1.01	70.001	0.32209	1103.772179
8	3.98	1693.1	4599.3	2.717	1.01	49.258	0.22664	1231.415932
9	2.51	1015.7	3238.3	3.188	1.01	34.11	0.15695	1352.132387
10	1.58	596.88	2237.6	3.749	1.01	23.276	0.1071	1465.722146
11	1.00	345.79	1522.5	4.403	1.01	15.692	0.072203	1561.274151
12	0.63	198.98	1009.1	5.071	1.01	10.337	0.047563	1630.001456
13	0.40	114.69	659.32	5.748	1.01	6.726	0.030948	1681.459633
14	0.25	67.535	428.39	6.343	1.01	4.3586	0.020055	1727.81164
15	0.16	44.637	278.14	6.231	1.01	2.8312	0.013027	1782.905005
16	0.10	29.538	180.95	6.126	1.01	1.8427	0.0084788	1833.450189
1	16	EX4RMC1						
Point No.	Angular Frequency	Storage Modulus	Loss Modulus	Loss Factor	Shear Strain	Shear Stress	Torque	Complex Viscosity
	[rad/s]	[Pa]	[Pa]	[1]	[%]	[Pa]	[mN·m]	Pa.s
1	100.00	20744	21856	1.054	1	302.7	1.3928	301.3300967
2	63.10	15254	18091	1.186	1.01	237.82	1.0943	375.018381
3	39.80	10889	14623	1.343	1.01	183.24	0.84311	458.0881274
4	25.10	7551.7	11539	1.528	1.01	138.6	0.63771	549.4205826
5	15.80	5088.5	8888.5	1.747	1.01	102.94	0.47364	648.2269227
6	10.00	3331.9	6692	2.008	1.01	75.138	0.34572	747.5588379
7	6.31	2127	4927.7	2.317	1.01	53.945	0.24821	850.5792909
8	3.98	1328.1	3550	2.673	1.01	38.097	0.17529	952.335872
9	2.51	817.43	2514.5	3.076	1.01	26.575	0.12228	1053.398965
10	1.58	498.04	1754.4	3.523	1.01	18.331	0.084344	1154.25465
11	1.00	305.88	1202	3.93	1.01	12.466	0.057359	1240.309064
12	0.63	189.86	812.68	4.281	1.01	8.3885	0.038597	1322.603994

13	0.40	121.78	545.27	4.477	1.01	5.6155	0.025838	1403.777954
14	0.25	82.812	364.12	4.397	1.01	3.7529	0.017268	1487.722177
15	0.16	58.595	244.82	4.178	1.01	2.53	0.011641	1593.255675
16	0.10	44.213	165.46	3.742	1.01	1.7213	0.0079198	1712.652941

Table 21: Rheological test results recycled blend stabilisation at each cycle

1	16	EX1RMEX						
Point No.	Angular Frequency	Storage Modulus	Loss Modulus	Loss Factor	Shear Strain	Shear Stress	Torque	Complex Viscosity
	[rad/s]	[Pa]	[Pa]	[1]	[%]	[Pa]	[mN·m]	Pa.s
1	100.00	25522	26821	1.051	1	371.94	1.7114	370.2348613
2	63.10	18783	22212	1.183	1.01	292.36	1.3452	460.9995353
3	39.80	13442	17979	1.338	1.01	225.62	1.0381	564.0307901
4	25.10	9352.7	14213	1.52	1.01	171	0.78682	677.8558298
5	15.80	6315.4	10968	1.737	1.01	127.21	0.58533	801.030074
6	10.00	4146.9	8270.8	1.994	1.01	92.992	0.42787	925.2184188
7	6.31	2650.1	6094.6	2.3	1.01	66.797	0.30734	1053.223334
8	3.98	1650.9	4393.6	2.661	1.01	47.175	0.21706	1179.278036
9	2.51	1009.8	3106.6	3.076	1.01	32.833	0.15107	1301.43329
10	1.58	610.11	2162.3	3.544	1.01	22.582	0.10391	1421.978169
11	1.00	370.05	1485.7	4.015	1.01	15.389	0.070808	1531.091602
12	0.63	224.07	995.17	4.441	1.01	10.252	0.047173	1616.614374
13	0.40	139.93	661.78	4.729	1.01	6.7985	0.031281	1699.5276
14	0.25	91.634	438.73	4.788	1	4.5044	0.020725	1785.646539
15	0.16	62.559	289.83	4.633	1.01	2.98	0.013712	1876.612242
16	0.10	43.928	194.14	4.419	1.01	2.0004	0.0092044	1990.47755
1	16	EX3RMEX						
Point No.	Angular Frequency	Storage Modulus	Loss Modulus	Loss Factor	Shear Strain	Shear Stress	Torque	Complex Viscosity
	[rad/s]	[Pa]	[Pa]	[1]	[%]	[Pa]	[mN·m]	Pa.s
1	100.00	22886	24693	1.079	1	338.21	1.5562	336.6768844
2	63.10	16714	20316	1.215	1.01	264.4	1.2165	416.9215356
3	39.80	11864	16329	1.376	1.01	202.86	0.9334	507.1337371
4	25.10	8179.1	12811	1.566	1.01	152.77	0.70293	605.5506885
5	15.80	5483.5	9814.3	1.79	1.01	112.99	0.5199	711.5378268
6	10.00	3567.1	7346	2.059	1.01	82.077	0.37765	816.6267104
7	6.31	2259.9	5374.2	2.378	1.01	58.595	0.2696	923.9339888
8	3.98	1397.4	3848.1	2.754	1.01	41.147	0.18933	1028.635986
9	2.51	848.11	2701.5	3.185	1.01	28.458	0.13094	1128.08769
10	1.58	509.03	1867.6	3.669	1.01	19.455	0.089516	1225.144044
11	1.00	306.54	1276.6	4.165	1.01	13.195	0.060713	1312.887783
12	0.63	185.18	846.29	4.57	1.01	8.7069	0.040062	1372.920928
13	0.40	116.07	563.99	4.859	1.01	5.787	0.026627	1446.758377
14	0.25	74.518	371.46	4.985	1.01	3.8078	0.01752	1509.405358
15	0.16	53.665	247.71	4.616	1.01	2.5474	0.011721	1604.1548

Point No.	Angular Frequency	Storage Modulus	Loss Modulus	Loss Factor	Shear Strain	Shear Stress	Torque	Complex Viscosity
16	0.10	37.375	165.36	4.424	1.01	1.7038	0.0078395	1695.311777
1	16	EX5RMEX						
Point No.	Angular Frequency	Storage Modulus	Loss Modulus	Loss Factor	Shear Strain	Shear Stress	Torque	Complex Viscosity
	[rad/s]	[Pa]	[Pa]	[1]	[%]	[Pa]	[mN·m]	Pa.s
1	100.00	21422	22128	1.033	1	309.37	1.4235	307.9854652
2	63.10	15813	18353	1.161	1	243.44	1.1201	383.9252002
3	39.80	11342	14878	1.312	1.01	188.03	0.86515	470.0546725
4	25.10	7910.7	11787	1.49	1	142.66	0.6564	565.5582225
5	15.80	5352.4	9115.5	1.703	1.01	106.24	0.48884	669.0341229
6	10.00	3513.9	6879.8	1.958	1.01	77.645	0.35726	772.5227586
7	6.31	2242.4	5073.7	2.263	1.01	55.751	0.25652	879.1034006
8	3.98	1389.4	3658.7	2.633	1.01	39.334	0.18098	983.3247072
9	2.51	843.78	2583.3	3.062	1.01	27.313	0.12567	1082.713108
10	1.58	505.41	1789.4	3.54	1.01	18.687	0.085984	1176.839403
11	1.00	301.48	1215	4.03	1.01	12.581	0.057888	1251.844715
12	0.63	176.39	809.7	4.59	1.01	8.3285	0.038321	1313.296743
13	0.40	109.94	535.45	4.87	1.01	5.4938	0.025278	1373.417273
14	0.25	68.33	355.71	5.206	1.01	3.6403	0.01675	1443.081527
15	0.16	46.47	234.12	5.038	1.01	2.3989	0.011038	1510.679222
16	0.10	34.064	156.13	4.583	1.01	1.6061	0.0073899	1598.027941

Table 22: Rheological test results recycled blend stabilisation at first cycle with Rec. Stab.

Point No.	Angular Frequency	Storage Modulus	Loss Modulus	Loss Factor	Shear Strain	Shear Stress	Torque	Complex Viscosity
1	16	EX1RMRS						
Point No.	Angular Frequency	Storage Modulus	Loss Modulus	Loss Factor	Shear Strain	Shear Stress	Torque	Complex Viscosity
	[rad/s]	[Pa]	[Pa]	[1]	[%]	[Pa]	[mN·m]	Pa.s
1	100.00	24617	25945	1.054	1	359.21	1.6528	357.6506276
2	63.10	17973	21397	1.191	1	280.81	1.2921	442.8506872
3	39.80	12745	17216	1.351	1.01	215.29	0.99058	538.196398
4	25.10	8780.9	13515	1.539	1.01	162	0.74539	642.1137054
5	15.80	5879.1	10357	1.762	1.01	119.7	0.55077	753.7527376
6	10.00	3831.2	7753.2	2.024	1.01	86.924	0.39995	864.8132959
7	6.31	2435.4	5680.7	2.333	1.01	62.124	0.28584	979.5147824
8	3.98	1517.2	4081.8	2.69	1.01	43.77	0.20139	1094.133468
9	2.51	934.29	2883.8	3.087	1.01	30.469	0.1402	1207.71688
10	1.58	575.31	2011.5	3.496	1.01	21.029	0.096758	1324.148931
11	1.00	360.19	1389.3	3.857	1.01	14.426	0.066378	1435.232151
12	0.63	228.55	939.09	4.109	1.01	9.7145	0.044698	1531.698083
13	0.40	150.37	632.89	4.209	1.01	6.5382	0.030084	1634.442657
14	0.25	101.84	426.31	4.186	1.01	4.4052	0.020269	1746.236554
15	0.16	73.471	288.48	3.926	1.01	2.9919	0.013766	1884.107143
16	0.10	54.668	195.32	3.573	1.01	2.0384	0.0093792	2028.262622
1	16	EX3RMRS						
Point No.	Angular Frequency	Storage Modulus	Loss Modulus	Loss Factor	Shear Strain	Shear Stress	Torque	Complex Viscosity

		[rad/s]	[Pa]	[Pa]	[1]	[%]	[Pa]	[mN·m]	Pa.s
1		100.00	22827	24307	1.065	1	334.97	1.5413	333.4519723
2		63.10	16695	20038	1.2	1.01	262.12	1.2061	413.335922
3		39.80	11870	16134	1.359	1.01	201.31	0.92627	503.2675585
4		25.10	8195.2	12681	1.547	1.01	151.75	0.69823	601.5396193
5		15.80	5495	9731.9	1.771	1.01	112.33	0.51686	707.3472275
6		10.00	3579	7295.9	2.039	1.01	81.677	0.37581	812.646281
7		6.31	2271.6	5351.4	2.356	1.01	58.432	0.26885	921.3271798
8		3.98	1406	3841.4	2.732	1.01	41.115	0.18918	1027.794522
9		2.51	857.04	2712.9	3.165	1.01	28.595	0.13157	1133.488469
10		1.58	516.72	1884.7	3.647	1.01	19.643	0.090382	1236.867183
11		1.00	313.37	1294	4.129	1.01	13.382	0.061571	1331.404055
12		0.63	190.55	863.28	4.531	1.01	8.8857	0.040885	1401.04558
13		0.40	118.57	577.97	4.875	1.01	5.9298	0.027284	1482.429448
14		0.25	77.884	385.25	4.946	1.01	3.9503	0.018176	1565.911813
15		0.16	54.013	256.06	4.741	1	2.63	0.012101	1656.295712
16		0.10	38.941	172.43	4.428	1.01	1.7766	0.0081745	1767.724707
1	16	EX5RMRS							
Point No.	Angular Frequency	Storage Modulus	Loss Modulus	Loss Factor	Shear Strain	Shear Stress	Torque		Complex Viscosity
		[rad/s]	[Pa]	[Pa]	[1]	[%]	[Pa]	[mN·m]	Pa.s
1		100.00	24125	24421	1.012	1	344.83	1.5866	343.2784389
2		63.10	17836	20328	1.14	1.01	271.81	1.2506	428.5814957
3		39.80	12826	16530	1.289	1.01	210.28	0.96752	525.6886549
4		25.10	8957.1	13122	1.465	1.01	159.69	0.73475	632.9729775
5		15.80	6075	10161	1.673	1.01	118.99	0.54749	749.2760646
6		10.00	3998.3	7677.9	1.92	1.01	87.007	0.40033	865.659005
7		6.31	2552.5	5665	2.219	1.01	62.449	0.28734	984.7055265
8		3.98	1589.2	4086	2.571	1.01	44.064	0.20275	1101.550425
9		2.51	964.87	2882.2	2.987	1.01	30.549	0.14056	1210.922797
10		1.58	574.23	1991.4	3.468	1.01	20.831	0.095849	1311.732956
11		1.00	338.74	1351.4	3.99	1.01	14.003	0.064428	1393.20736
12		0.63	194.29	891.38	4.588	1.01	9.1693	0.04219	1445.813883
13		0.40	116.46	582.9	5.005	1.01	5.9743	0.027489	1493.518022
14		0.25	70.542	376.62	5.339	1.01	3.851	0.017719	1526.571362
15		0.16	45.333	242.96	5.359	1.01	2.484	0.011429	1564.259968
16		0.10	31.628	156.05	4.934	1.01	1.6003	0.0073634	1592.229031